A New Performance Test for Evaluating the ASR Potential of Job Mixtures

by

Michael J. Laskey

B.Sc. E., University of New Brunswick, 2015

A Thesis Submitted in Partial Fulfillment
of the Requirements for the Degree of

Masters of Science in Engineering

in the Graduate Academic Unit of Civil Engineering

Supervisors: Michael Thomas, PhD, P.Eng., Civil Engineering
                          Edward Moffatt, PhD, EIT., Civil Engineering

Examining Board:

                          Alan Lloyd, PhD, Civil Engineering
                          Xiomara Sanchez-Castillo, PhD, P.Eng., Civil Engineering
                          Guida Bendrich, PhD, P.Eng., Chemical Engineering

This thesis is accepted by the Dean of Graduate Studies

THE UNIVERSITY OF NEW BRUNSWICK

May, 2018

ABSTRACT

Alkali-silica reaction (ASR) is a problem that plagues many concrete structures worldwide, from dams to residential structures. At the moment, standardized are testing methodologies encounter problems such as leaching of alkalis, extensive testing time, or the inability to test "job-mixtures". The University of New Brunswick concrete cylinder test (UNBCCT) was developed to overcome such difficulties through the storage of concrete samples in alkali host solutions designed to negate leaching, increase the storage temperature to accelerate the reaction, and the use of job mixture designs.

With these modifications, cylinders were cast with various aggregate and cementitious material combinations (100% portland cement, and combinations of cement and SCMs such as fly ash, ground granulated blast furnace slag, and silica fume) to the dimensions of 145 mm in diameter by 285 mm in height. The cylinders were stored in containers (150mm by 300 mm in height) filled with a host solution matching the alkalinity of the concrete pore-solution. The samples were then stored in either 38°C or 60°C to determine if an accelerated version of the test was plausible. The resulting expansion was periodically measured and compared to other test methods such as the concrete prism test (CPT) and long-term exposure blocks.

Alkali-leaching occurrence was also investigated through the casting of non-reactive limestone samples. These samples were periodically tested for alkali contents in a profile from the center to the surface. These profiles were generated by dissolving milled powder via hydrochloric acid or water, and measuring alkalis by inductively coupled plasma mass

spectrometry (ICP-MS). Testing was also conducted on pore-solution extracted from the concrete and the host solution.

The results to date indicate that the storage conditions used in the UNBCCT minimize the reduction or enrichment of alkalis in the test specimen, and that the expansion results compare well with the behavior of long-term exposure blocks. The test appears to have promise as a performance test for "job mixtures", although further studies are required with a wider range of mixes.

ACKNOWLEDGEMENTS

I would like to acknowledge the following people for their support and assistance:

Table of Contents

List of Tables

List of Figures

x

List of Symbols, Nomenclature or Abbreviations

AAR	Alkali-aggregate reaction
ASR	Alkali-silica reaction
ACR	Alkali-carbonate reaction
AMBT	Accelerated mortar bar test
CPT	Concrete prism test
CCT	Concrete cylinder test
CSH	Calcium-silicate hydrate
ICP-MS	Inductively coupled plasma mass spectrometry
Na_2O_e	Equivalent sodium oxide content
RH	Relative humidity
SCM	Supplementary Cementing Material
UNBCCT	University of New Brunswick concrete cylinder test
UNBCCT-38°C	UNBCCT samples stored at 38°C
UNBCCT-60°C	UNBCCT samples stored at 60°C
w/cm	Water-to-cementitious-materials ratio

1. Introduction

1.1. Background Information

Alkali-silica reaction (ASR) is a problem that plagues many types of concrete infrastructure worldwide. A great example of this is the Mactaquac Dam located just outside of Fredericton, New Brunswick. The dam has grown in height by approximately twenty-three centimeters, and has had more than fifty centimeters removed horizontally (through slot cutting) over a period of forty years (Fletcher, 2016). This expansion has dramatically damaged the functionality of the dam and thusly cost the province and its taxpayers millions annually to mitigate the problem. In the 1960s, when the dam was constructed, the aggregates used were found to be non-reactive according to the standard test method of the time (ASTM C227) (Beaman, 2005). Unfortunately, this test method has shown, in later years, failure for the detection of the susceptibility of slowly-reactive aggregates. The dam began to show expansion within a decade of construction, due to the presence of a slowly reacting aggregate, and the expansion has continued up to this day.

Just like ASTM C227, other test methods can also give misleading information. The current test methods and programs used for the detection of ASR have many problems, such as the length of time for testing (some taking up to 10 years or more, such as the use of outdoor exposure blocks) and inconsistency between tests (i.e. some tests indicate that a certain aggregate is reactive, while others indicate otherwise). The goal of this research is to develop a new test method that can be conducted in a relatively short time frame, which yields consistent data, and uses project mix designs (meaning that the alkali level does not

need to be artificially increased, such as with ASTM C1293). With this new test method, the accurate prediction of expansion would be determined in a timely manner, and could save companies and governments in the future millions if not billions of dollars in mitigation, repairs, and replacement costs.

1.2. Problem Statement

Current standardized tests, developing tests, and other testing programs lack the ability to accurately predict the performance of a job mixture, and to do so in a sufficient amount of time. Job mixtures are real world mix designs composed of portland cement and/or supplementary cementitious materials (slag, silica fume, or fly ash), combined with a coarse and fine aggregate. The testing of job mixtures is of great importance due to ASR being a function of the reactivity of the aggregate, composition of the binder, and exposure conditions. The aggregate determines whether the reaction will indeed take place, where the composition of the binder determines the intensity of the reaction, and the exposure conditions determine the reaction rate. The ability to test unaltered mixes is of great importance due to it rendering superior and more useful results for field scenarios.

Under current standards, the alkalinity of mix designs are altered through boosting in the case of the concrete prism test (CPT), to account for leaching, or through submerging the specimen in a high-temperature, high-alkali environment, such as the accelerated mortar bar test (AMBT), thusly providing an essentially unlimited source of alkalis. In these cases, the results generated can either be understated (CPT) or exaggerated (AMBT) when compared to field data. The ideal test would be one where the movement of alkalis is

prevented and the relative humidity of the sample remains constant to promote the reaction. The University of New Brunswick concrete cylinder test (UNBCCT) attempts to achieve this through the creation of job mix specimens, and submerging the sample in a small quantity of host solution mimicking the alkali content of the pore solution.

1.3. Hypothesis

The submerging of a concrete specimen in a low-volume of host solution surrounding the sample and emulating the alkalinity of the specimen will provide adequate moisture to drive ASR in a manner that neither augments nor reduces the alkalinity of the sample significantly.

1.4. Goals and Objectives

The goal of this research was to develop a new, more rapid, and reliable test method for the detection of the potential for damaging expansion due to alkali-silica reaction. An aspect of this goal was to overcome the leaching of alkalis through submerging the samples in a host solution, mirroring the alkali level of the concretes' pore solution. The submerging of a sample in a host solution negates the need to artificially boost the alkali content to compensate for leaching. The prevention of leaching allows the operator to conduct the experiment with "Job Mixtures", meaning concrete that is found in a production plant can be tested unaltered. Another aspect of this goal was to reduce the amount of time by storing the sample at an elevated temperature. In theory, an elevated temperature accelerates the rate of expansion. This phenomenon was examined through storage at two temperatures, these being 38°C and 60°C. The ultimate goal of this research was the adoption of the test

method by regulators. This would allow its widespread use by institutions when conducting durability tests. The objectives set for this project are listed below:

- Develop a testing program that can be easily replicated for further study

- Cast samples with and without SCMs to examine their benefits and effects on the length of time to complete the test

- Evaluate the extent of leaching associated with the new test method

- Establish correlations between the test method and other standardized and newly developed test methods

1.5. Scope

The scope of this research pertains only to concrete using portland cement and supplementary cementitious materials (SCMs) as binders. The mix designs that were used have reactive aggregates paired with non-reactive aggregates. This is to ensure that the reaction taking place can be allotted to a specific aggregate. The mix designs used match the alkali content and reactive aggregate source for the exposure blocks at the University of Texas in Austin, the CANMET exposure site in Ottawa, Ontario, and an exposure site in Kingston, Ontario. A mix design was also tested that matched the alkali content of the Mactaquac Dam in Fredericton, New Brunswick, but used a surrogate aggregate of similar properties. Other mixes that were tested are those having no blended cements (plain portland cement mixes) and no boosted alkalis, as well as one mix design conducted with non-siliceous aggregate, to monitor the effect of the storage in host solution.

Concrete was cast in accordance with ASTM C1293, with the exception of the alkali content. The same concrete was used in the casting of 285 x 145 mm cylinders. These cylinders were split into two groups, such that half were stored at 38°C and the others at 60°C. These temperatures were chosen as they are commonly used in concrete testing for regular and accelerated methods. Each sample was stored in a sodium hydroxide solution matching the estimated alkali content of their respective pore-solution. The cylinders were stored in a sealed 6 x 12 in. (152 x 305 mm) concrete mould. They were only unsealed to measure length change and to top up with distilled water.

2. Literature Review

2.1. History

Alkali-silica reaction (ASR) is one of two forms of alkali-aggregate reaction (AAR), the other being alkali-carbonate reaction (ACR); ACR was not studied in this research program. ASR was first discovered in the early 1930s in California, U.S.A., by Thomas Stanton (1940) . Upon discovering a new type of expansion in a number of concrete structures, Stanton conducted a series of mortar-bar tests and concluded that expansion occurred when both a reactive siliceous aggregate was present in addition to alkalis in the cement, and that "the intensity of the reaction is related to the alkali content" within the system (Stanton, et al., 1942). Since its discovery, a valiant effort has been undertaken to understand, predict, and prevent ASR from occurring in future construction. Many laboratory test methods have been developed to investigate the potential reactivity of aggregates. However, the users of these tests are given a choice, either test using a rapid method that has poor correlation to field results, or test using more reliable methods that take a substantially longer time to generate results (Thomas, et al., 2013a).

2.2. Requirement for ASR

There are three constituents required to initiate and sustain ASR. These include moisture, a source of reactive silica, and sufficient alkalis. All three are required to initiate ASR, therefore if one is missing, the reaction will not occur. In order for ASR to become deleterious, the presence of available calcium is needed. The basic mechanism of ASR is that a gel forms around the perimeter of the aggregate, absorbs water, expands, and when

the expansive forces exceed the tensile strength of the concrete, cracking occurs. A more detailed look at the reaction mechanism will be discussed in Section 2.3.

2.2.1. Moisture

Unless constructed in an arid environment, it is generally assumed that all concrete structures at some point during their lifetime will be exposed to moisture. In order for the alkali-silica gel to expand and cause damage, it must be exposed to moisture whether it is from concrete structures exposed to bodies of water, or rain. Stark (1991) demonstrated the need for moisture, and found that no damaging expansion occurs where moisture is not available. Stark (1991) also found that a relative humidity in excess of 80% is required to initiate and sustain ASR.

2.2.2. Reactive Silica

Silica is provided through the aggregate (fine, coarse, or both) used in the concrete. However not all silica is reactive. What makes the aggregate reactive is its ability to be broken down in a concrete's high pH (typically between 13.2 and 14), that is provided within the concrete's pore solution. A list of reactive minerals and aggregates can be found in Table 2.1. Research has shown that the more rapidly reacting aggregates tend to be the ones with minerals of poor crystallinity (Broekmans, 2004). The shape, size, and mineralogy all affect the potential of the aggregates reactivity and will be discussed in more detail below.

Table 2.1: Deleteriously Reactive Rocks, Minerals and Synthetic Substances (ACI Committee 201, 1991)

Reactive substance (mineral)	Chemical composition	Physical character
Opal	$SiO_2 \cdot nH_2O$	Amorphous
Chalcedony	SiO_2	Microcrystalline to cryptocrystalline; commonly fibrous
Certain forms of quartz	SiO_2	Microcrystalline to cryptocrystalline; crystalline, but intensely fractured, strained, and/or inclusion-filled
Cristobalite	SiO_2	Crystalline
Tridymite	SiO_2	Crystalline
Rhyolitic, dacitic, latitic, or andesite glass or cryptocrystalline devitrification products	Siliceous with lesser proportions of Al_2O_3 , Fe_2O_3, alkaline earths and alkalis	Glass or cryptocrystalline material as the matrix of volcanic rocks or fragments in tuffs
Synthetic siliceous glass	Siliceous, with lesser proportions of alkalis, Al_2O_3, and/or other substances	Glass
Opaline cherts	Rhyolites and tuffs	Opaline concretions
Chalcedonic cherts	Dacites and tuffs	
Quartzose cherts	Andesites and tuffs	Fractured, strained, and limestone-filled quartz and quartzites
Siliceous limestones	Siliceous shales	
Siliceous dolomites	Phylites	

2.2.3. Alkalis

The alkalis that are required for ASR are provided from many sources, such as portland cement, supplementary cementing materials (SCMs), de-icing salts, aggregates and mix

water. The most abundant source is attributed to portland cement, which contains both

sodium and potassium. During the hydration process of cement in concrete, sodium and

potassium are released into the pore solution from alkali sulfates and clinker minerals, as

shown in Figure 2.1 (Brouwers & van Eijk, 2003). In cases where non-reactive aggregates

are used, the bulk of the alkalis end up in the pore solution balanced by hydroxyl ions. A

portion of the alkalis may be bound by the C-S-H hydrates. This binding increases with the

presence of SCM's and even more so when the SCM's are high in silica and low in calcium.

If reactive aggregates are present in concrete, the alkalis from the pore solution will react

with silica found in the aggregate and form alkali silica-gel, as well as bond to calcium

silicate hydrate (C-S-H). In the presence of calcium hydroxide, alkalis in the gel can be

replaced by calcium and react again with silica to form more gel (see Figure 2.1) through

the phenomenon known as 'alkali recycling' (Thomas et al., 2013a).

Figure 2.1: Fate of Alkalis in Concrete (Thomas, 2016a)

9

The fate of alkalis is critical to the potential for ASR, where the more alkalis available at the onset of the reaction, the greater the potential for the reaction to occur. This can be combated through the usage of SCMs such as fly ash and slag, which sequester alkalis from the pore solution, thus lessening the potential for gel to form.

A performance test for "job mixtures" in an ideal world would account for the impact of alkalis on the potential for ASR. These alkalis are contributed by the cementitious materials, where the alkalinity of the material is represented by the equivalent amounts of sodium oxide. The equivalent alkali content is determined using Equation 1 through the summation of sodium and potassium oxides.

$$Na_2O_e = Na_2O + 0.685 \times K_2O \quad \textbf{[1]}$$

The dissolution of aggregate is attributed to the pH of the pore solution as presented in Figure 2.2. It can be seen that at a pH of between 13.2 and 14, which is lower than that typically found in the concrete's pore solution, the dissolution of amorphous silica is much higher than at a lower pH.
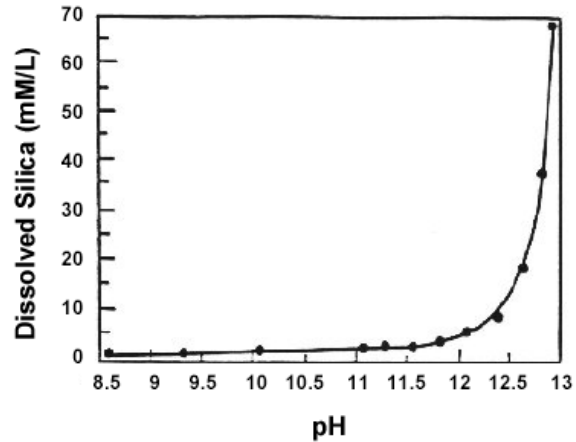
Figure 2.2: Dissolution of Amorphous Silica (Tang & Su-fen, 1980)

2.2.4. Calcium

Calcium, more specifically calcium hydroxide, is seen as the fourth constituent needed for ASR. Theories surrounding calcium's involvement have been around since 1944, and range from calcium replacing the alkalis in the gel (Hansen, 1944), to its role in the development of semi-permeable membranes around reactive aggregates, thus allowing expansion to occur (Bleszynski & Thomas, 1998). It is still unclear what its function is exactly, but a common theory is that of "alkali recycling" (Thomas, 2001).

Alkali recycling concerns the replacement of alkalis in the already-formed gel, with calcium from surrounding calcium hydroxide in the cement matrix. This chemical reaction is presented in Equation 2, developed by Hansen (1944), where the products of the reaction are that of a calcium silicate and alkali hydroxide. Hansen was the first to postulate this reaction due to the presence of two forms of gel. The first being clear (an alkali silicate) and the second white and opaque (a calcium silicate). He also found that the reaction

11

"would tend to convert the alkali-silicate solutions to calcium silicates, and regenerate the alkali hydroxide for further reaction with silica". Meaning that the alkalis are able to be reintroduced back into the pore solution and are available to react with silica again. With the presence of alkali recycling, ASR will therefore continue to occur until either all reactive alkalis or calcium hydroxide has been consumed (Thomas, 2001).

$$Na_2SiO_3 + Ca(OH)_2 \rightarrow Ca_2SiO_3 + 2NaOH \quad [2]$$
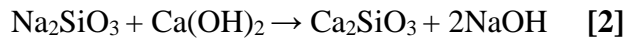
The effect of calcium on the properties of the gel have been well defined by Urhan (1987) and can be seen in Figure 2.3. Urhan showed that there are multiple phases of gel depending on the level of calcium, the first of them being with low calcium and high alkalis. This gel was found to have a low viscosity and high absorption, as well as be prone to swelling/shrinkage. Over time, the alkalis are replaced by calcium, raising the viscosity, lowering absorbency and proneness to shrinking/swelling. Once the alkalis in the gel are completely replaced by calcium, the physical properties of the gel tend towards those of CSH.
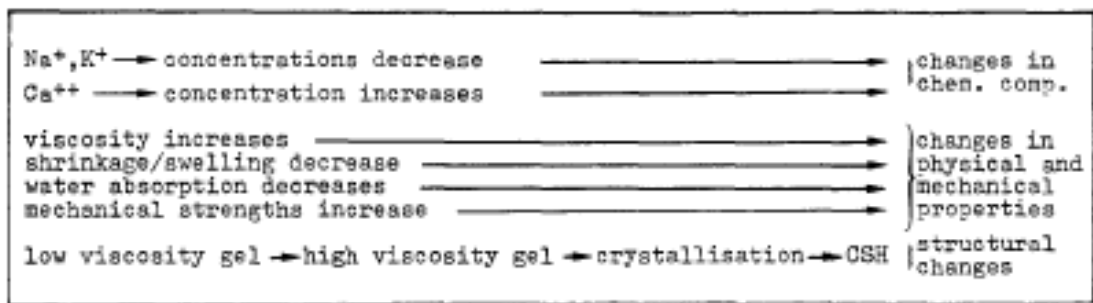
Figure 2.3: Changes in ASR gel with the increase of calcium (Urhan, 1987)

2.3. Mechanisms of ASR

There are three theories that are widely accepted as the mechanism in which ASR causes expansion. These mechanisms are osmosis, imbibition, and a combination of the two. These mechanisms start in the same manner and only differ for the method in which the expansion occurs.

ASR is initiated once the tetrahedral structure of the silica in the aggregate is attacked by hydroxyl ions found in the pore solution. The silica tetrahedra's found on the surface are naturally incomplete, and thus have a charged surface as presented in Figure 2.4A (Powers & Steinour, 1955);(Thomas, 2016a). This leads to water molecules breaking up into hydrogen and hydroxyl ions to balance the charged surface. Once this occurs, hydrogen ions are drawn back into the pore solution to lower the pH, due to a high presence of disassociated alkali hydroxides. Hydrogen ions then bond with the hydroxyl ions to form water, and the alkalis bond with the silica to balance the system as seen in Figure 2.4B (Powers & Steinour, 1955). This reaction is presented in Equation 3, where sodium is used to represent alkalis in general.

$$Si\text{-}OH + OH^- + Na^+ \rightarrow Si\text{-}O\text{-}Na + H_2O \qquad \textbf{[3]}$$
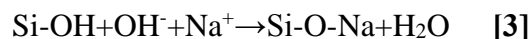
Once the reaction has taken place, any residual alkalis will propagate deeper into the crystal structure, as presented in Figure 2.4C, and start attacking the siloxane (Si-O-Si) bonds (Powers & Steinour, 1955). The hydroxyl ions first attack the structure by bonding with the silica and liberating oxygen ions. The hydroxyl ions then lose their hydrogen ions, and water is formed with the now free oxygen and hydrogen ions, which can be seen in Figure

13

2.4D (Powers & Steinour, 1955). The sodium ions then bond with the oxygen attached to the silica structure, thusly completing the reaction. Equation 4 shows the reaction stated above.

$$\text{Si-OH} + 2\text{OH}^- + 2\text{Na}^+ \rightarrow 2(\text{Si-O-Na}) + \text{H}_2\text{O} \qquad \textbf{[4]}$$
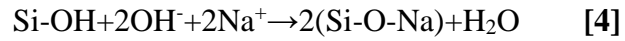
It should be noted that, as stated above, the more unorganized the crystal structure, the more reactive the aggregate is. This is due to the alkali hydroxides being able to penetrate easier into the structure.
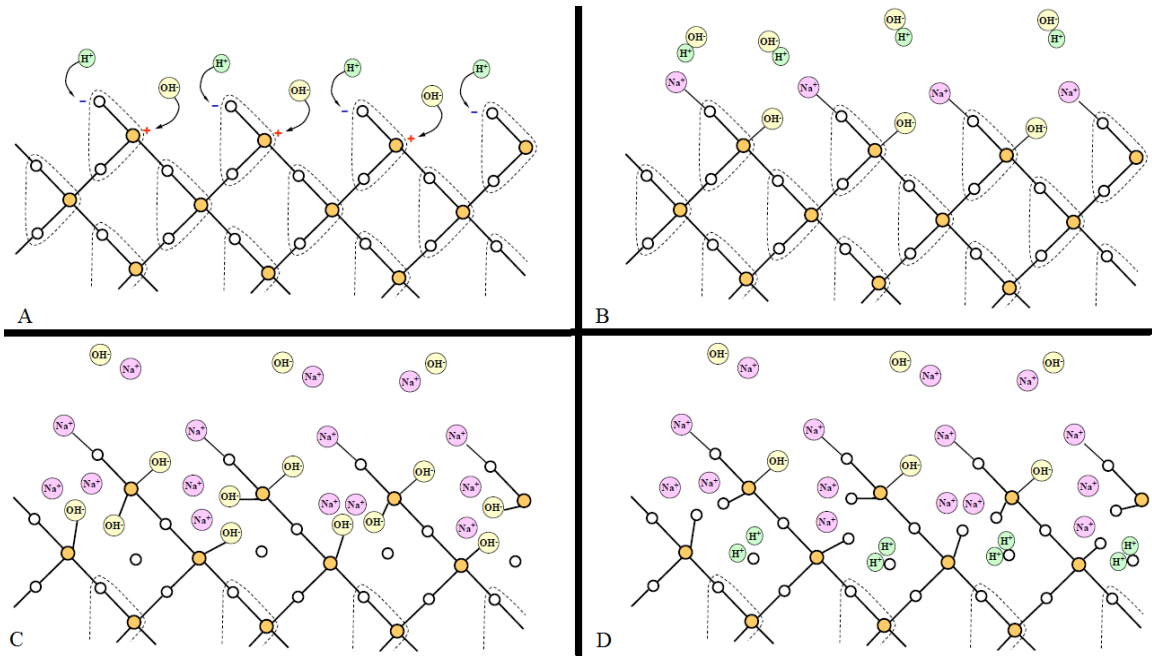
Figure 2.4: The chemical steps for alkalis attacking silica (Thomas, 2016a)

2.3.1. Osmosis Mechanism

In 1944, Hansen proposed that ASR was a result of osmosis. He stated that the hardened cement-paste acts as a semipermeable membrane that does not allow the larger complex silicate ions to move away from the aggregate and into the pore solution, but still allows water and alkali hydroxides to diffuse in. Water is drawn in by the reactions shown above, which then causes hydrostatic pressure to build between the gel formed around the aggregate and the cement paste. Pressure also builds between the aggregate and cement paste due to the production of alkali-silicates. The silicates are larger in size than the silica of the original aggregate, leading to them to exert pressure due to confinement. The cement-paste holds back these pressures until it fails in tension, leading to the expansion of the concrete (Hansen, 1944).

2.3.2. Imbibition Mechanism

Not long after Hansen proposed his theory, McGowan and Vivian (1952) presented the theory of imbibition. They argued that once the cement paste membrane had cracked, the pressure would be released and no further expansion would occur. The manner in which they theorized expansion occurred was through water being absorbed by the alkali-silica gel, leading to its expansion.

2.3.3. Combined Mechanism

In 1955, Powers and Steinour developed the notion that expansion was not solely caused by imbibition or osmosis, but a combination of the two. They found that the osmotic

pressure and imbibition mechanisms were fundamentally alike, and could occur simultaneously (Powers & Steinour, 1955).

The mechanism upon which Powers and Steinour theorized caused the swelling relies on the rigidity and viscosity of the alkali silica gel. If the gel is in a fluid phase and confined, then hydraulic pressure will build as described by Hansen (1944). However, if the gel is solid it will imbibe water and swell as described by McGowan and Vivian (1952), even when unconfined. Finally if the gel is solid yet still plastic, it can swell as well as have hydrostatic pressure develop (Powers & Steinour, 1955).

2.4. Factors Affecting ASR Expansion Rate

The rate at which ASR affects concrete is dependent on a multitude of aspects, from the concrete itself to its exposure conditions. This section examines a number of these factors including the characteristics of the aggregate, type or types of cementitious materials, properties of the mix design, and the exposure conditions of the concrete.

2.4.1. Aggregate

As previously mentioned, the size, shape, and mineralogy all play a role in the level of reactivity for a given aggregate. Aggregates of a similar physical appearance can have drastically different levels of reaction, therefore it is important to first understand its mineralogy, and then proceed to examine its physical properties.

The mineralogy of an aggregate is typically determined through petrographic characterization. The minerals found in the aggregate can then be compared to a list of

known reactive and non-reactive aggregates. Reactive aggregates have minerals that are amorphous or poorly crystalline, where nonreactive aggregates have a crystalline mineralogy (Thomas et al., 2013a) . Once the aggregates have been classified, their reactivity still cannot be categorized due to difference in geological history, which necessitates further testing. An example stated by Lindgard et al. (2012), was that quartz (when crystalline) is known to be nonreactive, however if the quartz has been deformed by temperature, pressure, or both, and its crystalline structure altered it can become highly reactive.

The primary physical properties of aggregates that affect its reactivity are size and angularity. Fine aggregates (less than 4.75mm in diameter) tend to be more rapidly reactive than coarse aggregates (greater than 4.75mm). This is due to the fine aggregates having more surface area to react with alkalis. However, if the aggregates are crushed very fine (below approximately 250 microns), the resulting expansion will be less than that of coarse aggregates. This phenomenon is known as the pessimum effect, and is attributed to the aggregate reacting during the curing process, as well as being more uniformly distributed in the sample (Thomas et al., 2013a). Another characteristic of the aggregate that can affect the reaction is its angularity. The more angular the aggregate, the more surface area it has, and the more it can react (Ramyar et al., 2005).

2.4.2. Binder Composition

The composition and type of binder plays an important role in ASR. Certain binders aid in the initiation of the reaction through providing sufficient alkalis (mostly high-alkali

cements), while others aid in the prevention, primarily through binding the alkalis before the silica can react (certain SCMs). Therefore, it is important to understand what promotes and hinders the reaction.

Cements, more specifically portland cements, are predominant contributors to alkalis in the pore solution system. The higher the content of equivalent sodium oxide (Na_2O_e), the more likely the concrete will see increasingly damaging expansion. Figure 2.5 presents the relationship between a certain type of aggregate and various levels of alkalis at a cement content of 400 kg/m³ (Sibbick & Page, 1992). It is noticeable that as the alkali content increases from 3.0 kg/m^3 to 7.0 kg/m^3 Na_2O_e, the strain levels within the concrete become substantially larger.

Figure 2.5 also demonstrates the phenomenon of alkali thresholds. The alkali threshold is the required amount of alkalis to initiate damaging expansion (Thomas et al., 2006). It can be seen that an alkali content of 3.0 kg/m^3 does not produce a high level of expansion, however, 3.5 kg/m^3 does. This means that the alkali threshold for this aggregate and cement combination is between the two values.
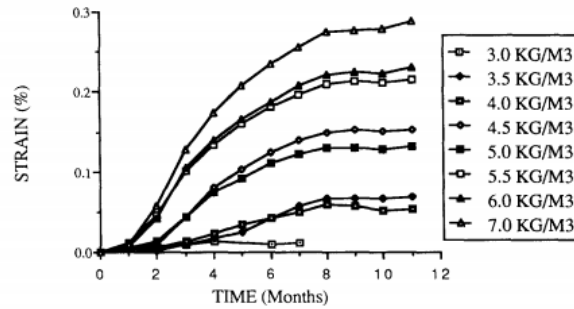
Figure 2.5: Strain vs. Time of a British aggregate as a factor of alkalis contents in kg/m^3 (1 kg/m^3=0.25% $Na_2O_{e)}$ (Sibbick & Page, 1992)

Supplementary cementitious materials (SCMs) have a different effect on ASR, and they are often used to mitigate the reaction. SCMs such as fly ash, ground granulated blast furnace slag, and silica fume are all used to partially replace the level of portland cement in concrete mixtures. The use of SCMs is an environmentally friendly alternative to ordinary portland cement, as they are natural by-products from industry. The presence of SCMs not only reduces the effect of ASR, but helps improve the durability performance of the concrete when exposed to various environments. These other durability issues are, however, outside the scope of this research.

SCMs mitigate ASR by lowering the alkali content of the pore solution during the hydration of the concrete. As concrete hydrates, alkalis are bound in the hydration products formed by SCMs (Lindgård et al., 2012). The sequestering of alkalis lowers the equivalent sodium oxide content of the pore solution, and, in cases where enough SCMs are used, prevents damaging expansion from occurring. This phenomena is presented in Figure 2.6

where the pore solution of concrete at various portland cement replacement levels all show

a decrease in the alkali hydroxyl ion concentration over time.
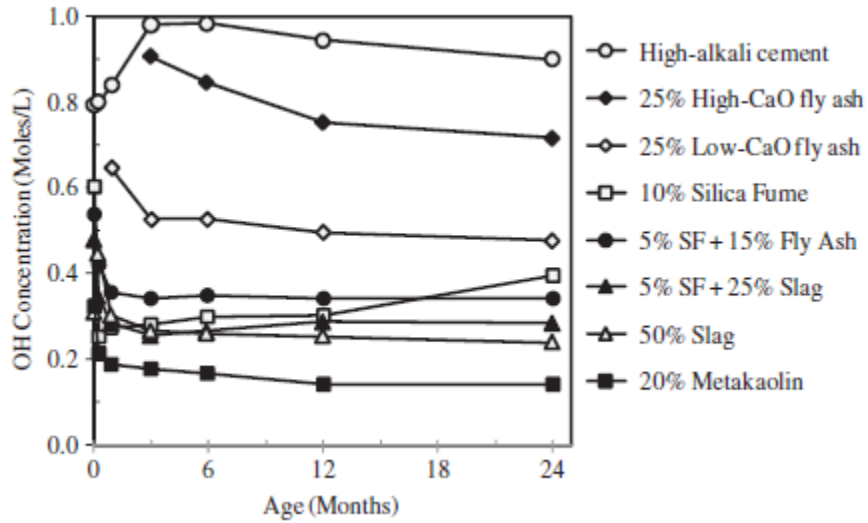
Figure 2.6: The effects of SCMs on pore solution over time (Thomas et al., 2017)

The effects of increasing the replacement levels of SCMs on pore solution hydroxyl ion

concentrations can be seen in Figure 2.7. As expected, the increase in replacement yields a

decrease in hydroxyl ions, which leads to a system where less expansion occurs, as

demonstrated by Figure 2.8.
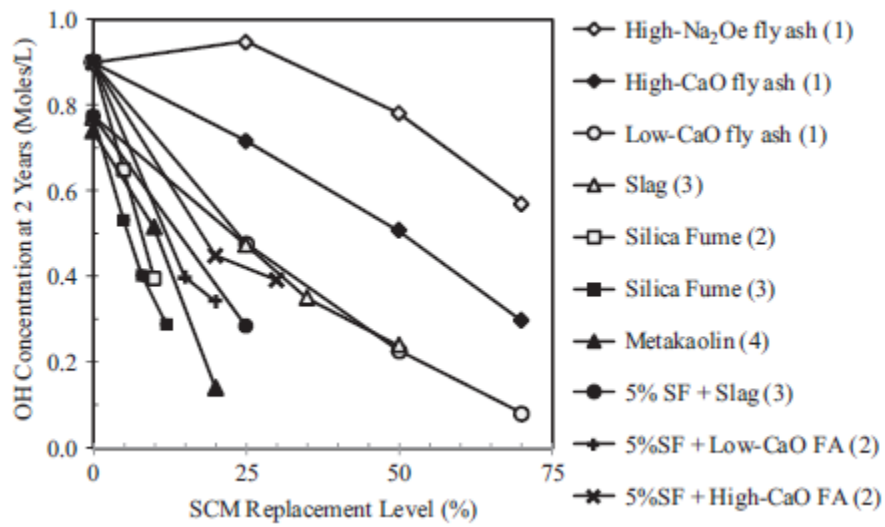
Figure 2.7: The effects of increase portland cement replacement levels with various SCMs (Thomas et al., 2017)
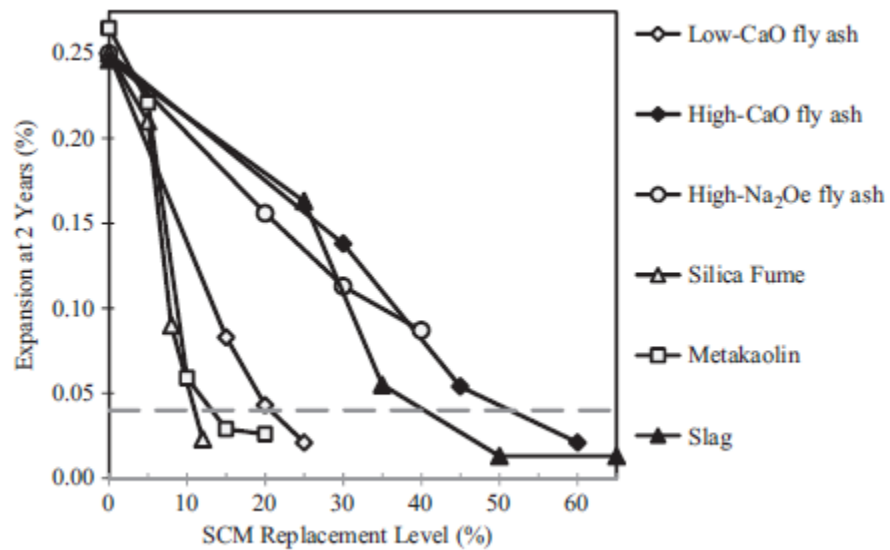
Figure 2.8: Effects of increasing SCMs on expansion (Thomas et al., 2017)

21

It should be noted that in some instances, SCMs such as silica fume and pozzolans can agglomerate together. These agglomerated particles can act like reactive siliceous coarse aggregates resulting in ASR (Thomas et al., 2013a).

2.4.3. Mixture properties

The various mixture components and proportions required to generate a concrete mixture greatly affect the level of reactivity. The alkali content within the hydrated concrete is affected by a number of factors including the water-to-cementitious-material ratio (w/cm), amount and type of binder, the chemical composition of the binder, and the presence of additives such as chemical admixtures. Changes in these factors can increase or decrease the susceptibility of the concrete to ASR. Therefore, knowing how each factor influences the pore solution is of upmost importance.

The water-to-cementitious-material ratio affects the alkali concentration in the pore solution. Decreasing the w/cm will cause the hydroxide ions to become more concentrated than that of a high w/cm. This higher hydroxide concentration causes the pore solution's pH to increase, which triggers a more rapid degradation of the silica, leading to alkalis being able to penetrate deeper in the aggregate structure, and generating more alkali-silica gel.

On the other hand, decreasing the w/cm can have beneficial effects such as densifying the paste structure of the concrete; making it less permeable to the ingress of water and other molecules and compounds. After the initial hydration process has finished, additional

moisture is required to continue the alkali-silica reaction. This additional moisture will have difficulty penetrating the dense matrix, leading to the lowering of the relative internal humidity of the concrete. If the RH drops below 80% Lingard et al. (2012) has shown that damaging expansion is very unlikely to occur.

The overall impact of w/cm ratio is very little when in comparison to the amount of alkalis and alkali content of cement. Figure 2.9 was generated with a variety of w/cm (ranging between 0.38 and 0.64), cement contents, and alkali contents. It can be seen that the biggest influence on expansion was the alkali content of the cement.
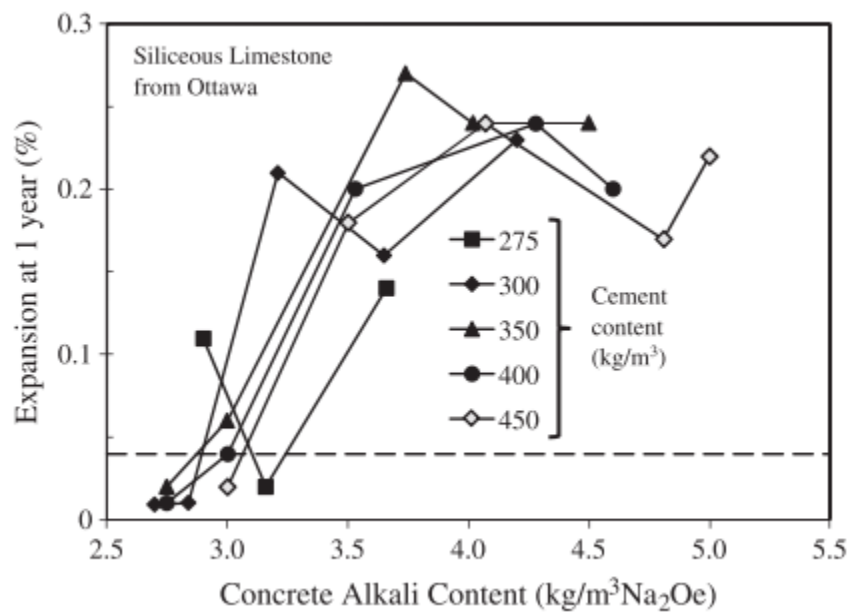
Figure 2.9: Expansion of concrete prisms as a function of alkali content (produced from unpublished data from the Building Research Establishment, U.K.) (Lindgård et al., 2012)

23

The binders used in the concrete as discussed above, can either promote or hinder ASR. However, the quantity, and combinations dictate whether or not damaging expansion will occur. In order for SCM's to be effective they have to be used at a sufficiently high replacement level. The minimum level required will depend on the type and composition of the SCM, the reactivity of the aggregate, the alkalis available for the portland cement and the concrete's exposure conditions. CSA A23.2-27A is a standard practice that takes these factors into account in determining a prescribed minimum level of SCM. Currently there is not a reliable test method to permit an accurate determination of the minimum level of SCM by testing.

The presence of chemical admixtures do not contribute to ASR, unless they contain a substantial quantity of alkali such as sodium, potassium, or lithium. Sodium and potassium, as denoted above, are part of the four constituents that contribute to the reaction; meaning that their addition to a concrete mixture will increase the likelihood of damaging expansion. The cases where sodium and potassium are added to concrete are for boosting the alkali concentrations to combat the effects of leaching during the testing procedure, such as in ASTM C1293. Alkalis are typically added in the form of NaOH solution, however KOH has been used as well (Xu et al., 2002)

Lithium on the other hand is used as a preventative measure for ASR. Lithium is added in the form of a salt. The most commonly thought mechanism for the manner in which lithium prevents damaging expansion is through an alkali-silica reaction similar to that of sodium and potassium. Instead of the product absorbing water, the insoluble lithium silicate creates

a barrier around the aggregate preventing further attack from sodium and potassium (Thomas et al., 2013a). A summary of lithium used in new concrete conducted by Feng et al. (2005) shows that lithium can be effective when used in the appropriate amount in new concrete.

2.4.4. Exposure Conditions

Temperature and humidity also play an important role in alkali-silica reaction. Gautam and Panesar (2017) found that prisms cast with the same aggregate and cured at 50°C expand at a rate of approximately 1.7 times more rapidly than prisms cured at 38°C. This is demonstrated in Figure 2.10, where the ACPT was conducted at 50°C. It should be noted that the ACPT reached its ultimate expansion at an early age, however, the expansion it reached was lower than that of the ultimate expansion of the 38°C samples. The reduction in expansion was minimal in comparison to samples stored at more elevated temperatures, such as at 60°C. Figure 2.11 shows the difference in results for two types of aggregate stored at 38°C and 60°C. For both aggregate types, the ultimate expansion happened much sooner at the higher temperature, but was significantly lower.
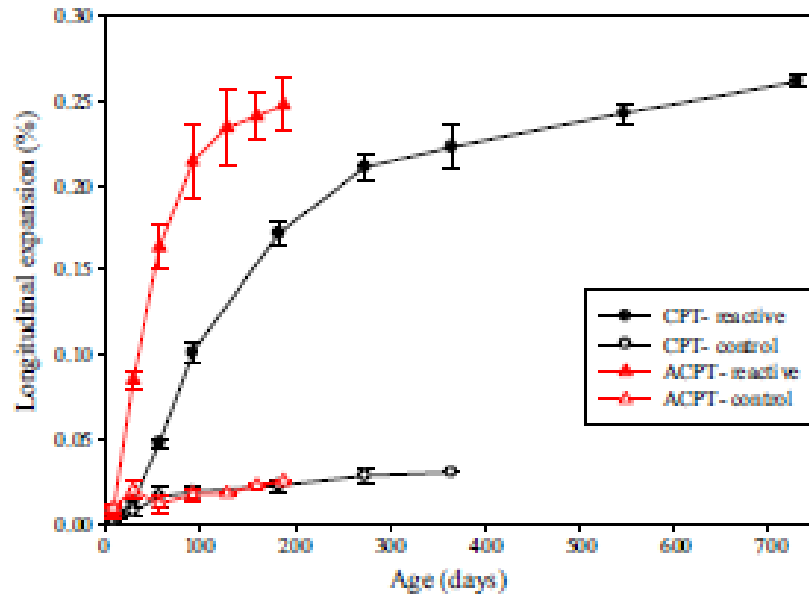
Figure 2.10: Expansion of samples at 38°C and 50°C temperatures (Gautam & Panesar, 2017)
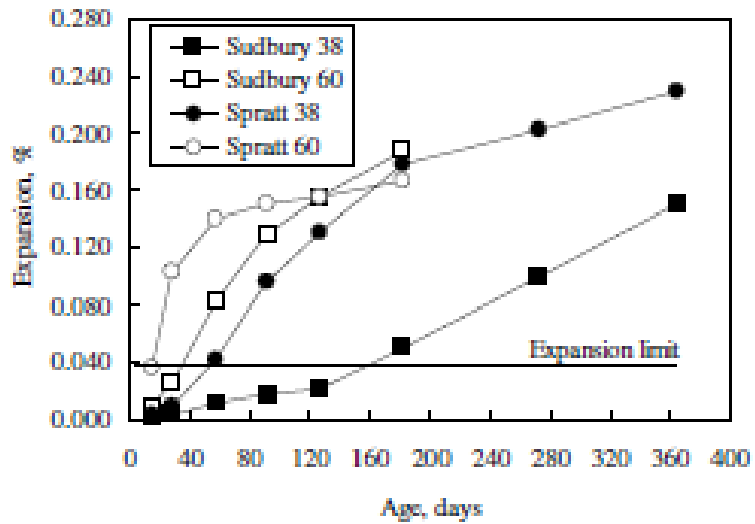
Figure 2.11: Expansion of samples at 38°C and 60°C temperatures (Fournier et al., 2004)

The reasoning for the variation in expansion of samples stored at different temperatures is a result of two issues, the increase of leaching of alkalis and the increase in sulfate content found in the pore solution (Fournier et al., 2004). The increase in leaching occurs due to the ponded water evaporating and condensing on the sample at a higher rate, thusly removing alkalis from the sample's surface. This causes more alkalis to migrate to the surface from the interior of the sample. The increase in sulfates is caused by the solubility of ettringite increasing with respect to an increase temperature. The relationship between temperature and sulfate content in pore solution can be seen in Figure 2.12. In both cases, the pH of the sample is lowered, resulting in a lower rate of silica dissolution, which leads to decreased rate of expansion (Fournier et al., 2004).
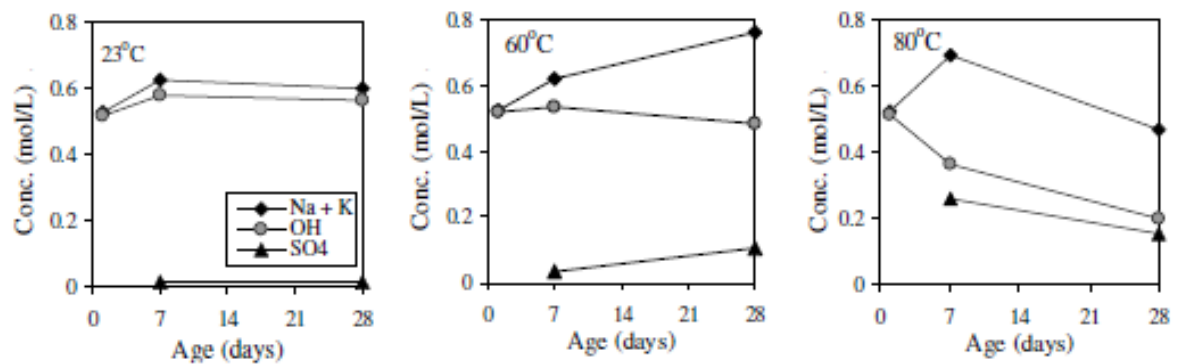
Figure 2.12: Relationship between sulfates in pore solution and temperature (Shehata – Ryerson University and Thomas – University of New Brunswick, unpublished data)

An increase in temperature can also lead to false data by means of other expansion methods, such as delayed ettringite formation, or reacting with aggregates that would not normally react at lower temperatures. Delayed ettringite formation (DEF) occurs when concrete is

27

cured at high temperatures (70°C and above) (Diamond, 1996). This elevated temperature destroys normally forming ettringite, causing it to dissolve and its constituents (particularly sulfate) to be encapsulated in calcium-silicate-hydrate (CSH). Once the concrete temperature is reduced, sulfates and alumina are slowly released, resulting in the formation of additional ettringite in fine pores (Thomas, 2016b). This delayed formation of ettringite causes expansion, which can be mistaken for ASR, if not properly investigated.

As temperature increases, so does the solubility of silica (Fournier & Rowe, 1977). Figure 2.13 shows that the solubility for both amorphous silica and quartz (crystalline silica) increases with increasing temperature. With more silica in the system, a greater degree of alkali-silica reaction can occur, resulting in misleading information for the aggregate's expansion levels.
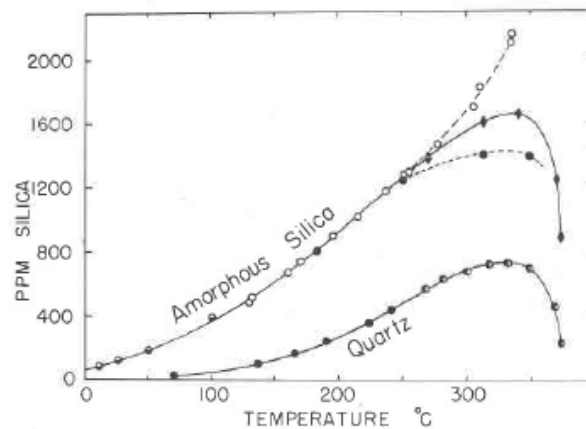
Figure 2.13: Solubility of silica in water with respect to temperature (R. O. Fournier & Rowe, 1977)

Humidity also plays and important role, due to moisture being one of the four main components required to initiate ASR. In laboratory testing, samples are often kept at an RH of 95% or greater, to ensure adequate moisture is provided. Figure 2.14 demonstrates that a small change in RH can have drastic effects on the outcome of expansion.
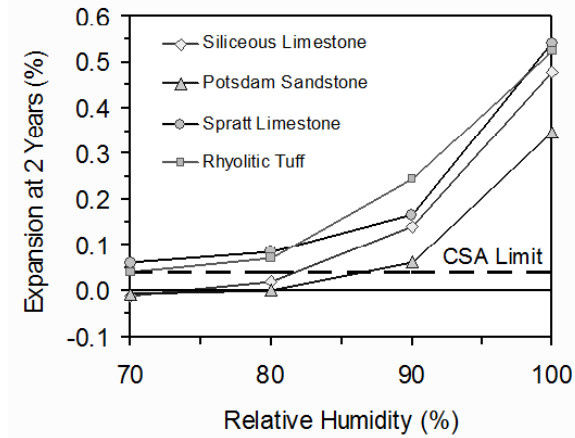
Figure 2.14: Effects of humidity on expansion after two years (Pedneault, 1996)

In field work, the abundance of moisture varies depending on the exposure conditions. This variation can lead to concrete members suffering damage in sections prone to moisture, and little damage in other dryer sections, as shown in Figure 2.15 (Thomas et al., 2013a).

29

Figure 2.15: Damage difference of concrete exposed to and sheltered from moisture (Thomas, 2016a)

2.5. Pore Solution

During the first day of hydration, the concrete's pore solution is primarily comprised of alkali sulfates. However, as the concrete ages, sulfate-bearing phases such as calcium mono-sulfo-aluminate (ettringite) form, resulting in an equivalent amount of hydroxide ions being released. The hydroxide ions are then combined with alkalis found in the pore solution to ensure charges are balanced. The level of equivalent alkalis that can be approximately found in pore solution is 0.7 mol/L per 1% equivalent alkalis in the cement, as shown in Figure 2.16 by work conducted by Diamond and Penko (1992).
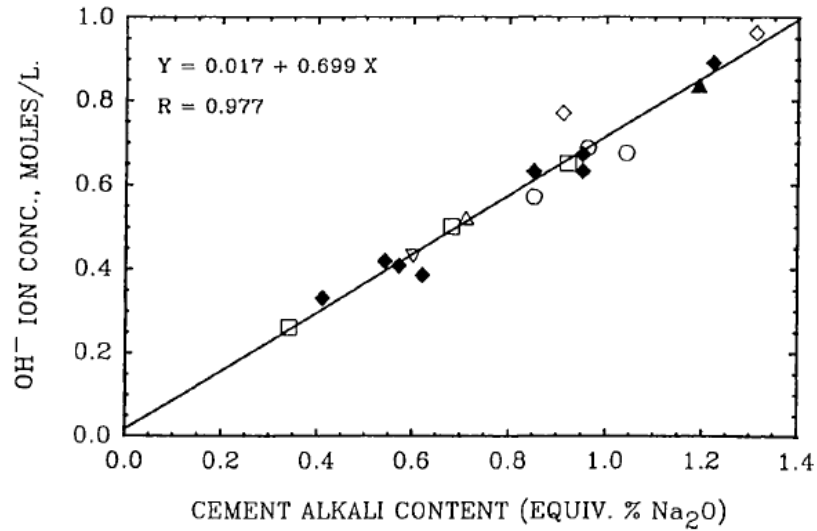
Figure 2.16: Relationship between alkalis found in cement and pore solution (Diamond & Penko, 1992)

2.6. Leaching

Leaching is the process by which alkalis from the interior of the concrete migrate to the surface. This can occur in the field or laboratory through wetting and drying cycles. Blanks and Meissner (1946) were the first to discover leaching in a laboratory setting, where they were testing mortar bars suspended over water in a sealed environment. They noticed the samples had agglomerates of moisture rolling down their sides and decided to test the reservoir. What they found was an increased presence of alkalis and other compounds originating from the sample.

The same mechanism for leaching found in the mortar bar test, also occurs in the CPT. Figure 2.17 and Figure 2.18 show the effects of leaching during the course of ASTM

31

C1293, where the white staining on the sample in Figure 2.17 depicts leached alkalis, and

Figure 2.18 shows the change of the alkali concentration over time.

Figure 2.17: CPT leaching alkalis
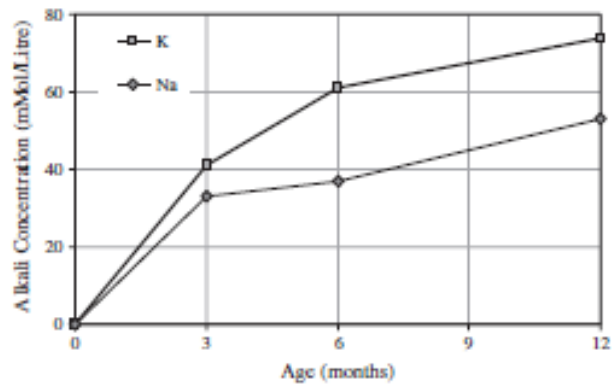
Figure 2.18: Concertation of sodium and potassium found is reservoir for CPT (Thomas et al., 2006)

The leaching of alkalis is less predominant in field samples then in the lab. This is a result

of a number of factors, such as the size of the sample being tested, and the relative humidity

(RH) to which it is exposed. The larger the sample, the further the alkalis have to migrate to the surface in order to be washed away. The higher the humidity the samples encounter, the more moisture there is to wash the alkalis away. This is why laboratory samples made in accordance with ASTM C1293 seem to require more alkalis to cause damaging expansion compared to blocks in the field of similar mixtures (Thomas et al., 2006).

2.7. Standard Test Methods

There currently exists a number of laboratory and field test methods used to evaluate aggregate reactivity. They can be broken down into two categories, those using mortar and those using concrete. The differences between these two categories mainly pertain to the size of the aggregate and testing conditions. For mortars, the aggregate used is a sand or coarse aggregate that has been crushed to a nominal diameter of 4.5 mm or less. The aggregates used in concrete are a combination of sand and coarse aggregate, where the coarse aggregate typically ranges in size between 4.5 mm and 20 mm.

2.7.1. Mortar Tests

ASTM C227: Standard Test Method for Potential Alkali Reactivity of Cement-Aggregate Combinations (Mortar Bar Method) was standardized as an aggregate reactivity test as a result of some of the first work on ASR by Thomas Stanton in 1940. The test requires the casting and curing of prisms (25.4 mm in cross section x 250 mm in gauge length). The test procedure starts with mortar bars being cured for one day in the moulds at laboratory temperature at a high RH (above 80%). The moulds are then striped at one day and the initial length of the samples are recorded. The mortar bars are then suspended over water

in a sealed container stored at 38°C for 12 days, after which the container is placed at lab temperature for 16hrs. The 14 days length change is then recorded and the samples once again stored in a sealed container suspended over water at 38°C. Subsequent measurements are taken periodically over the next year. Unfortunately, this test method has many drawbacks, such as leaching of alkalis and the inability to positively identify known reactive aggregates, especially slow reactive aggregates.

The cement's alkali content leads to the majority of the problems encountered in this test, such as leaching, and in some cases, insufficient amounts of alkalis to initiate the reaction. The only requirement specified by ASTM C227 for the cement's alkali content is that if multiple cements are to be used for a job, then the cement with an alkali content above 0.60% Na_2O_e should be tested. This limit is due to the findings of Stanton (1940) where he found that cements of an Na_2O_e below 0.60% show negligible expansion. The flexibility in the equivalent alkali content allows for an inconsistent rate of reaction to be seen by samples, leading to various degrees of reactivity for the same aggregate. This test method was criticized for a number of reasons, which resulted in the development of a number of other laboratory test methods, such as the accelerated mortar bar test (AMBT).

The AMBT was developed by Oberholster and Davies in 1986 (Oberholster & Davies, 1986), and was later modified and standardized in 1994 by ASTM and CSA (ASTM C1260/C1567 and CSA A23.2-25A, respectively). The test is comprised of casting mortar samples and curing them in a humid environment. They are then stripped at one day and immersed in a water-filled container at laboratory temperature. The container is then

transferred to an oven at 80°C for 24 hours. At an age of 2 days the mortar bars are removed from the water, measured to determine the length and then transferred to a container filled with 1 M NaOH at 80°C, which is placed in an oven at 80°C. The length change of the mortar bars is measured periodically for at least 14 days and the 14 day expansion is reported (the mortar bars are 16 days old at this time). The major drawback of this test is the harsh exposure conditions and the inability to detect the effect of cement alkalinity on susceptibility to ASR. Due to the specimens being stored in a NaOH solution, there is virtually an inexhaustible source of alkalis. This leads to an exaggerated level of expansion; meaning the reliability of the test is in question.

The obtained results can, in some cases, lead the tester to believe that an aggregate may cause harmful expansion, but in the field the opposite may be observed. Due to this major flaw, this test is mostly used to determine if an aggregate should be accepted, but not rejected. Further testing is often needed to reject aggregates.

2.7.2. Concrete Tests

Testing for aggregate reactivity using concrete specimens can be achieved using both laboratory and field specimens. In the laboratory, the reactivity of aggregate in concrete specimens is tested in accordance to the concrete prism test (CPT), which is standardized (ASTM C1293 and CSA A23.2-14A). Field exposure blocks are not a test method, but a technique to determine the reactivity over time when exposed to a natural environment.

The motivation behind the development of the CPT came after results generated from ASTM C227 showed discrepancies between laboratory and field tests. The CPT is performed by casting prisms (75 mm x 75 mm x 250 mm gauge length). The mix design used is composed of a well-graded coarse aggregate, fine sand, w/cm of 0.42, and cement content of 420 kg/m^3. The alkalis of the cement are boosted to 1.25% Na$_2$O$_e$ with the addition of sodium hydroxide to the mixing water. The samples are demoulded after 24 hours, then measured and stored over water in a sealed container at 38°C. Length-change measurements are taken periodically over the course of a year to determine the potential reactivity of aggregates. Mixtures containing SCMs (and chemical admixtures used to prevent ASR) are measured for two years to determine the efficiency of preventative measures for controlling expansion.

Similar to other test methods, the CPT has issues associated with it as well. Although results have been shown to be more reliable than the test methods previously introduced. Figure 2.19 presents a comparison between the AMBT and CPT. It is evident that there is great disagreement between the two, with the CPT being much more conservative. It is generally considered (Thomas et al., 2006) that the concrete prism testis more reliable than the AMBT to determine aggregate reactivity as the results from the test correlate well with field performance.
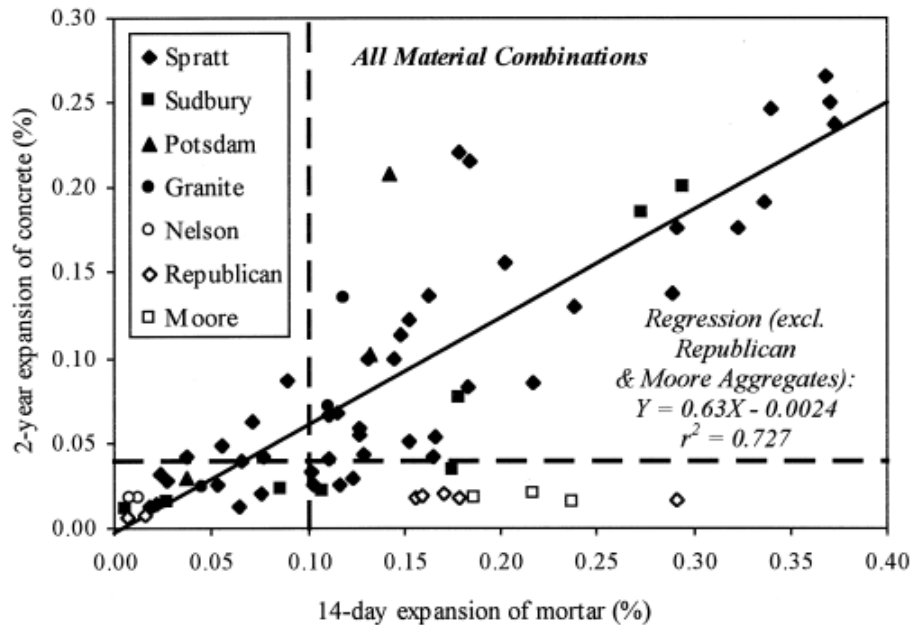
Figure 2.19: Expansion compassion between CPT and AMBT (Thomas & Innis, 1999)

One of the major flaws of the CPT is the leaching of alkalis, and the manner in which it attempts to compensate for it (alkali boosting). Thomas et al. (2006) showed that for a specific set of samples, over a year approximately 35% of the alkalis leached into the reservoir, with 20% in only 90 days. To compensate for the drastic amount of leaching, standards call for the alkali content to be boosted to 1.25% Na_2O_e. This leaching in turn also renders the CPT unsuitable for job mixture testing, as job mixtures would not likely have alkali boosting.

Concrete exposure blocks are used mainly as a tool for validating (or calibrating) laboratory test methods. Blocks range in size and shape, as there is no standard for their manufacturing. Examples of exposure blocks can be seen in Figure 2.20. The main purpose

of exposure blocks is to replicate how a potential job mix design will perform over time, and to use these results in comparison with other test methods.

Figure 2.20: BRE exposure blocks (Thomas et al., 2006)

It should be noted that there are other test methods that are used for the reactivity of aggregates, such as petrographic testing and the chemical method (ASTM C856 and ASTM C289, respectively). However, these tests will not be discussed as they are outside the scope of this research.

2.8. Comparison of Standard Test Methods

Each of the existing test methods stated above is not without its flaws. These flaws include the time to complete the experiment, poor correlation with field performance, leaching of alkalis, and the inability to test job mix designs. A general observation that has been made in the literature is that the larger the sample, the less impact leaching has, but the longer it takes for the sample to reach its ultimate expansion. This is shown in both Figure 2.21 and Figure 2.22, where there is a noticeable difference between field exposure blocks (and slabs

38

in the cases of Figure 2.21) and the expansion seen by the CPT. It is evident that leaching

has a profound effect on the expansion seen with the CPT.
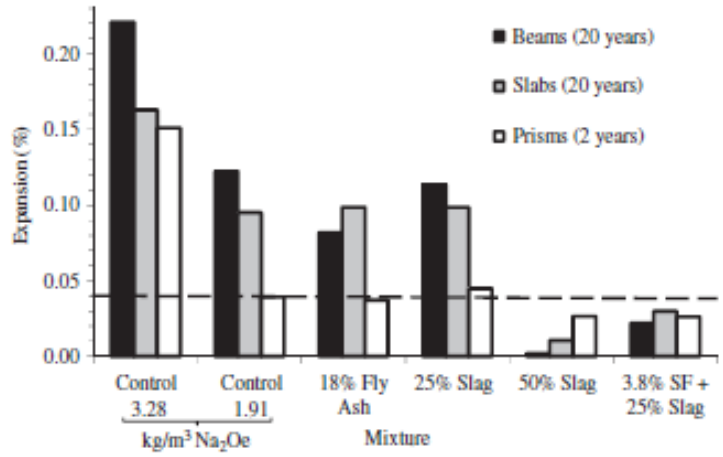
Figure 2.21: Comparison of expansion between CPT, beams, and slabs (Thomas et al., 2017)
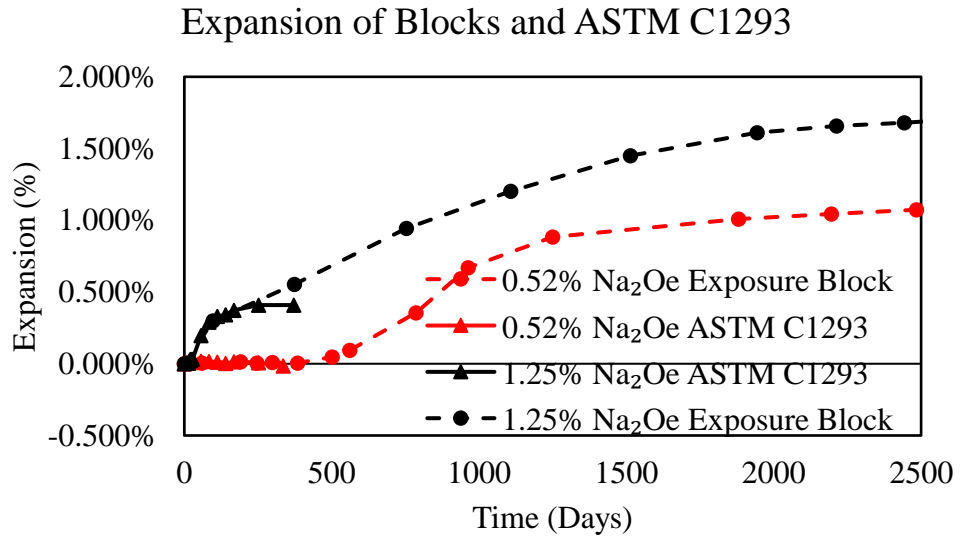
Figure 2.22: Exposure block and ASTM C1293 Data (data from Stacey et al. 2016)

The CPT and mortar bar test also have difficulty testing low range alkali mixes, as evident in Figure 2.23 (and in Figure 2.22 in the case of the CPT) where they show significantly less expansion then their counterpart blocks. In some instances, the blocks show damaging expansion, where the CPT and mortar bar tests do not. This variation is due to the leaching of alkalis, and is why samples are boosted (CPT) or submerged in solution (AMBT). The inability to test low alkali mixtures, results in the incapacity for these tests to assess job mix designs, resulting in inconclusive data for aggregate reactivity under real world circumstances.
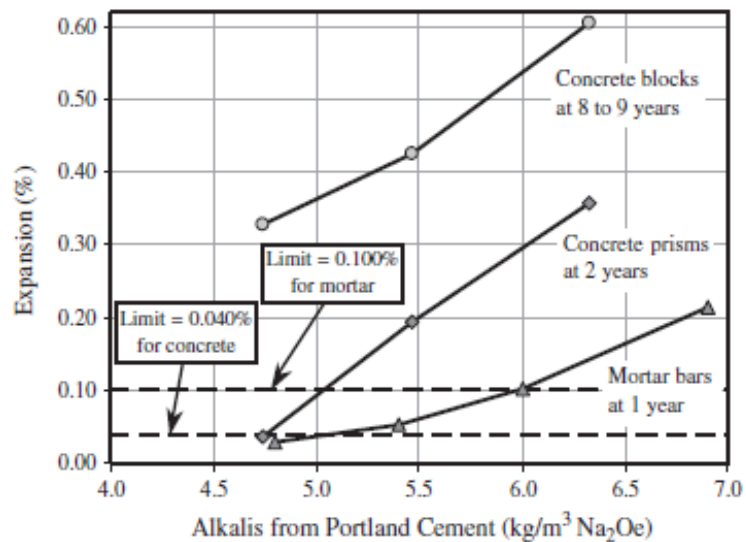
Figure 2.23: Comparison of test method expansion (Thomas et al., 2006)

2.9. Current Research

One of the primary issues facing our industry is the development of a rapid and reliable test method to better predict the long term performance and reactivity of "job mixtures".

40

Significant research is being conducted in order to generate more reliable laboratory test methods that can be performed in a short period of time. Some of the most current advancements have been the creation of the concrete cylinder test (Stacey et al., 2016), the miniature concrete prism test (Latifee & Rangaraju, 2015), and the autoclave concrete prism test (Giannini & Folliard, 2013). These three tests were chosen due to their test duration being shorter than the CPT.

2.9.1. Concrete Cylinder Test (CCT)

The Concrete Cylinder Test (CCT) is comprised of casting 100 x 200 mm cylinders with the interior of the mould wrapped in a filter paper in order to allow solution to surround the sample. The cylinders are cast just short of 200 mm in height to allow for ponding of solution, and have pins (for subsequent length-change measurements) imbedded in both ends. The lower pin protrudes through the concrete mould as presented in Figure 2.24 to allow for periodic length measurements. Some of the samples tested reached their ultimate expansion in as little as fifteen weeks without leaching due to ponding with solution (Stacey et al., 2016).
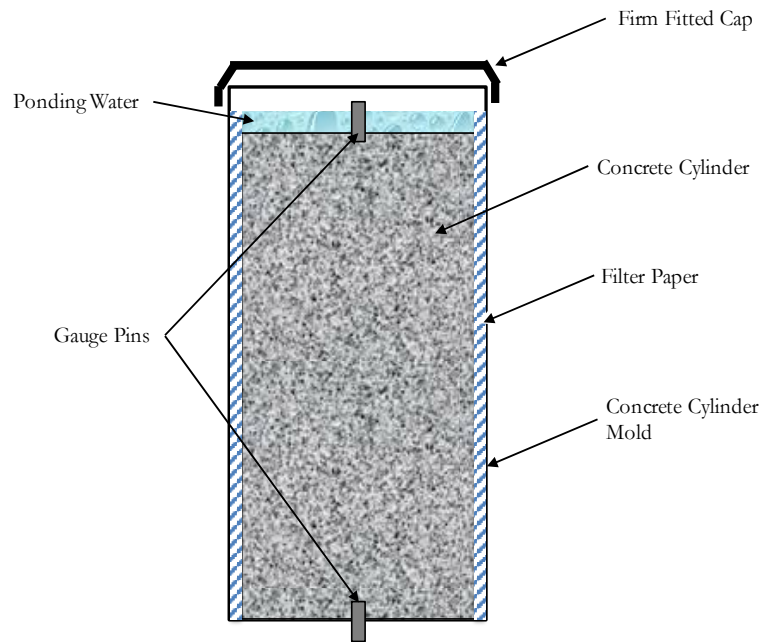
Figure 2.24: The concrete cylinder test setup (Stacey et al., 2016)

The data produced by Stacey et al. (2016) can be seen in Figure 2.25. It can be seen that the ultimate expansions achieved by the CCT are drastically lower than those of their respective exposure blocks. It can also be noted that the low alkali mix of 0.52% did not reach a damaging expansion level where its block counterpart did.

The downfall for this test method is that it struggled to demonstrate that concretes produced using low-alkali cements can be damaging. This was noted by Stacey et al. (2016) for their samples having an alkali content of 0.52% Na_2O_e and below. It was suggested that these low alkali samples required a longer amount of time to reach damaging expansion under these conditions.
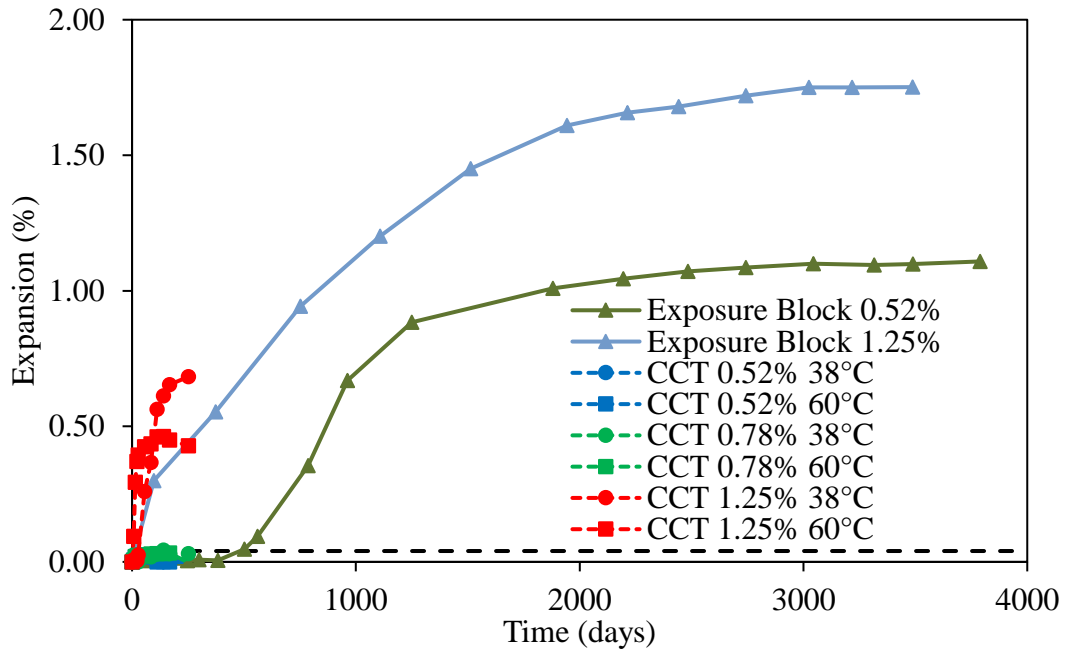
Figure 2.25: CCT and Exposure Block Data (Data from Stacey et al., 2016)

2.9.2. Miniature Concrete Prism Test

The miniature concrete prism test (MCPT) consists of casting and curing 50x50x285 mm

concrete prisms (see Figure 2.26). The prisms, once cured, are placed in 60°C water for 24

hours, and then placed in a 1 molar NaOH solution at 60°C, with periodic measurements

over 84 days (Latifee & Rangaraju, 2015). There are a few concerns pertaining to this test

method, such as the boosting of the alkalis to 1.25% Na_2O_e, which removes the possibility

to test job mixtures and alkali thresholds. Submerging the samples in water also promotes

leaching of alkalis, and the storage in NaOH gives the sample a virtually unlimited source

of alkalis, which could lead to false positives, similar to that of the AMBT. However,

results found at 56 days correlated with those found in the CPT at one year.

43

Figure 2.26: Sample in solution for MCPT (Latifee & Rangaraju, 2015)

2.9.3. Autoclave Concrete Prism Test

Samples for the autoclave concrete prism test are cast in a similar manner as those in ASTM
C1293, with the exception of the equivalent alkalis being boosted to 3% Na_2O_e instead of
1.25%. After the samples have moist cured for 24 hours, they are demoulded and allowed
to moist cure for an additional 24 hours. The samples are then placed in an autoclave for
24 hours at 133°C and 0.20 MPa. After 24 hours, the samples are cooled for 1 hour in
running water at room temperature and length change measurements are taken (Giannini
& Folliard, 2013). A schematic of samples in the autoclave can be seen in Figure 2.27. The
major flaw with this test method is the extreme heat and boosting of alkalis. The
temperature to which the samples are subjected to at such an early age can result in dramatic
changes to possible ultimate expansion found otherwise, potentially leading to inaccurate

results. The boosting of alkalis also hinders the test from being used to test job mixtures and alkali thresholds.
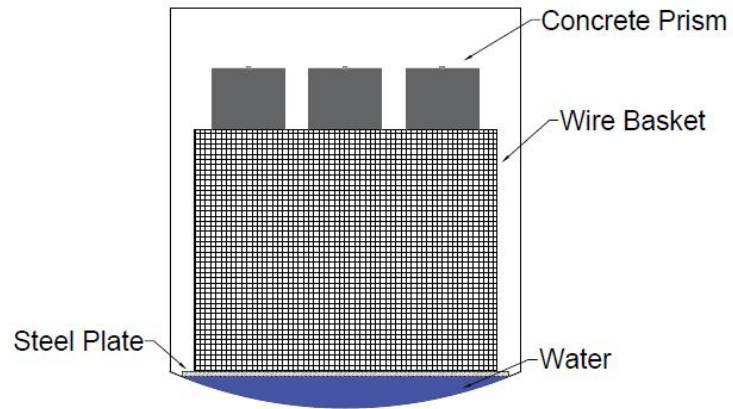
Figure 2.27: Schematic of the autoclave interior with CPT inside (Wood et al., 2016)

3. Methodology

The goals set out by this research were achieved using the experimental procedures outlined in this chapter. The procedures are grouped into three main sections, materials and casting, storage and measuring, and alkali inventory. Each section is outlined below with the protocols and materials used.

3.1. Mix Design

The mix designs used for the entirety of this research conform to ASTM C1293, except the equivalent sodium alkali content. The material and proportion used in the experimental program were selected to match those used to cast blocks at various exposure sites. Various equivalent alkali contents were used during the experimental program to examine alkali thresholds between 0.36% to 1.25% Na_2O_e. All mix designs had a water-to-cementitious materials (w/cm) ratio of 0.42, and a sand to aggregate ratio of 40%; both within the acceptable ranges of ASTM C1293. The total cementitious material quantity used for all mixes was 420kg/m³, with mixes of only portland cement, binary systems of fly ash and slag combined with portland cement, and a ternary system of portland cement, slag, and silica fume. A complete mix design for each set of samples can be found in Appendix A, along with the respective slump and 28 day compressive-strength data.

3.1.1. Aggregate Selection

The aggregates used for this project originated from a variety of sources. Table 3.1 outlines the aggregate mineralogy, source, and gradation size, where Table 3.2 outlines the specific gravity and absorption of the aggregates.

Table 3.1: Aggregate Source and Mineralogical Description

Aggregate Source, Location	Gradation	Reactivity and Mineralogy
Blagdon, New Brunswick	Coarse	Low Reactivity, Granite
Springhill, New Brunswick	Coarse	Highly Reactive, Greywacke/Argillite
Zealand, New Brunswick	Fine	Non-Reactive, Quartz/Argillite/Feldspar
Spratt, Ontario	Coarse	Highly Reactive, Siliceous Limestone
El Paso (Jobe), Texas	Fine	Highly Reactive, Quartz/Chert/,Feldspar
San Antonio, Texas	Coarse	Non-Reactive Dolomitic Limestone
Austin, Texas	Fine	Non-Reactive Limestone

Table 3.2: Properties of Aggregate

Aggregate Source	Specific Gravity	Absorption (%)
Blagdon, New Brunswick	2.691	0.44
Springhill, New Brunswick	2.535	0.40
Zealand, New Brunswick	2.594	0.53
Spratt, Ontario	2.670	0.61
El Paso (Jobe), Texas	2.589	0.54
San Antonio, Texas	3.120	2.47
Austin, Texas	2.680	2.54

To examine the expansive properties of reactive aggregates, they were paired with a non-reactive counterpart. The only mix design which did not use any reactive aggregates was that used for alkali inventory, due to the goal of the test being to monitor the movements of alkalis and not consume them (see Section 3.3).

3.1.2. Alkali Content and Cement Selection

In order to create a range of alkali contents, three cements were used. The chemical compositions of each portland cement can be found in Table 3.3.

Table 3.3: Chemical Composition of Portland Cements

Chemical Composition (%)	Brookville	Paulding	Whitehall
SiO_2	20.6	20.82	18.70
Al_2O_3	4.90	5.03	5.80
Fe_2O_3	3.50	2.12	2.70
CaO	64.10	64.78	61.30
MgO	0.70	2.86	2.70
SO_3	2.80	2.37	4.00
Na_2O	-	0.21	-
K_2O	-	0.33	-
Na_2O_e	0.36	0.43	0.92
CO_2	1.06	-	1.40
LOI	2.40	1.58	2.30

These three cements were combined to achieve the required alkali contents up to 0.92% Na_2O_e. The concrete mixtures with alkali contents above 0.92% Na_2O_e were achieved through dissolving NaOH pellets into the concrete's mixing water, as per ASTM C1293. The calculation for the required amount of NaOH will be discussed below

The determination of the composition of the blended cements was achieved through the use of Equation 5 and 6, where Equation 5 was used to calculate the proportions of low alkali cement, and Equation 6 for high alkali cements. In these equations $Na_2O_{e\ req}$ is the required alkali content for the mix design, $Na_2O_{e\ high}$ is the alkali content of the high alkali

cement, $Na_2O_{e\,low}$ is the alkali content of the low alkali cement, and $420(kg/m^3)$ is the total

cement content for the mix design.

$$Low\ Alkali\ Cement\ Amount = \frac{Na_2O_{eReq} - Na_2O_{ehigh}}{Na_2O_{elow} - Na_2O_{ehigh}} * 420(kg/m^3) \qquad \text{[5]}$$

$$High\ Alkali\ Cement\ Amount = \left(1 - \frac{Low\ Alkali\ Cement}{420(kg/m^3)}\right) * 420(kg/m^3)\ \text{[6]}$$

For mixes with an alkali content above the highest alkali cement (above 0.92 Na_2O_e)

Equation 7 was used, which determines the required NaOH content to achieve the desired

alkali content where 39.997 is the molar mass of NaOH, and 61.980 is the molar mass of

Na_2O_e. Table 3.4 shows the alkali content, cements, and aggregates used for 100% portland

cement mix designs.

$$NaOH = \left(Na_2O_{eReq} - Na_2O_{ehigh}\right) * 420(kg/m^3) * \frac{39.997}{61.980}/100\ \text{[7]}$$

Table 3.4: Cement combination, alkali contents and aggregate combinations

Cements		Blagdon & Jobe	Springhill & Zealand	Spratt & Zealand	San Antonino & Austin
Brooksville		0.36			
Brooksville	Paulding		0.40†	0.40†	
Brooksville	Paulding	0.41*			
Paulding		0.43			
Paulding	Whitehall		0.49	0.49	
Paulding	Whitehall	0.52*			
Paulding	Whitehall	0.70‡	0.70‡		0.70‡
Paulding	Whitehall		0.90†	0.90†	
Whitehall		0.92			
Whitehall		0.95*			
Whitehall		1.25*	1.25†	1.25†	

Key: *Exposure Bocks at University of Austin Texas, †Exposure Blocks at CAMNET in Ottawa, Between alkali contents of blocks, ‡Alkali Content of Mactaquac Dam, Alkali Content of Cement

The mixtures with Jobe reactive sand closely replicate mixtures used for blocks on the exposure site at the University of Texas in Austin (UTA). On the UTA site there are Jobe blocks constructed with 420 kg/m^3 of portland cement with cement alkali levels of 0.41, 0.52, 0.95 and 1.25% Na$_2$O$_e$. These same alkali loadings were used in this study plus a few additional mixes were cast at other alkali loadings.

The mixtures with the reactive greywacke from Springfield and the reactive siliceous limestone from Spratt were cast with alkali levels to match blocks at the CAMNET exposure site in Ottawa where levels of 0.40, 0.90, and 1.25% Na$_2$O$_e$. A few additional alkali levels were used also. The mix combining Springfield with a cement with alkali

content of 0.70% was selected to represent the suspected alkali content of the Mactaquac Dam which was constructed with a greywacke aggregate similar to that from the Springfield Quarry

3.1.3. SCM Selection

Binary systems of slag or fly ash combined with portland cement, and a ternary system of slag, silica fume, and portland cement were also used in the testing program. Table 3.5 presents the chemical composition of the slag, fly ash, and silica fume used. The SCM and alkali contents for each mix are found in Table 3.6.

Table 3.5: Chemical Composition of SCMs

Chemical Composition (%)	Belledune Fly Ash	Illinois GGBS	Silica Fume
SiO_2	55.60	34.1	96.7
Al_2O_3	20.12	9.42	0.3
Fe_2O_3	5.74	0.33	0.1
CaO	4.41	40.1	0.4
MgO	-	11.56	0.3
SO_3	1.72	2.68	-
Na_2O	-	0.37	0.1
K_2O	-	0.18	0.7
Na_2O_e	1.55	0.49	-
LOI	2.26	-	-

Table 3.6: Cementing material combinations, alkali contents, and aggregate combinations

Cements		SCM Type	SCM (%)	Blagdon & Jobe	Springhill & Zealand	Spratt & Zealand
Whitehall		Fly Ash	30	1.25*		
Whitehall		Fly Ash	56	1.25*		
Paulding	Whitehall	Fly Ash	20			0.90†
Paulding	Whitehall	Fly Ash	30		0.90†	0.90†
Paulding	Whitehall	Fly Ash	56		1.25†	
Paulding	Whitehall	GGBS	50			0.90†
Paulding	Whitehall	GGBS	65			0.90†
Paulding	Whitehall	GGBS	25			1.25‡
		Silica Fume	4			
Key: *Exposure Bocks at University of Austin Texas, †Exposure Blocks at CAMNET in Ottawa, ‡Kingston Exposure Site						

The mixtures with Jobe sand closely replicate mixtures used for blocks on the exposure site at UTA. These blocks were made with a cement alkali level of 1.25% Na_2O_e and total cementitious content of 420 kg/m^3. Fly ash was used at two replacement levels, 30 and 56% of cementitious content.

The mixtures with Springfield and Spratt aggregates were cast at alkali contents of 0.90 and 1.25% Na_2O_e matching exposure blocks found at the CAMNET exposure site. The mixes found at the Ottawa site had cement replacement levels of 20, 30, and 56% of fly ash as well as 50 and 65% ground granulated blast furnace slag.

The only ternary system tested matched blocks found at the CAMNET exposure site in Kingston. This mix has a cement alkali content of 1.25% Na_2O_e. The SCM's used were

both ground granulated blast furnace slag and silica fume at replacement levels of 25 and 4% respectively.

3.1.4. Specimen Fabrication

All concrete was cast in 50-Liter batches using a high-shear concrete mixer in accordance with ASTM C192. The batching sequence went as follows, coarse aggregate placed in the mixer with a portion of water and admixture, then the start of rotation of the mixer. Once the mixer was stopped, fine aggregate, cement, and the rest of the water was added and mixed for three minutes, allowed to rest for three minutes and then mixed again for two minutes. All mixes were prepared with a 19-mm aggregate, which was graded in accordance with ASTM C1293 in addition to a fine aggregate meeting the gradation of ASTM C33. The batch quantities for each mix are presented in Table 3.7.

Table 3.7: Batch quantities for all mix designs

Mix	Batch Quantities (kg/m³)						
	Water	Cement	Slag	Fly Ash	Silica Fume	Fine Agg.	Coarse Agg.
Jobe 0.36	176	420	-	-	-	729	1045
Jobe 0.41							
Jobe 0.43							
Jobe 0.52							
Jobe 0.7							
Jobe 0.92							
Jobe 0.95							
Jobe 1.25							
Jobe 30FA		294		126		697	
Jobe 56FA		184.8		235.2		693	1020
Springhill 0.40		420		-		694	
Springhill 0.49							
Springhill 0.70							
Springhill 0.90							
Springhill 1.25							
Springhill 30FA		294		126		662	
Springhill 56FA		184.8		235.2		634	
Spratt 0.40		420		-		698	1070
Spratt 0.49							
Spratt 0.90							
Spratt 1.25							
Spratt 20FA		336		84		677	
Spratt 30FA		294		126		666	
Spratt 50SG		210	210			475	
Spratt 65SG		273	147	-		409	
Spratt 25SG 4 SF		298.2	105		16.8	649	1000
Alkali Inventory		420	-		-	673	

The slump of each mixture was measured in accordance with ASTM C143, where the slump cone was filled in thirds, with every layer receiving 25 blows protruding approximately 25 mm (1 in.) into the layer below, or in the case of the bottom layer, striking the slump board. For each mix the following specimens were cast:

- Three 75 x75 x 285 mm prisms in accordance with ASTM C1293

- Three concrete cylinders (100 x 200 mm)

- Six custom made cylinders (145 x 280 mm).

The samples were cast in accordance with ASTM C192, with the exception of the custom cylinders. Custom-made moulds were manufactured (see Figure 3.1A). These cylinders had gauge pins in both top and bottom surfaces which were embedded into the top and bottom of the specimen using plates as seen in Figure 3.1B. These plates were used to locate the machined ¼ x 1 ¼ in. bolts, with the bottom (smaller plate) sitting inside the mould, and the top plate being placed on top of the mould after it has been filled with concrete. Figure 3.1C shows the custom moulds filled with concrete before placement of the top plate. These pins allowed the sample to be measured at various increments in time in accordance with ASTM C157.

The casting procedure for both sets of cylinders commenced with the moulds being filled in thirds, with every layer receiving 25 blows protruding approximately 25 mm (1 in.) into the layer below, except in the case for the bottom layer where the rod struck the bottom of the mould. The 100 mm diameter cylinders were rodded with a 10mm rod, where the

custom moulds were rodded with a 16mm rod. The prisms were cast in in two layers with each layer receiving 32 blows. Once the moulds were filled, the sides of the moulds were struck with a rubber mallet to aid in consolidation of the sample, and the moulds were struck off removing excess concrete.

The cylinders and prisms were cured under wet-burlap for 24 hours, after which they were demoulded. Cylinders (100 x 200 mm) were then placed in a moist curing room (100% RH at 23±2°C) until they were to be tested, whereas the prisms and UNBCCT samples were measured and stored in accordance to ASTM C1293, respectively. Figure 3.1D shows a UNBCCT sample after the mould and plates have been stripped, leaving only the concrete and the embedded gauge pins.
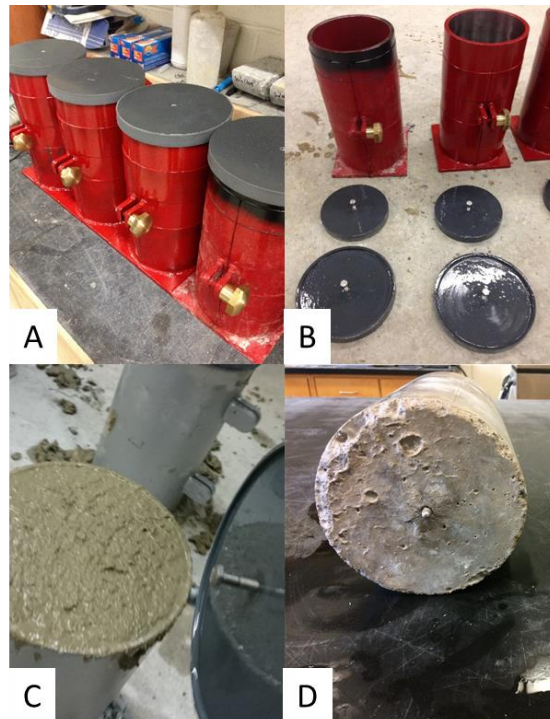
Figure 3.1: Mould, pin placement, casting and demoulded sample for UNBCCT

3.2. Storage Conditions

Once demoulded, specimens were placed in one of four conditions. Concrete cylinders (100 mm x 200 mm) were demoulded following 24 hours and then placed in a moist curing room (100% RH at 23 ± 2°C) until they were tested to determine the compressive strength at 28 days. Concrete prisms (100 x 100 x 285 mm) were initially measured following 24 hours of curing, and then suspended over water in a container stored at 38°C, as specified in ASTM C1293 and seen in Figure 3.2.

Figure 3.2: Open storage container for CPT samples

The UNBCCT cylinders were measured and placed in a standard 6 x 12 in. (152 x 305 mm) mould, where the annulus around the concrete cylinders was filled with a sodium hydroxide solution representative of the alkalinity of pore solution within the concrete specimen. The UNBCCT samples were subjected to two storage temperatures, 38°C and 60°C. A schematic of a sample with host solution can be seen in Figure 3.3. A different mould was used for each temperature condition. Figure 3.4 shows a thin walled mould on the left used for 38°C storage, and a thick walled mould on the right for 60°C storage. The thicker mould

was used to provide greater stability at the elevated temperature. Following each measurement, the top cap on each mould was either epoxied or taped into place to prevent evaporation of the host solution.
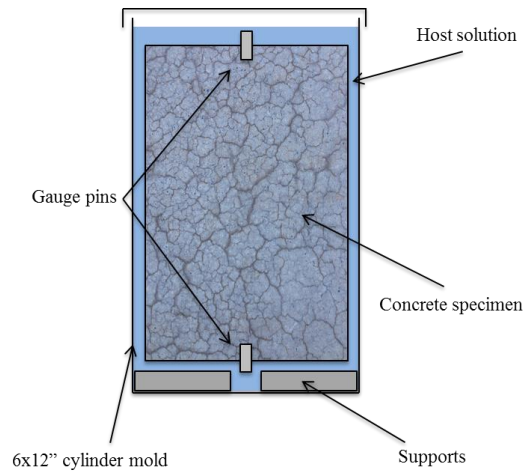
Figure 3.3: UNBCC sample with host solution

Figure 3.4: Thin (left) and thick (right) walled moulds

The NaOH concentration used to achieve equilibrium between the host and pore solution was calculated using Equation 8, where $NaOH_{con}$ is the required concentration of NaOH,

Na_2O_e Cement is the % equivalent alkalis in the cement, 0.7 is the conversion factor of equivalent alkalis to hydroxide ions, 17 is the molar mass of OH, and 40 is the molar mass of NaOH.

$$NaOH_{con}\left(\frac{g}{L}\right) = Na_2O_{e\ Cement}(\%) * 0.7\left(\frac{\frac{mol}{L}}{\%Na_2O_e}\right) * 17\left(\frac{g}{mol}OH\right) * \frac{40\left(\frac{g}{mol}NaOH\right)}{17\left(\frac{g}{mol}OH\right)}$$

[8]

3.2.1. Compressive Testing and Length-Change Measurement Schedule

The average compressive strength of three 100mm x 200mm cylinders was determined in accordance with ASTM C39 after 28 days of standard curing. The mix proportions and 28-day strength results for all mixes are presented in Appendix A. Length-change measurements were conducted on both CPT and UNBCCT specimens in accordance with ASTM C157, with a modification to the frequency of measurements. Specimens were initially measured at the time in which they were demoulded (1-day) and then measured on a weekly basis until an age of 56 days. Measurements were then done on a bi-weekly basis until 112 days, after which they were measured monthly. The samples were monitored until the length-change reached a plateau, or indefinitely. It should be noted that the length-change measurements for alkali inventory samples were only measured monthly until the alkali inventory was conducted, due to the aggregate being non-reactive. Figure 3.5 shows the calibration of the digital length comparator used for measurements, as well as a UNBCCT and CPT sample being measured.
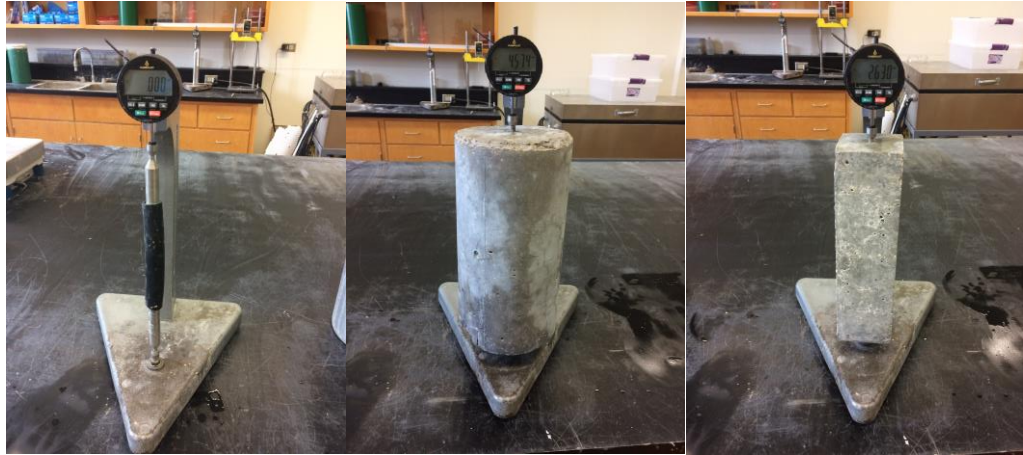
Figure 3.5: Calibration of digital length comparator (left) and length change measurement of UNBCCT (center) and CPT (right)

Before each measurement was taken, all samples were allowed to cool to room temperature for 24 hours. To retain as much host solution as possible, samples were allowed to dry on top of their storage container lid (see Figure 3.6). Any solution retained on the lid was poured back into the storage container, and topped up with distilled water to the original volume of solution. This was done to account for evaporation of water to ensure the concentration of alkalis did not change. It should also be noted that at the time of the writing of this dissertation, not all samples had reached their final expansion.
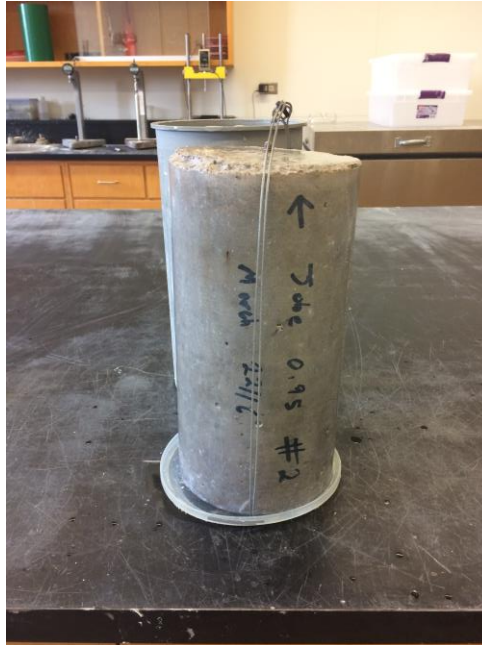
Figure 3.6: UNBCCT sample air drying on lid

3.3. Alkali Inventory

An alkali inventory was conducted on concrete samples cast with non-reactive carbonate (i.e. non-siliceous) aggregates. This was done in order to determine the fate of the alkalis in terms of mobility and partition between the pore solution, surrounding host solution, and solid phases (i.e. "bound" by aggregates or hydrates). This was achieved through the collection of pore and host solution, and the milling of concrete samples at various increments of time. These samples were then dissolved with either an acid or water solution, diluted, and tested for sodium and potassium levels.

Twelve samples were cast and stored in host solution, with half of them stored at 38°C and the others at 60°C. Specimens were measured for length-change monthly until tested at

ages of 1, 28, and 91 days, as well as 6, 12, and 24 months. When tested, one specimen from each storage condition was used. These specimens were cut into three portions as presented in Figure 3.7. It should be noted that at the time of writing this dissertation, not all samples had been tested.
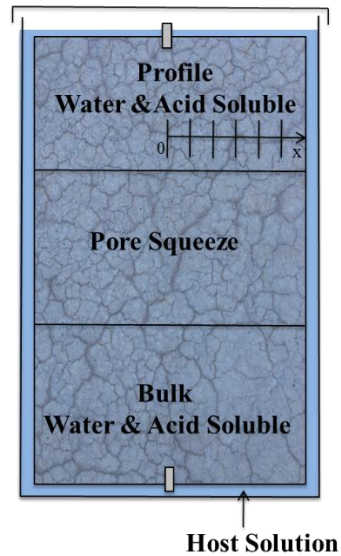
Figure 3.7: Sample division for alkali inventory

At the time of testing, each cylinder was cut into thirds using a wet diamond blade saw. The top third of the cylinder was used to generate both acid and water-soluble alkali profiles, the middle third was used to extract pore solution, and the bottom third was used for bulk acid and water-soluble alkali contents.

3.3.1. Alkali Profiles

As denoted above, the top third of the cylinder was used to determine alkali profiles. The alkali profiles were generated from the center outwards, where the center was the datum.

To obtain samples, the cylinder was cut in half, and milled in ten millimeter increments until a depth of 70 mm. The powder created during the grinding process was collected and stored in a desiccator until tested. Table 3.8 presents the depth at which samples were collected. It should be noted that as the milling approached the surface, the layer milled was thicker. This was due to the need to collect an adequate amount of sample for testing purposes. Figure 3.8 presents the milling process in order to determine sufficient material at all depths.

Table 3.8: Depth and layer thickness for milling

Depth outwards from center (mm)	Thickness of layer milled and tested (mm)
0	2
10	2
20	2
30	2
40	2
50	2
55	2
60	2
65	5
70	5
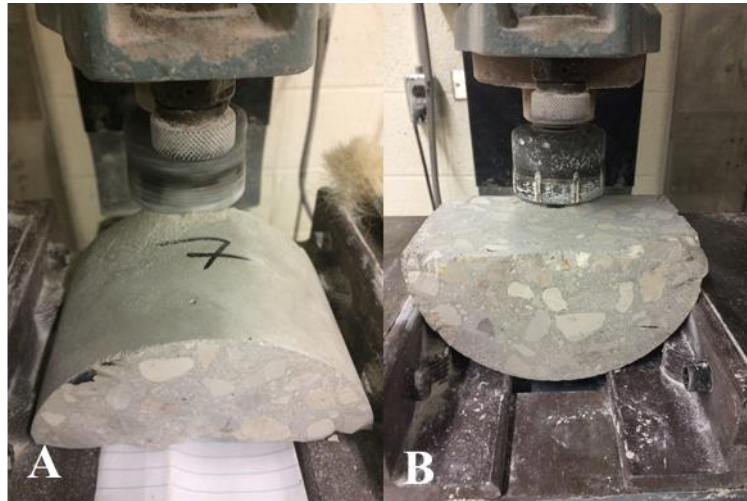
Figure 3.8: Milling of sample for acid and water soluble alkali profile

The collected powder was then tested in accordance to ASTM C114. The acid-soluble alkali content was determine by weighing one gram of material at each layer. This amount was then mixed with 25 mL of distilled water, dissolved in 5mL of hydrochloric acid, and then mixed with 20 mL of distilled water. The solution was then placed on a hotplate and allowed to boil for 10 minutes. Afterward the sample was allowed to cool, then vacuum filtered to remove solids. The filtrate was then diluted to 100 mL, inverted to ensure mixing, and tested using inductively coupled plasma mass spectrometry (ICP-MS) to determine the concentration of sodium and potassium.

The samples for water-soluble alkalis were prepared using 10 grams of powder. The powder was combined with 250 mL of distilled water and agitated for ten minutes. Once shaken, the solution was filtered to remove solids and 50 mL of the filtrate was measured out and combined with 9mL of calcium chloride stock solution and 0.5 mL of hydrochloric

acid. The solution was then diluted with 100mL of distilled water and inverted to ensure mixing, then tested via ICP-MS

3.3.2. Pore Solution Extraction

The middle third of the cylinder was used for pore solution extraction. The section of concrete was firstly cut in half to produce two smaller sections after which it was broken in multiple pieces using a hammer. This was conducted in order to separate the cementitious matrix from the coarse aggregate. The paste and mortar pieces were then collected for testing.

Pore solution extraction was performed in a similar manner as described by Barneyback et al. (1981). The overall procedure for the extraction is the placement of the mortar and paste in a shaft, were a piston presses down on the sample at various loads for a certain amount of time. Between loads, the piston pressure is reduced to allow for elastic rebound. The pore solution from the sample is forced outward into a vial below. The sample collected was stored at 5°C until testing. Figure 3.9 shows the apparatus setup for pore solution extraction.
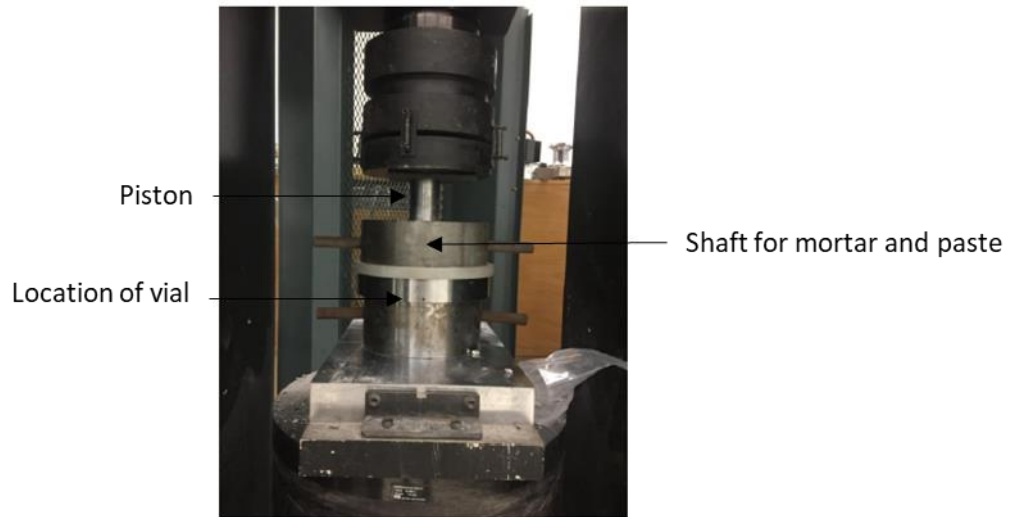
Figure 3.9: Pore solution extraction setup

To test the alkali content of the pore solution samples, 0.5 mL of the sample was mixed with 2.5 mL of hydrochloric acid and diluted to 50 mL. The sample was then tested via ICP-MS.

3.3.3. Bulk Water and Acid Soluble Alkali Content

The method used to determine the bulk acid and water-soluble alkali contents was determined by milling the bottom third of the cylinder to a depth of 5 mm. The powder collected was stored under vacuum, and was tested in the same manner as described in section 3.3.1.

3.3.4. Host Solution

Upon the removal of the alkali inventory cylinder from its host solution for processing, a sample of host solution was taken and stored at 5°C. This sample was then directly subjected to ICP-MS for the determination of sodium and potassium.

3.4. Exposure Block Data

The data generated during the course of this experiment was compared to exposure block data generated from the CAMNET exposure site in Ottawa, Ontario, the Kingston Ontario exposure site, and the University of Texas at Austin exposure site.

3.4.1. CAMNET Exposure Site

The CAMNET exposure site was developed in 1991 and contains blocks from over 150 concrete mixtures. For this study, results were compared to 12 mixes with an age between 15-18 years. The exposure blocks found at this location are comprised of 9 different reactive aggregates of sources found in both the United States and Canada. All blocks were cast with a cementitious content of 420 kg/m^3, and are 400x400x700 mm in size (Fournier et al., 2016). All blocks have stainless steel pins embedded in the front, back, and top surfaces which allows for periodic length change using a Demec gauge (Thomas et al., 2013b). Figure 3.10 shows a photograph of the CAMNET exposure site.

Figure 3.10: CAMNET exposure site in Ottawa (Thomas et al., 2006)

3.4.2. University of Texas in Austin Exposure Site

The University of Texas at Austin exposure site was initiated in 2001. The block age for the data used in this study was 9.5-10.5 years. There are over 131 blocks at this exposure site, but only 4 were used for this study. The exposure blocks found at this location are comprised of 24 different reactive aggregates (both coarse and fine) from locations in both the United States and Canada. These reactive aggregates were paired with non-reactive quarried limestone (for reactive fines) and manufactured limestone sand (for reactive coarse). The blocks were manufactured with various high and low alkali cements, as well as various SCMs. The cementitious content of all blocks is also $420kg/m^3$, and the blocks are of the same size as blocks on the CANMET exposure site (Ideker et al., 2012). Figure 3.11 shows the University of Texas in Austin exposure site.

Figure 3.11: University of Texas in Austin exposure site (Thomas et al., 2006)

3.4.3. Kingston Exposure Site

The Kingston exposure site was established in 1991. The block ages for the data used in this study was 20 years old. There are five different mix designs for this exposure site, but only one was used for this study. The blocks are made from one reactive coarse aggregate paired with a non-reactive fine. The size of the blocks are 600x600x2000 mm, and the blocks have 100 mm bolts vertically embedded in the finished surface. Periodic length measurements are conducted using surface bolts at a spacing of 508mm (Hooton et al., 2013). Figure 3.12 presents the Kingston exposure site.

Figure 3.12: Kingston exposure site (Hooton et al., 2013)

3.4.4. Expansion Monitoring Technique

Periodic length-change measurements are conducted using a Demec gauge, which spans between two gauge pins. The Demec gauge is initially calibrated to an invar reference bar (see Figure 3.14). Blocks on the Kingston exposure site only have pins on the top surface, whereas the CAMNET and Texas exposure sites have pins on the top, front and back surfaces in order to determine an average expansion. Figure 3.13 shows an example of an exposure block with pins located on the front and top (pins are in the red circles). Figure 3.15 shows length-change measurements being made on the top of an exposure block. Table 3.9 provides a summary of the expansion results and other properties of the exposure blocks used in this study to validate the UNBCCT and other test methods.

Figure 3.13: Exposure Block example

Figure 3.14: Demec gauge and reference bar

Figure 3.15: Exposure blocks being measured

Table 3.9: Summary of exposure block data

Reactive Aggregate	Exposure Site	PC Alkali (% Na₂Oₑ)	PC Alkali (kg/m³)	SCM Type	SCM % Replacement	Exposure Block Expansion (%)	Age of Blocks (years)	Source for Data
Jobe	UTA	0.41	1.72	N/A	N/A	0.094	9.5	Stacey et al., 2016
		0.52	2.18			1.108	10.4	
		0.95	3.99			1.434	10.4	
		1.25	5.25			1.751	9.56	
Spratt	CAMNET, Ottawa	0.4	1.68	N/A	N/A	0.085	15	Fournier et al., 2016
		0.9	3.78	N/A	N/A	0.206	15	
				FA	20	0.062	15	
				FA	30	0.016	15	
				GGBS	50	0.022	15	
				GGBS	65	0.014	15	
	CAMNET, Kingston	1.25	5.25	N/A	N/A	0.336	18.1	Thomas et al., 2013b
				GGBS, SF	25,4	0.03	20	Hooton et al., 2013
Springhill	CAMNET, Ottawa	0.4	1.68	N/A	N/A	0.029	15	Fournier et al., 2016
		0.9	3.78	N/A	N/A	0.391	15	
				FA	30	0.067	15	
		1.25	5.25	N/A	N/A	0.495	18	Thomas et al., 2013b
				FA	56	0.005	18.2	

The effects of alkali content and especially low-alkali content on exposure blocks can be seen in Figure 3.16. The time to the onset of expansion increase and the ultimate expansion (i.e. plateaus shown in Figure 3.16) decreases as the alkali content of the concrete decreases. The expansion for 1.25% alkali starts off almost immediately where as that of 0.41% alkali takes just over 4 years.
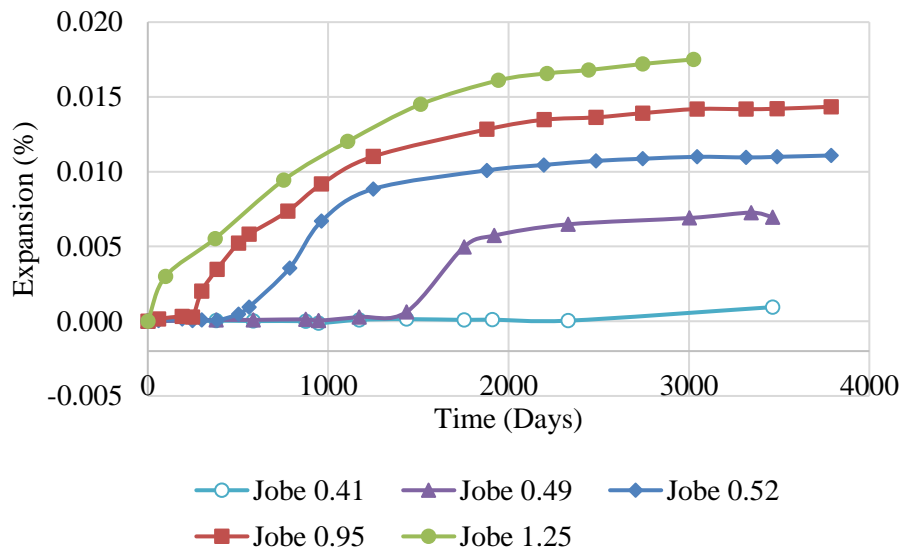
Figure 3.16: Jobe block expansion (Stacey et al., 2016)

The rate and ultimate expansion are also effected by the level of cement replacement by SCMs. Figure 3.17 shows that for systems all of the same cement alkali content (all boosted to 1.25% Na_2Oe) the cement replacement level has a profound effect. The control sample reached an expansion of 0.50% in 19 years where the next closest sample (with 20% fly ash) only reached 0.27% in the same time period.
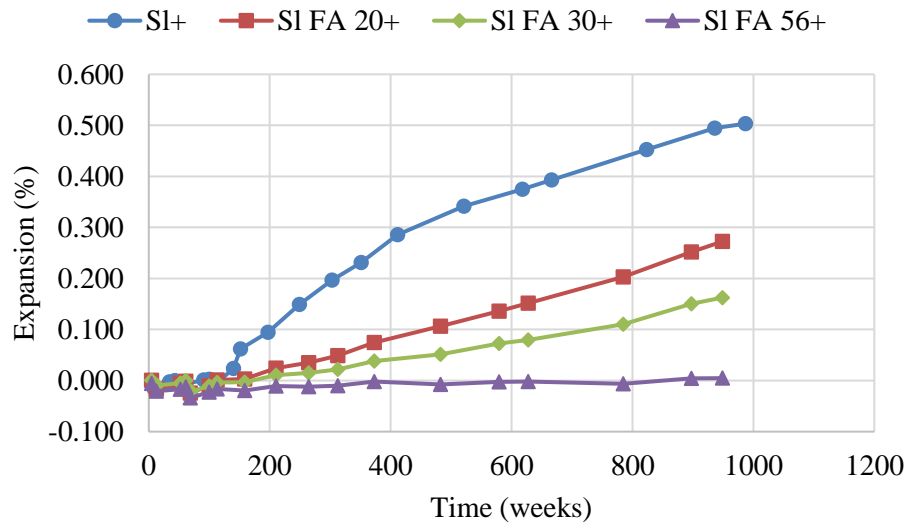
Figure 3.17: Effects of SCM on expansion (data from Thomas et al, 2013b using data from CAMNET)

4. Results

The results generated during the course of the experimental program are broken down into two sections, expansion and alkali inventory. The expansion data are further broken down into 100% PC mixes, binary and ternary mixes, and further again by aggregate types. The expansion data presented in this chapter is that of the UNBCCT and CPT samples generated concurrently. The data shown is that of an average from 3 samples. An example of a figure showing the data for all three samples can be seen in Appendix B. To better understand the effects of averaging three samples per measurement Appendix C shows a figure with error bars. Chapter 5 will present the data in comparison to field exposure blocks. This comparison will be used to validate the UNBCCT and its benefits over the CPT in regards to specific combinations of materials. All expansion graphs for individual mixes can be seen in Appendix D.

4.1. Results for Jobe Sand

The expansion results for mixes with 100% PC at a range of alkali contents with reactive Jobe sand are shown in Figure 4.1, 4.2 and 4.3, respectively, CPT at 38°C, UNBCCT at 38°C and UNBCCT at 60°C. The dashed line represents the 0.04% expansion limit defining failure in accordance with CSA A23.2-27A and ASTM C1778.
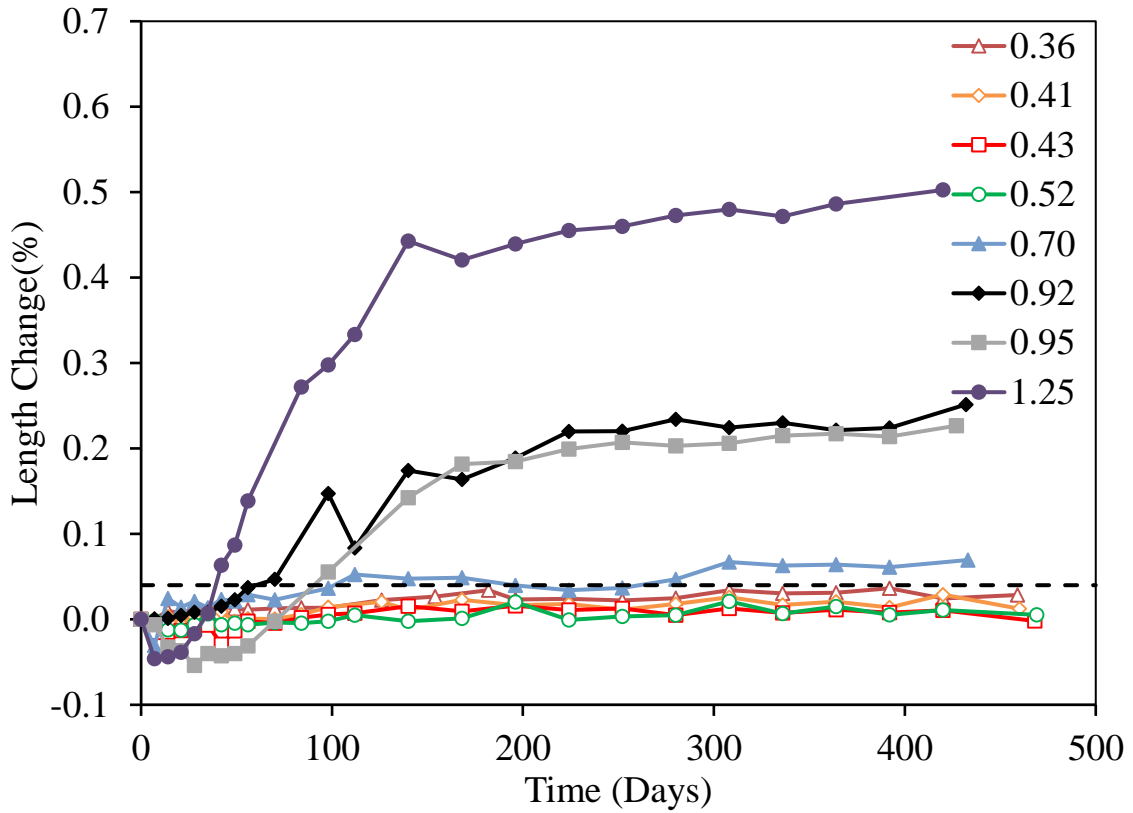
Figure 4.1: Summary of 100% portland cement Jobe sand CPT samples

The data presented in Figure 4.1 were collected from concrete prism test samples up to a minimum of 460 days. The standard CPT test (at 1.25% Na_2O_e) achieved deleterious expansion at approximately 35 days, and reached a plateau of approximately 0.47% after 7 to 9 months. The CPT samples that experienced deleterious expansion were those above a cement alkali content of 0.70% Na_2O_e. The onset of expansion for these samples commenced at approximately 90 days, with a maximum expansion of nearly 0.2% at 6 to 9 months. The mix with cement alkali content of 0.70% also showed some minor

expansion, however this did not occur until almost a year had passed. All other mixes did

not demonstrate damaging expansion.
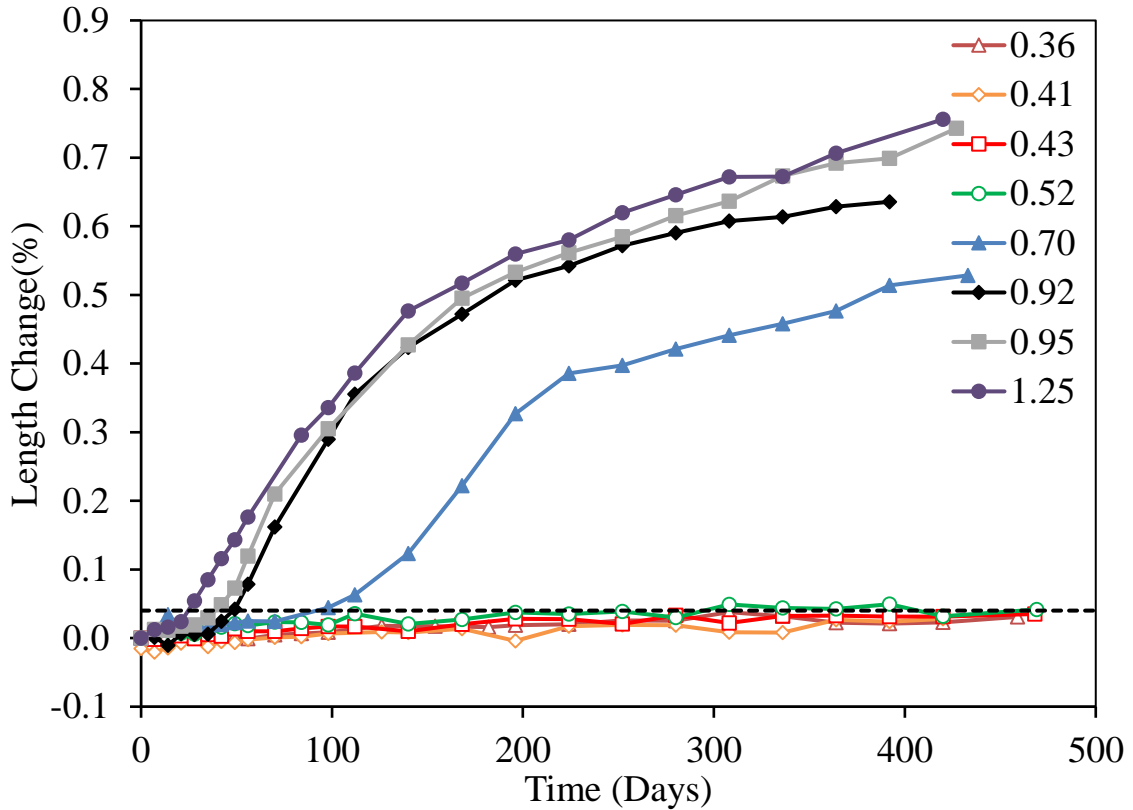
Figure 4.2: Summary of 100% portland cement Jobe sand UNBCCT samples at 38°C

The UNBCCT data presented in Figure 4.2 shows deleterious expansion for mixes with a

cement alkali content of 0.70% Na_2O_e and above. Samples at alkali content 0.92%, 0.95%,

and 1.25% saw similar expansion rates, with deleterious expansion commencing at

approximately 50 days. These three sets of samples started to plateau at around 170 days

at an expansion level of about 0.5%. The mix with a cement alkali level of 0.70% started

to expand after 100 days, and reached a plateau at around 0.40% at 224 days. All other mixes did not demonstrate damaging expansion.
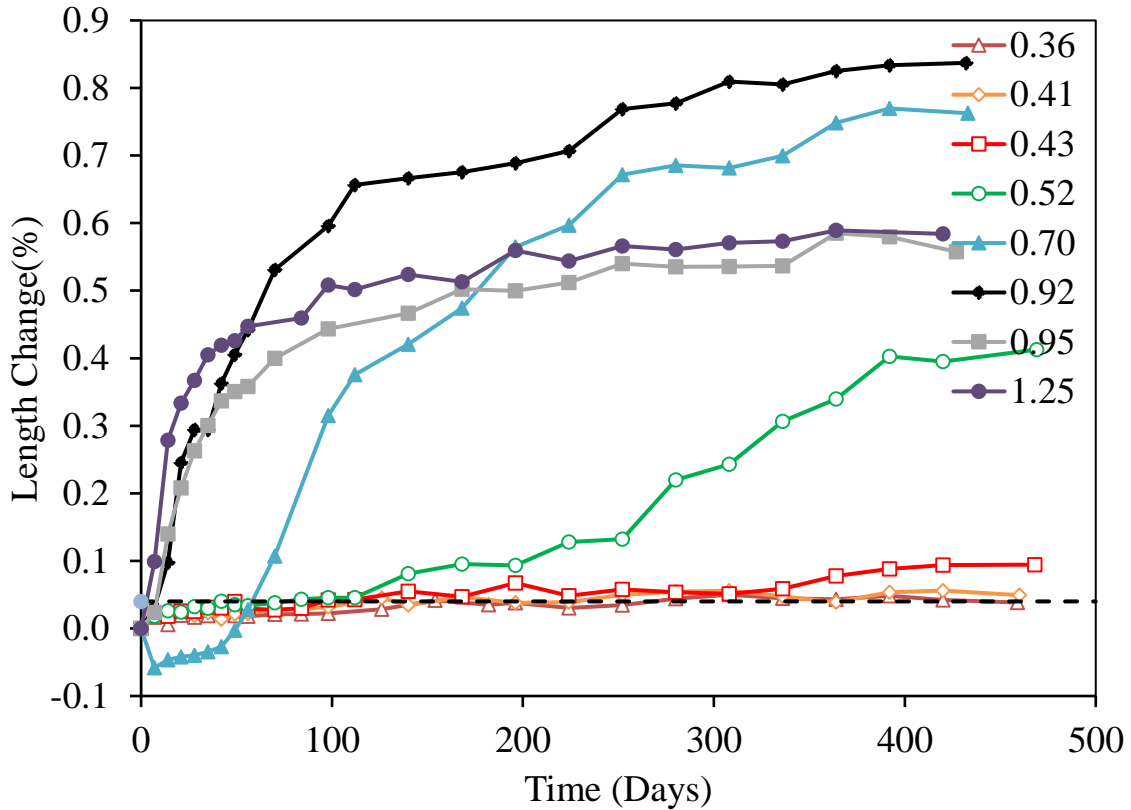
Figure 4.3: Summary of 100% portland cement Jobe sand UNBCCT samples at 60°C

The UNBCCT data presented in Figure 4.3 shows deleterious expansion for all mixes except for that with a cement alkali content 0.36% Na_2O_e. The samples at alkali content 0.92%, 95%, and 1.25% saw similar expansion rates, with deleterious expansion commencing at approximately 14 days. The onset of expansion for mixes with a cement alkali content of 0.70 and 0.52% was, respectively, approximately 50 and 100 days. Mixes

with low alkali contents (0.36 to 0.43) did not show any signs of expansion until around one year, with only 0.43% alkali content yielding deleterious expansion. The length change for the 0.70% alkali mix shows an abnormality at the onset of measurements. It seems to have shrunk a considerable amount before starting its expansion. This is likely due to an error in the initial zero-day measurement, as no other mixes presented in Figure 4.3 follow this trend.

4.2. Results for Springhill Aggregate

The expansion results for mixes with 100% PC at a range of alkali contents with reactive Springhill coarse aggregate are shown in Figure 4.4, 4.5 and 4.6, respectively, CPT at 38°C, UNBCCT at 38°C and UNBCCT at 60°C. The dashed line represents the 0.04% expansion limit defining failure in accordance with CSA A23.2-27A and ASTM C1778.
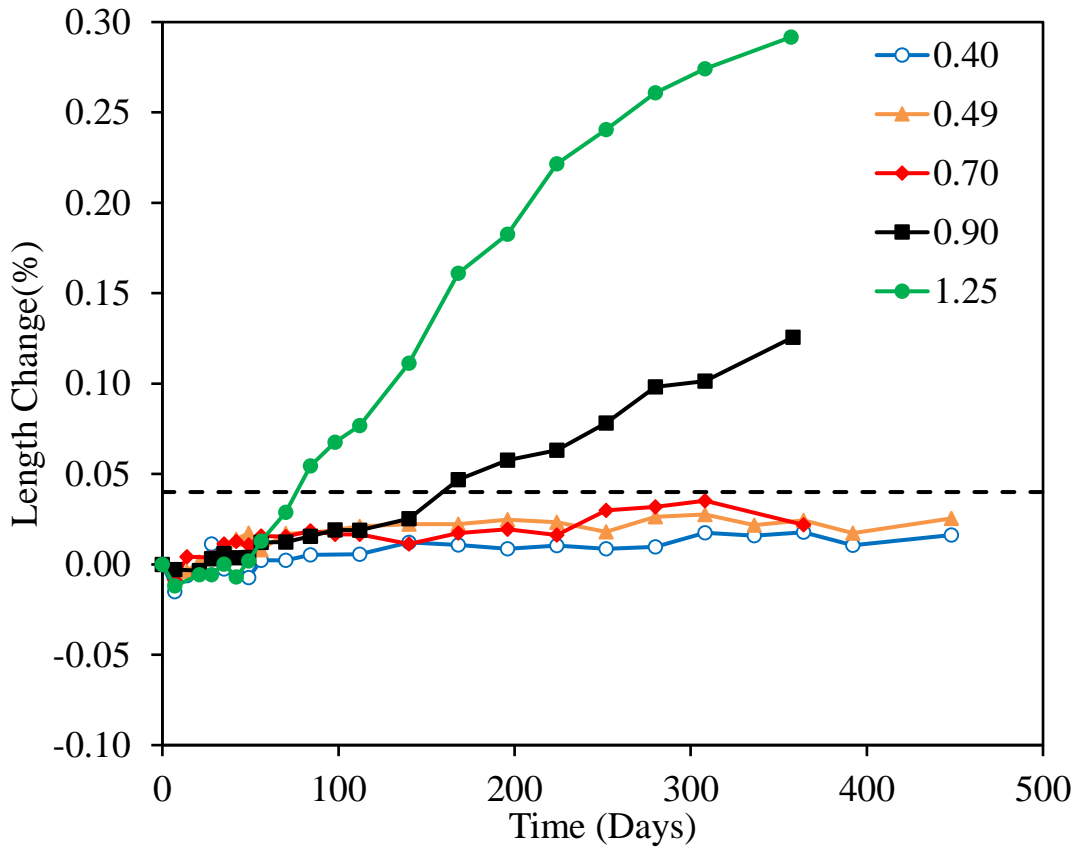
Figure 4.4: Summary of 100% portland cement Springhill coarse aggregate CPT samples

The data presented in Figure 4.4 were collected from concrete prism test samples up to a minimum of 360 days. The standard CPT test (at 1.25% Na_2O_e) achieved deleterious expansion at approximately 85 days, and reached a plateau of approximately 0.29% after a year. The concrete with cement alkali content of 0.90% also expanded failing the 0.04% limit at about 180 days. None of the other concretes have shown deleterious expansion to date.
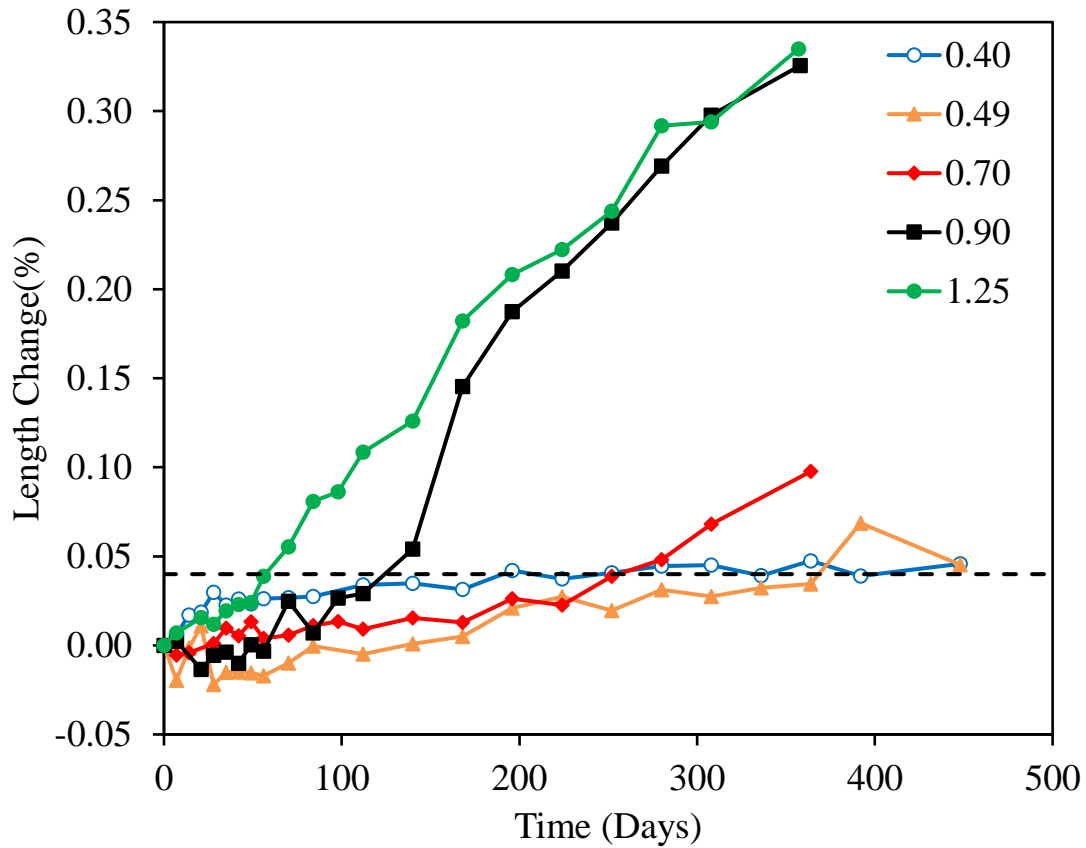
Figure 4.5: Summary of 100% portland cement Springhill coarse aggregate UNBCCT samples stored at 38°C

The UNBCCT data presented in Figure 4.5 shows deleterious expansion for all mixes. The samples at an alkali content of 0.40% Na_2O_e plateaued at the 0.04 mark at approximately 6 months, and therefore were deemed reactive. The high alkali samples of 0.90% and 1.25% had rapid expansion, but have yet to plateau at the time of last measurement. The concrete with 0.70% cement alkali surpassed the expansion limit of 0.04% at the 280 day mark resulting in deleterious expansion, but like the samples at 0.90 and 1.25% cement alkali content, have yet to reach a plateau.
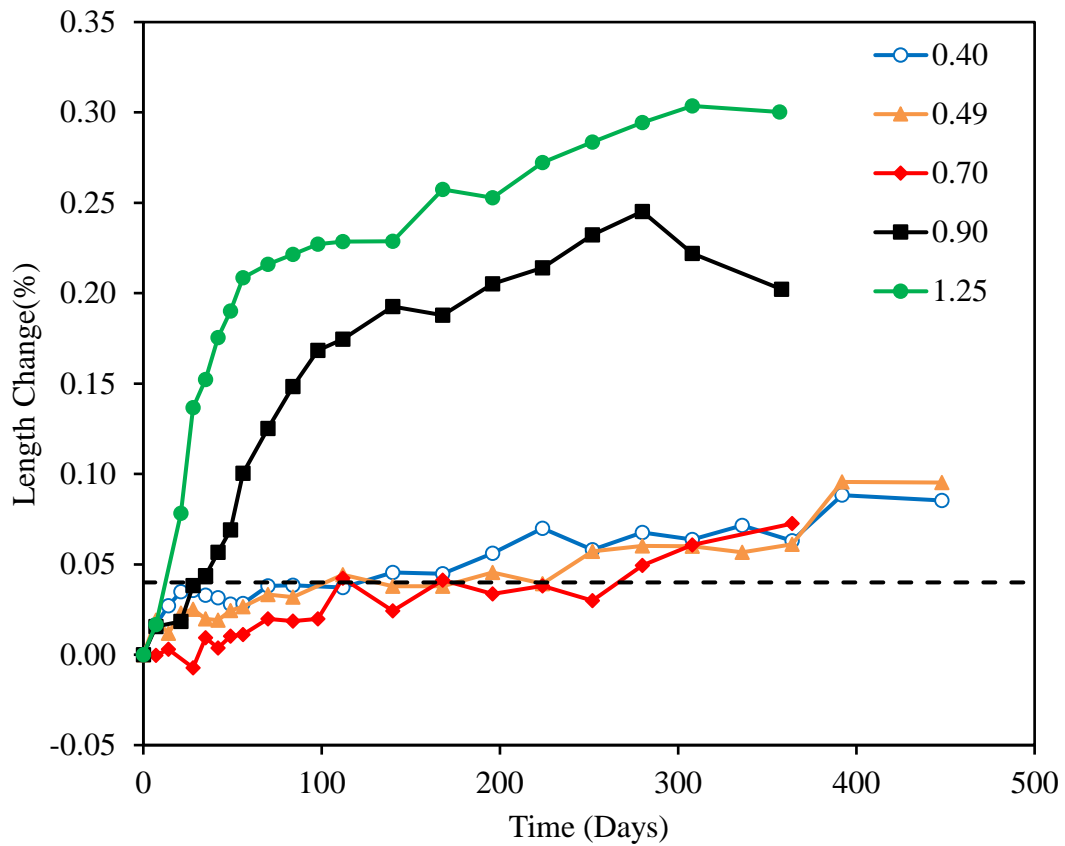
Figure 4.6: Summary of 100% portland cement Springhill coarse aggregate UNBCCT samples stored at 60°C

The UNBCCT data presented in Figure 4.6 shows deleterious expansion for all mixes. The mixes that have plateaued are those of cement alkali 0.90 and 1.25%. They commenced deleterious expansion at approximately 24 days, where the lower alkali samples commenced at 6 to 9 months.

4.3. Results for Spratt Aggregate

The expansion results for mixes with 100% PC at a range of alkali contents with reactive Spratt coarse aggregate are shown in Figure 4.7, 4.8 and 4.9, respectively, CPT at 38°C,

UNBCCT at 38°C and UNBCCT at 60°C. The dashed line represents the 0.04% expansion

limit defining failure in accordance with CSA A23.2-27A and ASTM C1778.
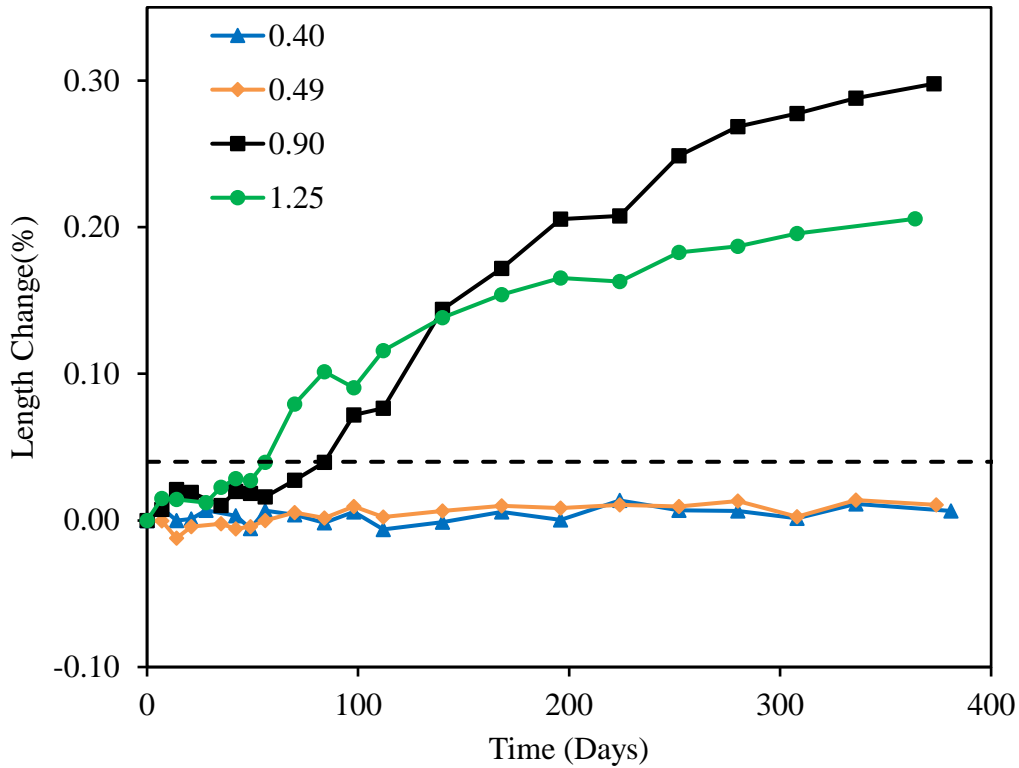
Figure 4.7: Summary of 100% portland cement Spratt coarse aggregate CPT samples

The data presented in Figure 4.7 were collected from concrete prism test samples up to a

minimum of 365 days. The standard CPT test (at 1.25% Na_2O_e) achieved deleterious

expansion at approximately 70 days, and reached a plateau of approximately 0.19% after

10 to 12 months. The CPT samples that experience deleterious expansion were those with

a cement alkali of 0.90 and 1.25%. The samples with lower alkalis (0.40 and 0.49%) have not expanded to date.
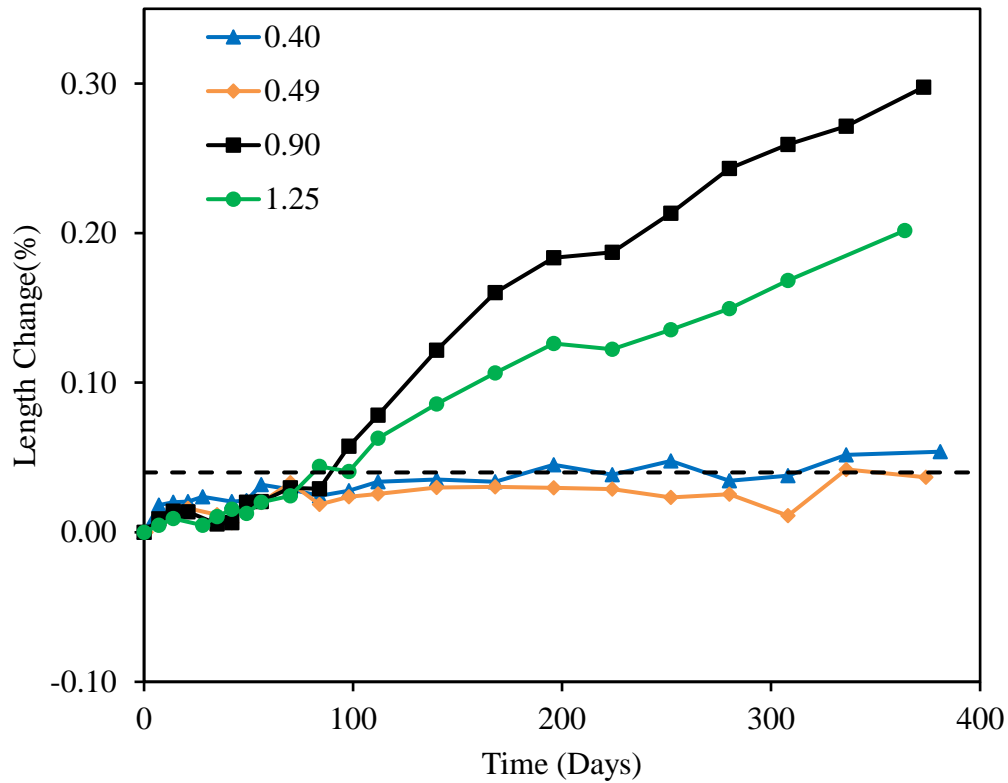
Figure 4.8: Summary of 100% portland cement Spratt coarse aggregate UNBCCT samples stored at 38°C

The UNBCCT data presented in Figure 4.8 shows deleterious expansion for all mixes except that with a cement alkali content of 0.49% Na_2O_e. The two most reactive sets of samples (0.90 and 1.25% Na_2O_e) commenced deleterious expansion at about the 70 day mark. Plateaus for these reactive samples had not been reached within the year of measuring. There is a discrepancy between the length changes between the low alkali

mixes where the expansion of the 0.40% alkali is higher than that of the 0.49% cement alkali content.
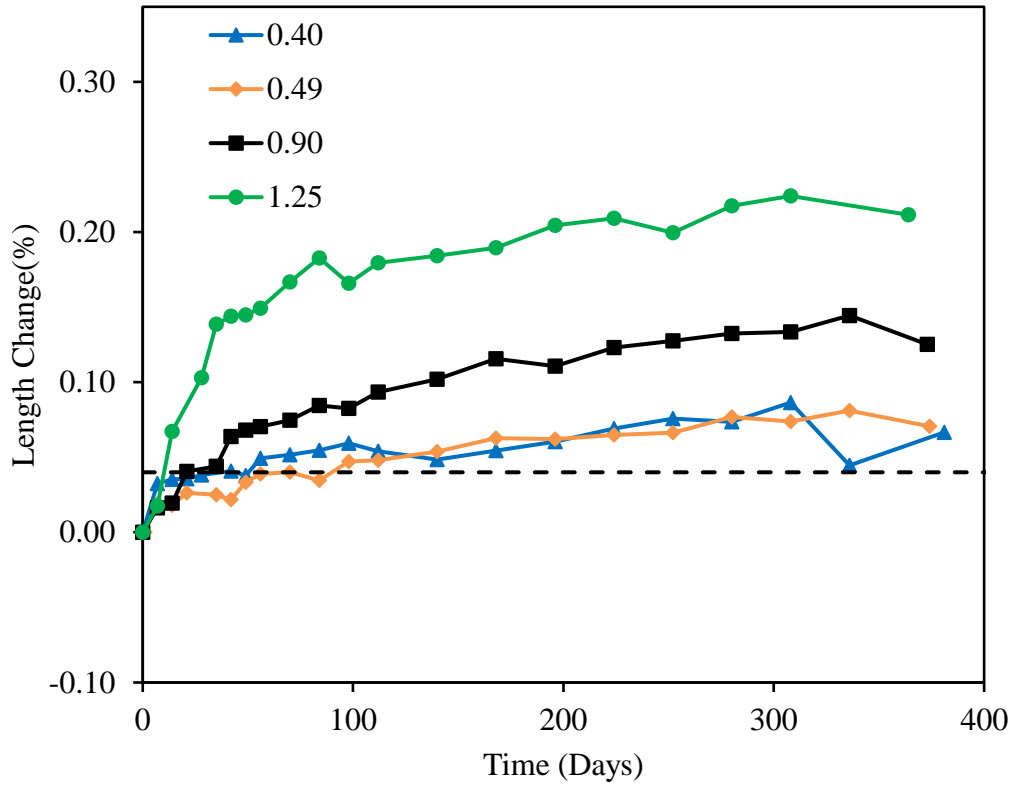
Figure 4.9: Summary of 100% portland cement Spratt coarse aggregate UNBCCT samples stored at 60°C

The UNBCCT data presented in Figure 4.9 shows deleterious expansion for all mixes. All samples have plateaued, with the highest alkali mixes (1.25% and 0.90% Na_2O_e)

commencing deleterious expansion at approximately 14 days, where the lower alkali samples commenced at 70 to 80 days.

4.4. Results for Binary and Ternary Systems

Figure 4.10, 4.11, and 4.12 present the expansion results for binary and ternary concrete mixes with a range of alkali contents, cement replacement levels, supplementary cementitious materials, and reactive aggregates. In each figure the data are labeled by first the reactive aggregate, then the cement replacement level, followed by the type of SCM, and in the case of the ternary system, the second replacement level and SCM. For example a mix made with a Spratt aggregate and 20% fly ash would be denoted as "Spratt 20% FA". Figure 4.10, 4.11, and 4.12 show results for the CPT at 38°C, UNBCCT at 38°C and UNBCCT at 60°C respectively. The dashed line represents the 0.04% expansion limit defining failure in accordance with CSA A23.2-27A and ASTM C1778.
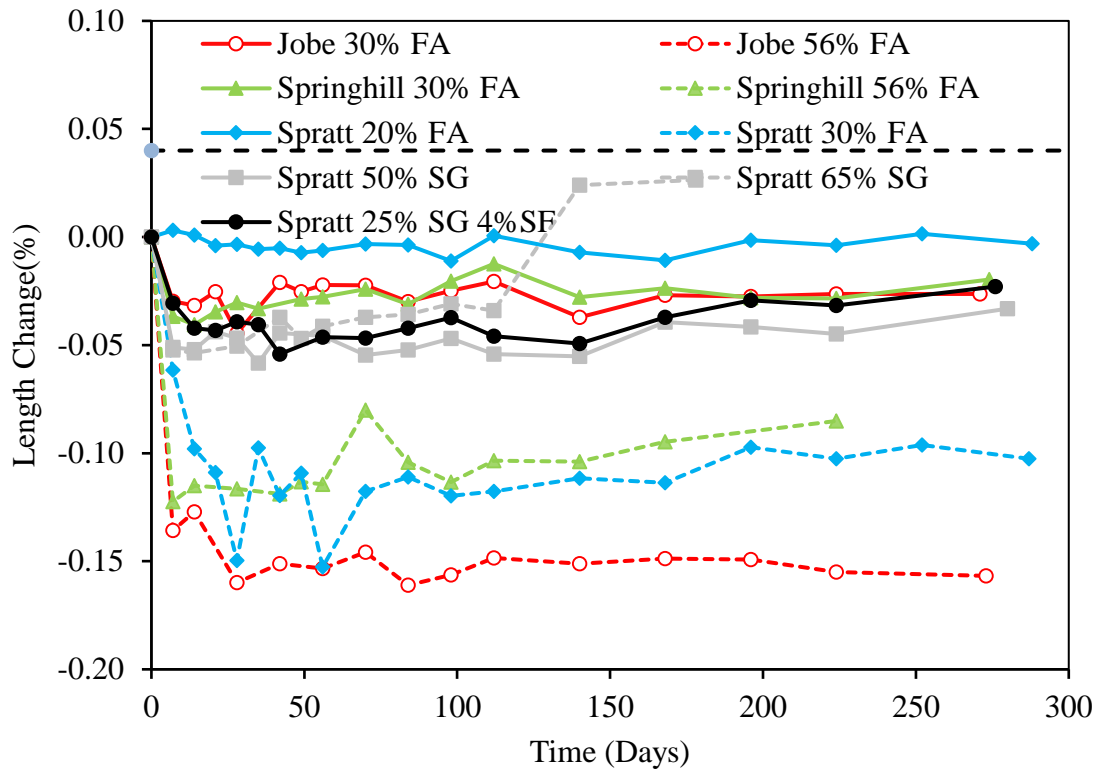
Figure 4.10: Summary of binary and ternary mixes for CPT

The data presented in Figure 4.10 were collected from concrete prism test samples up to a minimum of 180 days. All mixes presented in the figure have not reached a deleterious expansion level during the testing period. A trend that can be noted is that the higher the replacement level for a particular reactive aggregate, the less expansion seen by the sample. This trend is true for all mixes except for Spratt aggregates with slag replacement levels of 50 and 65%. These samples show that a higher replacement level achieved a higher expansion, therefore a mistake must have occurred in the fabrication of the Spratt 65% SG sample.
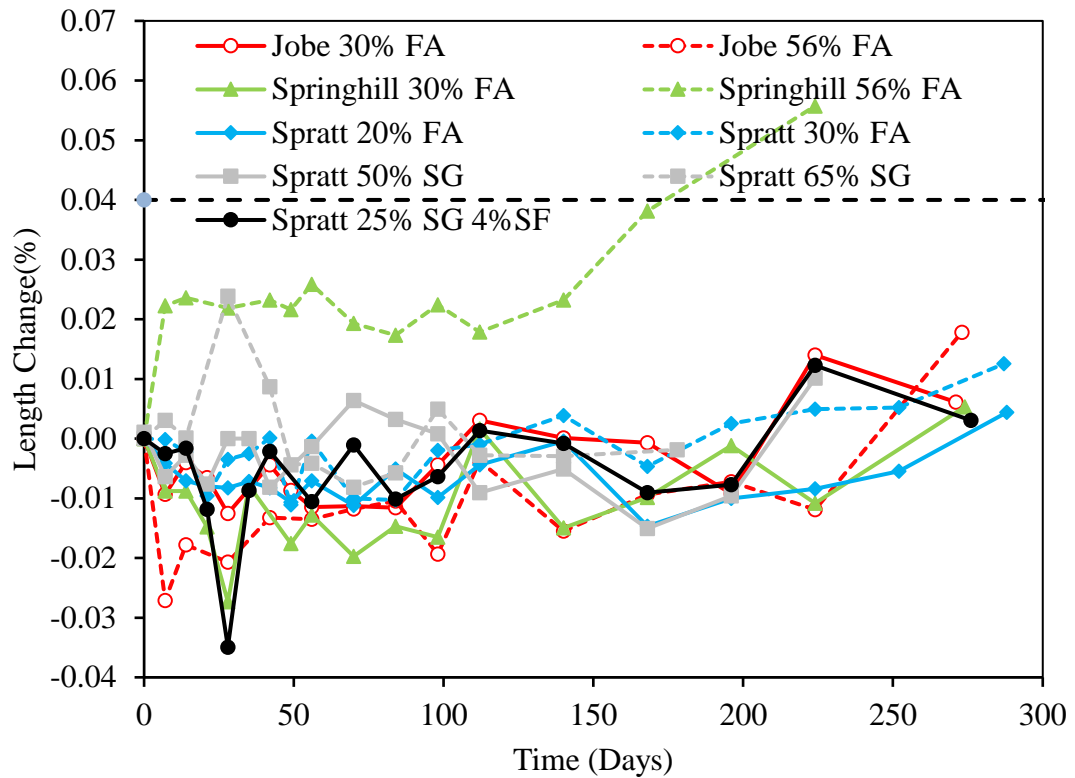
Figure 4.11: Summary of binary and ternary mixes for UNBCCT at 38°C

The UNBCCT (38°C) data presented in Figure 4.11 shows that the majority of replacement levels examined do not yield deleterious expansion. The one case that surpass the 0.04% length change limit was that of Springhill 56% FA. This mix had a higher equivalent alkali content then the Springhill 30%FA (1.25% to 0.9% respectively), leading to the higher expansion level. However, the expansion is unexpected as exposure blocks with similar composition have not expanded at an age of 18 years (see Table 3.9)
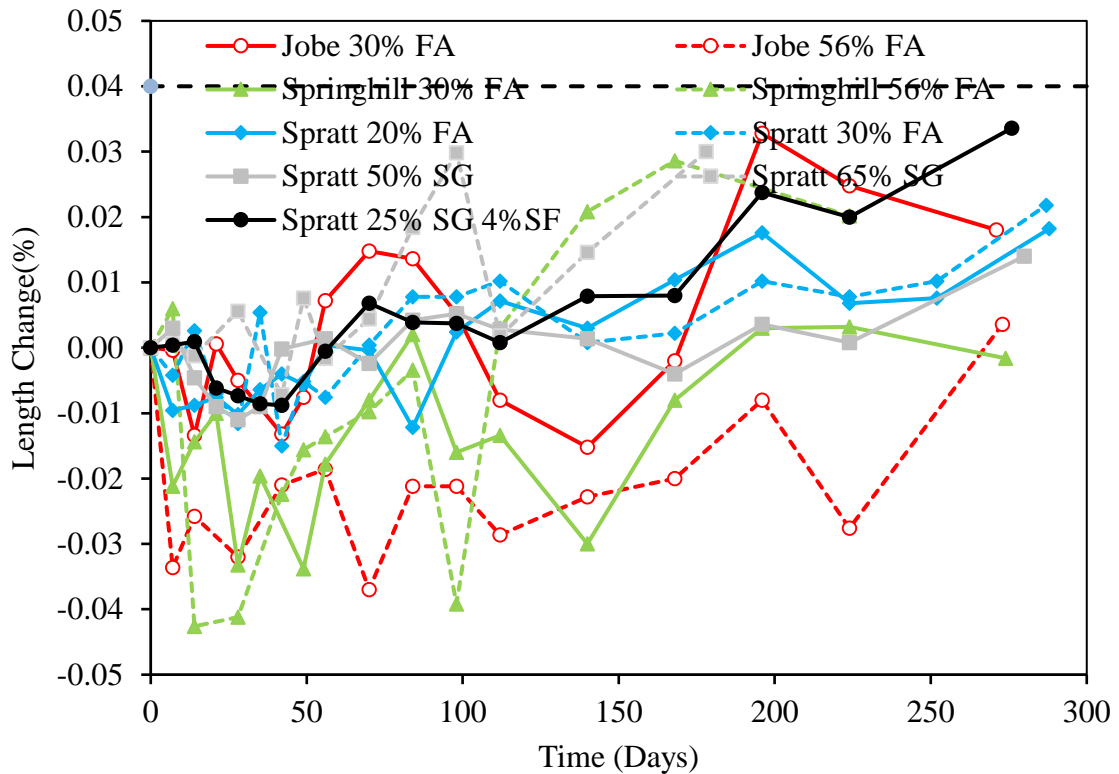
Figure 4.12: Summary of binary and ternary mixes for UNBCCT at 60°C

The UNBCCT (60°C) data presented in Figure 4.12 shows that all of replacement levels examined do not yield deleterious expansion during the time tested thus far. Multiple samples, at the time of the last measurement, had started to show an increase in levels of expansion, and could in the future, surpass the 0.04% expansion mark. The trend of mixes with higher replacement levels yielding lower expansion can be noted in Jobe mixes as well as the Spratt mixes with 20 and 30% cement replacement levels. The Spratt mixes with 50 and 65% slag replacement show the same trend at 38°C and in the CPT, further demonstrating that there may have been a problem with those samples.

4.5. Alkali Inventory Data

The alkali inventory testing can be broken down into three sets of data. The first being length change as seen in Figure 4.13, the second being alkali profiles (acid and water soluble) and bulk alkali contents as seen in Figure 4.14, 4.15, and 4.16, and lastly the alkali contents of host and pore solutions as seen in Figure 4.17. All measurements came from a series of samples cast with 100% portland cement and carbonate aggregates. Half of the samples were stored at 38°C with the others at 60°C. The alkali content that was chosen for this mix was 0.7% Na_2O_e, due to it showing damaging expansion in other mix designs and being in the middle of the range of alkali contents studied within this research.
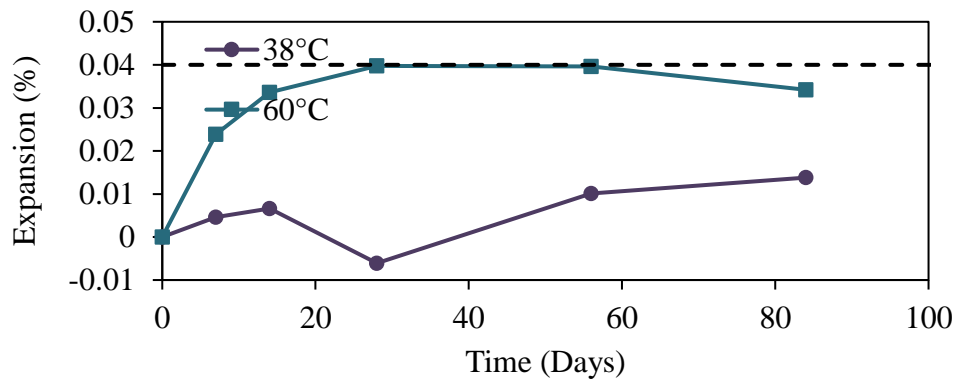
Figure 4.13: Non-reactive expansion data

Figure 4.13 presents the length-change data for the non-reactive samples up to 182 days. It can be seen that some expansion occurred, but stayed below the 0.04% threshold. Samples stored at 60°C expanded more than the companion samples stored at 38°C. These samples had plateaued just under the threshold after 28 days, whereas the 38°C samples continues

91

to show an upward trend, however, little expansion exists due to the aggregate being non-reactive.
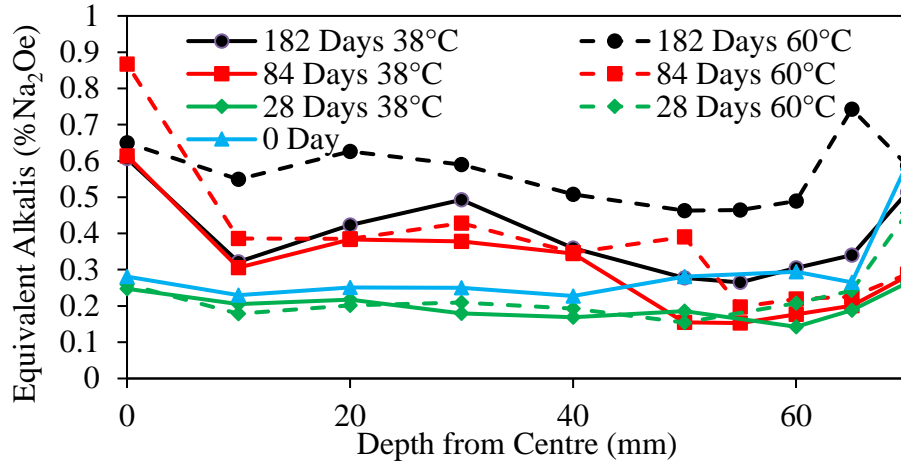
Figure 4.14: Acid-soluble profile

Figure 4.14 shows the acid soluble profiles taken at 0, 28, 84, and 182 days. The general trend for the data are a higher concentration of equivalent alkalis at the surface and center of the samples. Over time these concentrations build up with more found in samples stored at 60°C. It is conjectured that this was caused partly from alkalis that were bound by CSH early on, being replaced by calcium, and through the movement of alkalis to form an equilibrium.
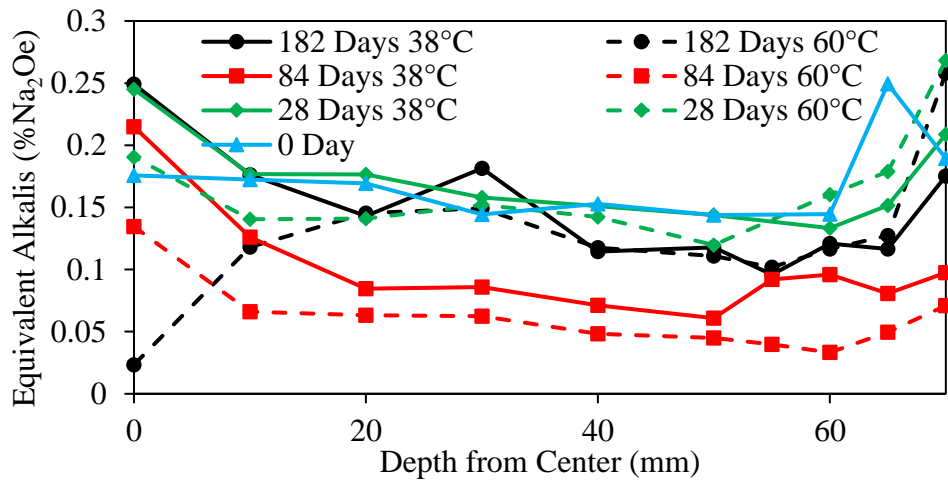
Figure 4.15: Water soluble profile

Figure 4.15 shows the water soluble profiles taken at 0, 28, 84, 182 days. The general trend for these data are a higher concentration of equivalent alkalis at the surface and center of the sample. Over time these concentrations reduce, with lower alkalis measured in samples stored at 60°C.
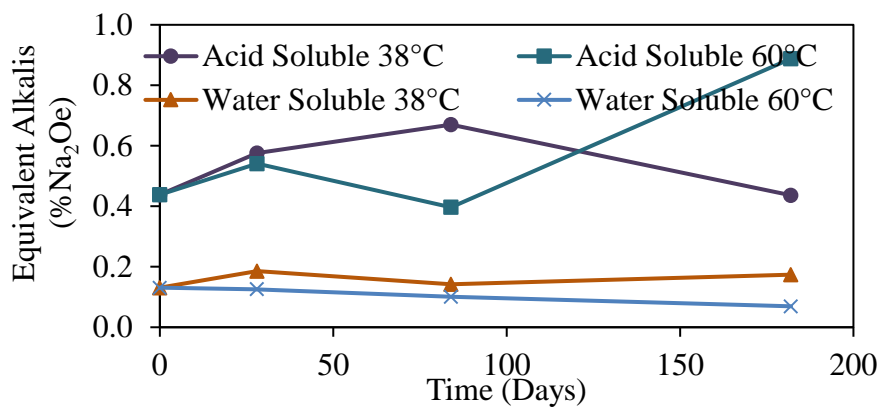
Figure 4.16: Bulk-alkali content over time

Figure 4.16 shows the change in the acid-soluble and water-soluble alkali content over time for the "bulk sample". As expected, the acid soluble alkali contents is greater than that of the water soluble. The acid-soluble alkali contents for 60°C relates well to the acid soluble alkali profiles, both showing an increase of alkalis over time. This trend seems to disagree for 38°C samples where the alkali content remains fairly constant over time. The trend of water soluble alkalis lowering overtime is again shown here for both temperatures.
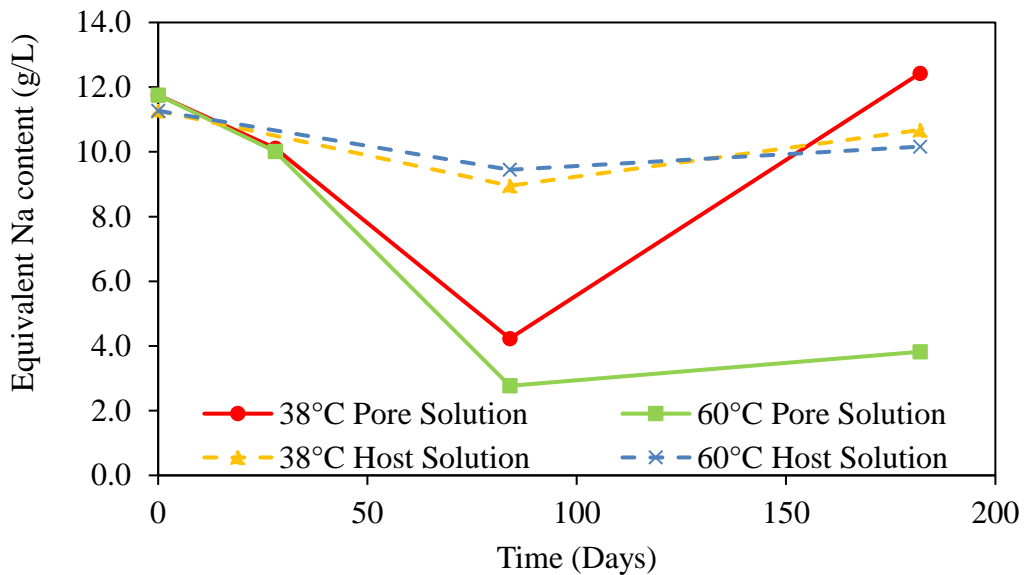
Figure 4.17: Equivalent sodium content of host and pore solution over time

Figure 4.17 shows the change in equivalent sodium content over time, where the equivalent sodium content is a combination of sodium and potassium found in the host and pore solutions. The alkali content found in the host solution for both 38 and 60°C has a slight decrease over time. This explains the increase of alkalis at the surface of the sample due to

94

alkali migration. The pore solution on the other hand was found to drop significantly at the 84 day mark at both temperatures, but after this drop an increase was observed. To better understand this drop in the pore solution alkalinity Figures 4.18 and 4.19 show the equivalent sodium content found in the pore and host solution in terms of sodium and potassium respectively.
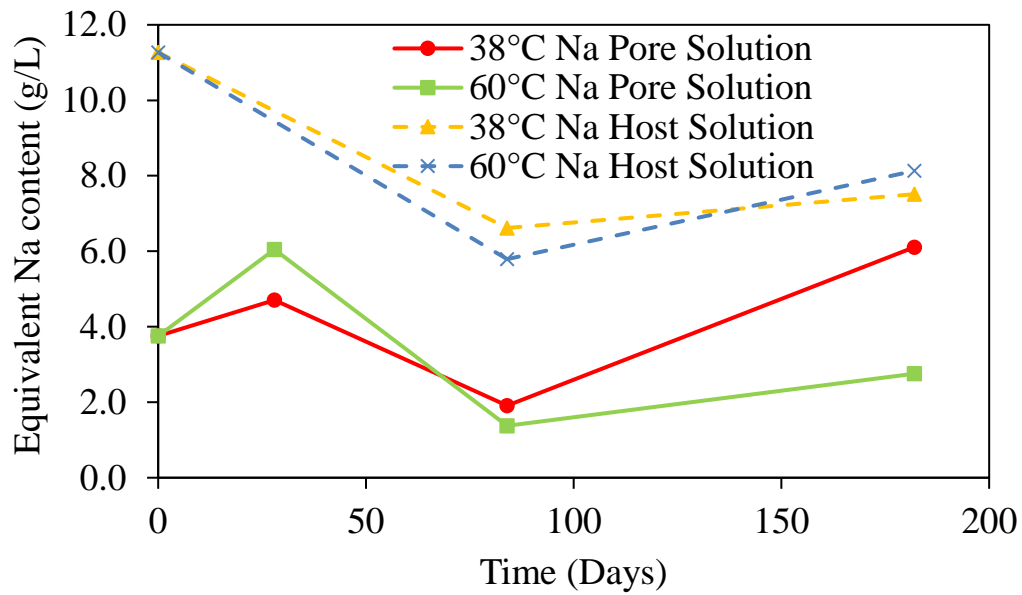
Figure 4.18: Sodium found in pore and host solution

Figure 4.18 shows that there is a 2 g/L drop in sodium at 84 days for both pore and host solutions at 38 and 60°C. This equal drop was caused by the binding of alkalis to CSH and the host and pore solution maintaining equilibrium.
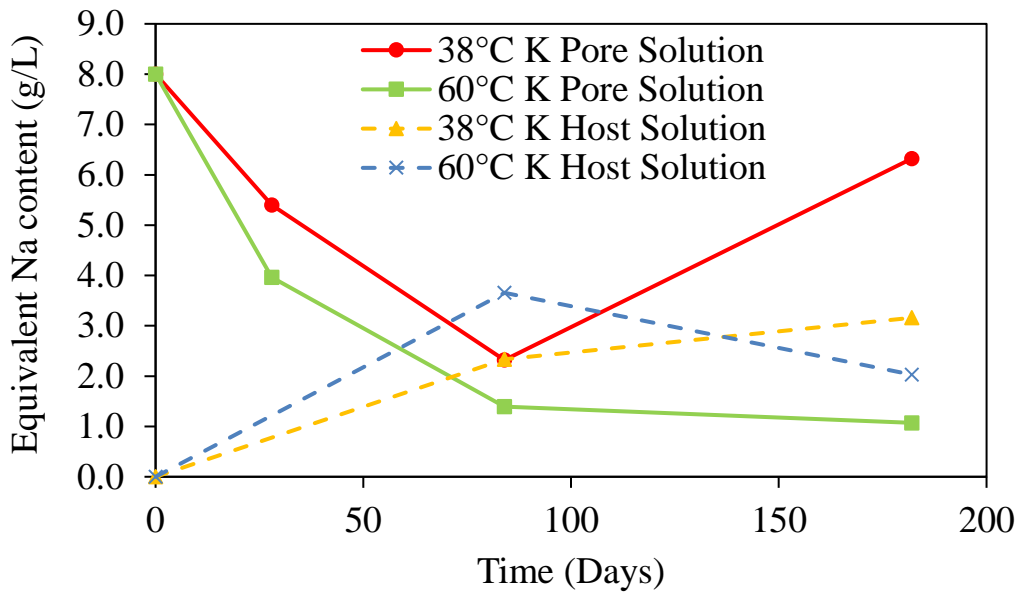
Figure 4.19: Potassium found pore and host solution.

Figure 4.19 shows that the large drop in the pore solution found in Figure 4.17 was caused by the movement of potassium from the pore solution to the host solution in order to maintain equilibrium. This was caused by the fact that the host solution was only made with sodium hydroxide and not a combination of sodium and potassium hydroxide. It is believed that the increase of potassium at the 182 day mark for 38°C pore solution was caused by an error and should have resembled that of the 60°C pore solution.

5. Discussion

The results previously presented will be discussed in two main sections, expansion data and alkali inventory. The expansion data will be examined and compared to field exposure site blocks, CPT, and other newly developed tests to verify if the UNBCCT produced similar results (in the sense that if both yielded passing results, failing results, or a combination of the two). Furthermore, alkali thresholds will be examined to verify the applicability of testing "job" mixes, as well as the effect of variation in temperature, and the usage of SCMs to gauge their effect on test duration. Finally, alkali inventory data will be examined to determine if there was a change in the availability of alkalis in the systems (leaching or absorption) to verify the effectiveness of the UNBCCT storage condition in terms of maintaining "alkali equilibrium"

5.1. Effects of Sample Composition and Storage Conditions on Expansion

The storage conditions, aggregates, and alkali contents all had considerable impact on the levels of expansion observed. To understand what the effects of each were, they will be examined below. The data for mixes with 100% PC will be examined in detail. However, the data for SCM mixes are not consider to be sufficiently advanced to allow for detailed interpretation at this time.

5.1.1. Storage Conditions

The storage conditions for the UNBCCT samples utilized two temperatures; half of the samples were stored at 38°C and the others at 60°C. The temperature of 38°C was chosen due to it being used for the concrete prism test (CPT – ASTM C1293) whereas a

temperature of 60°C was chosen due to higher temperatures accelerating expansion (Gautam & Panesar, 2017). A temperature greater than 60°C was not used because of the risk of a change in the pore solution composition and possibly the risk of DEF. Higher temperatures can cause sulfate ions to replace hydroxyl ions in the pore solution, thus lowering its concentration and pH in the concrete. Also higher temperatures can lead to delayed ettringite formation (DEF), and increase the dissolution of silica, leading to expansion that would not normally occur at lower temperatures.

The effect of higher temperature is shown to result in a significant increase in the onset of expansion. Figure 5.1 shows that for high alkali mixes (above 0.6% Na_2O_e) in early stages of testing; 60°C samples have accelerated levels of expansion. However, at later ages of expansion, the 60°C specimens are surpassed by the 38°C samples. This phenomenon was previously noted in work done by Fournier et al. (2004) where the authors observed the same trend in CPT samples, and attributed it to sulfate ions replacing hydroxyl ions due to the increase solubility of ettringite at higher temperatures, as well as an increase in leaching. The low-alkali mixes also observe an accelerated expansion at higher temperatures, but have yet to be surpassed by their lower temperature counterparts. If the test was to be run until ultimate expansion was achieved, it is thought that the trend would continue.
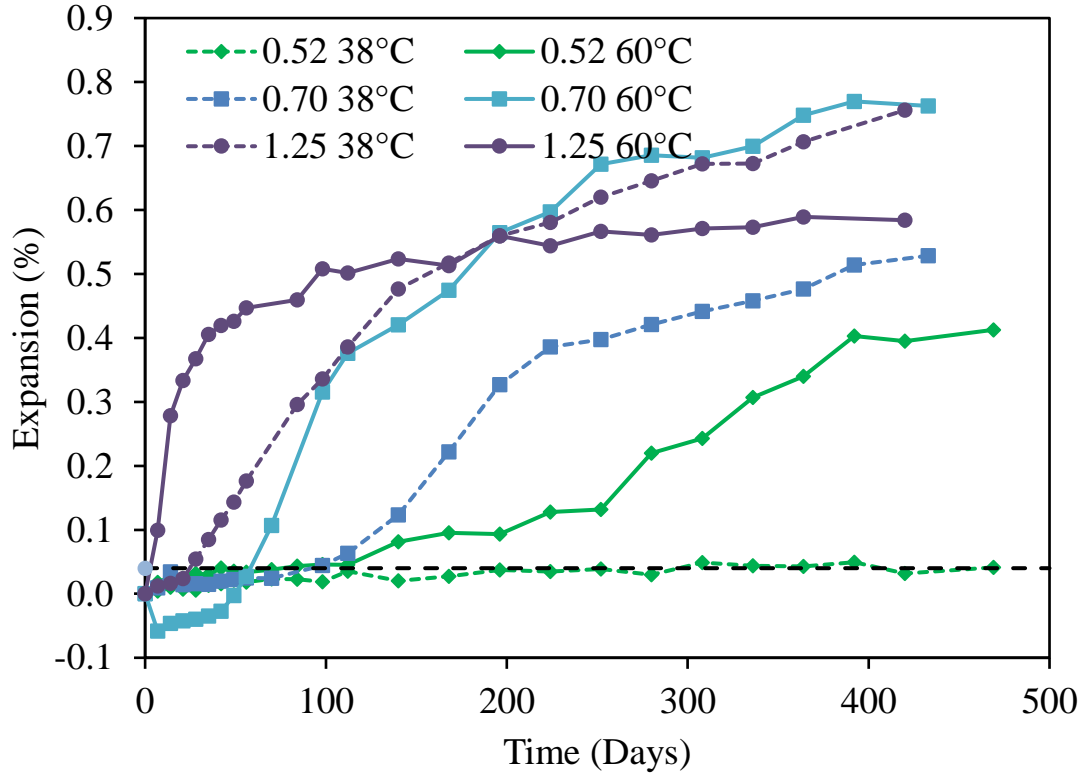
Figure 5.1: Effects of temperature on expansion for Jobe sand

5.1.2. Aggregate

The aggregates used for the experiment fall into two categories of reactivity using the criteria of CSA A23.2-27A: Standard practice to identify degree of alkali-reactivity of aggregates and to identify measures to avoid deleterious expansion in concrete (Canadian Standards Association, 2014b). The Spratt aggregate is classified as highly reactive, where Jobe and Springhill are classified as extremely reactive. Figure 5.2 demonstrates that the extremely reactive aggregates have a more destructive potential, with Jobe being the most

aggressive. Yet again, the trend of 38°C samples overtaking 60°C samples was demonstrated, even with aggregates of varying reactivity levels. For Jobe and Springhill aggregates, the expansion at 38°C surpassed that at 60°C within a year, whereas it took more than one year for this phenomenon to be observed with Spratt aggregate.
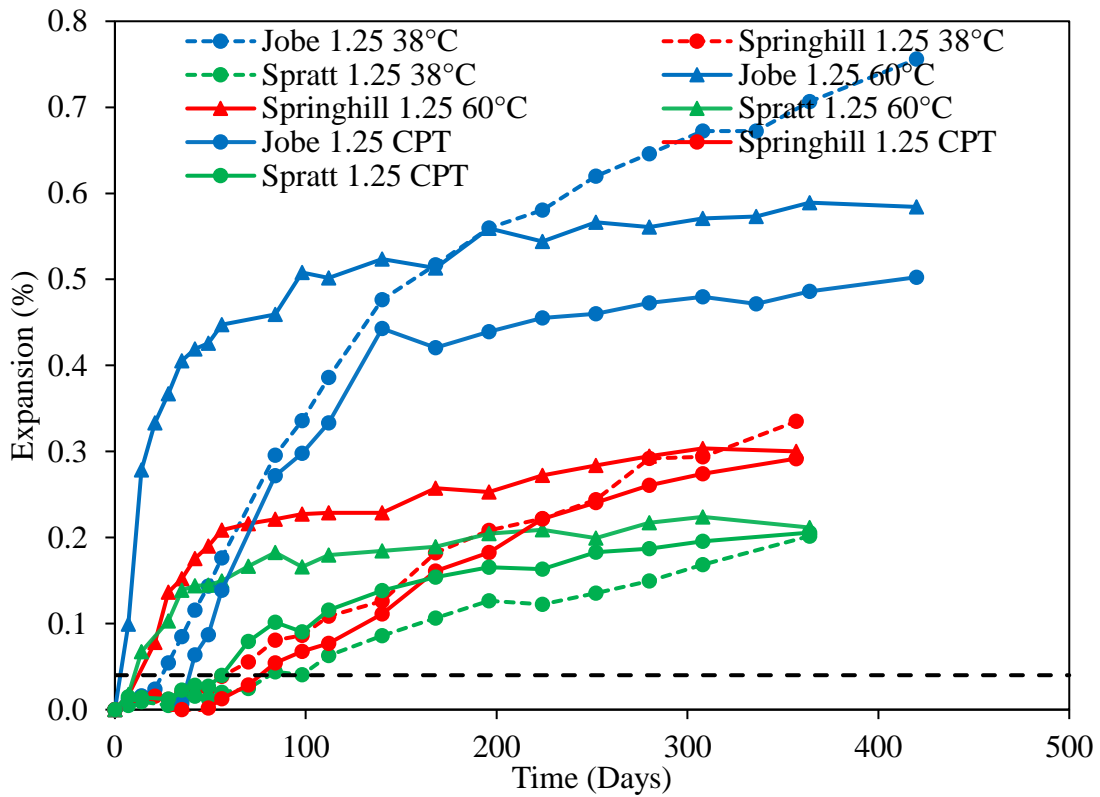
Figure 5.2: Expansion comparison of Jobe, Springhill, and Spratt, at 1.25% alkalis

5.1.3. Alkali Content

The alkali content of the concrete also has a direct relationship on the level of expansion. Figure 5.3, 5.4, and 5.5 shows that as the alkali content increases so does the expansion at

a given age. This is true across all test methods, due to alkalis being one of the four ingredients needed to fuel the reaction. The exceptions to this observation can be seen in Figure 5.3 and Figure 5.5. The 60°C samples in Figure 5.3 are shown to have a drop in expansion between 0.92% and 0.95% Na_2O_e, where Figure 5.5 has a drop after 0.9% for the CPT at 38°C. This drop in overall expansion is possibly the result of alkali leaching. The 0.92% mix was achieved through the use of only portland cement, where 0.95% and 1.25% were obtained through adding NaOH pellets to the mix water as described in ASTM C1293. Since the alkalis were added in the form of a solution, it is likely that they were immediately available to the pore solution. The alkalis could then have been consumed and therefore not contributed to later age expansion, or they could have migrated out of the sample into the surrounding host solution to balance the pH between the two, thus removing fuel from the reaction.

As for the variance seen in Figure 5.5, it is possibly due to error on the creation of the sample or host solution. Since both CPT and UNBCCT at 38°C observed a much greater expansion than that seen from an exposure block, it is expected that the mix was improperly made with a higher alkali content.
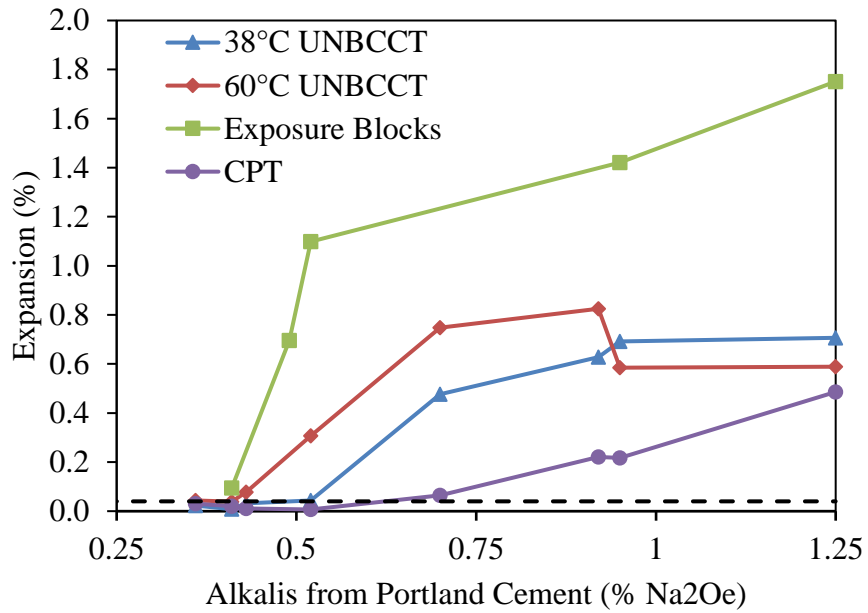
Figure 5.3: The expansion of Jobe samples at various alkali contents and test methods after 1 year compared to exposure blocks at about 10 years
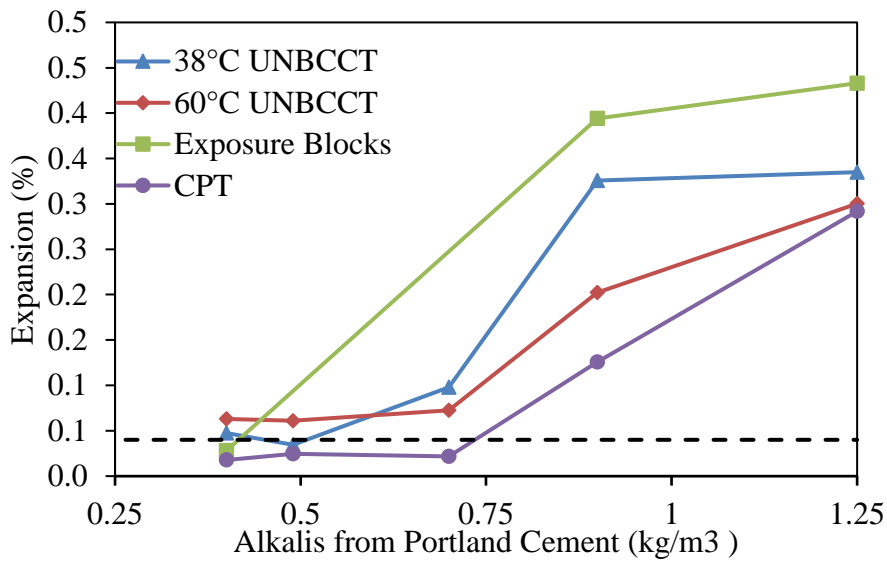
Figure 5.4: The expansion of Springhill samples at various alkali contents and test methods after 1 year compared to exposure blocks at between 15 and 18 year

102
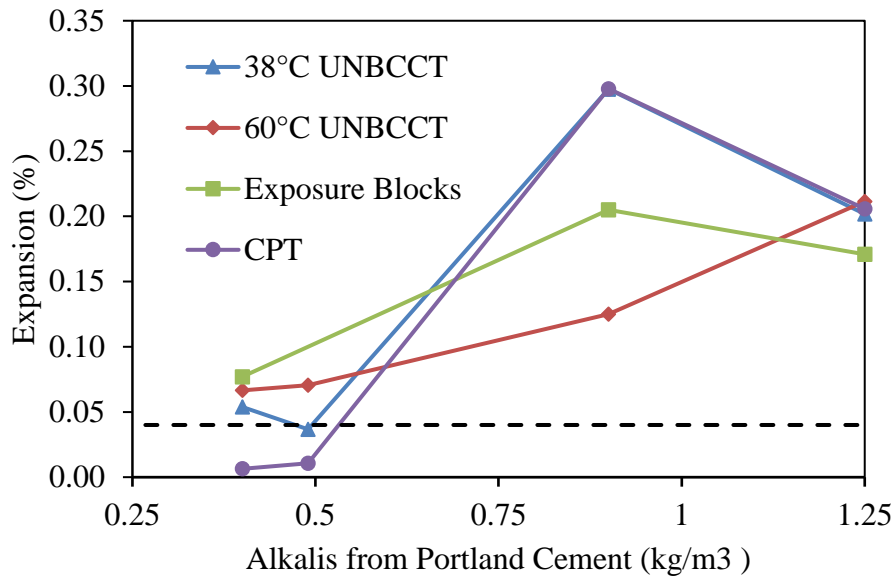
Figure 5.5: The expansion of Spratt samples at various alkali contents and test methods after 1 year compared to exposure blocks at between 15 and 18 years

5.1.4. Supplementary Cementitious Materials

The effects of SCMs on ASR reactive aggregates are well known, dating back to Stanton's research in 1940 (using natural pozzolans), as a proposed method of mitigation. The effects of SCMs used in the experimental work done can be seen in Figure 5.6, where the samples with no SCMs reached a higher level of expansion, a moderate level of SCMs had some expansion, and a sufficient level of SCMs had little to no expansion. It should be noted that the SCM samples have yet to reach the 2-year mark, as prescribed in ASTM C1293. It is therefore considered too early to determine whether the UNBCCT is effective for evaluating the performance of SCM's in "job mixtures".
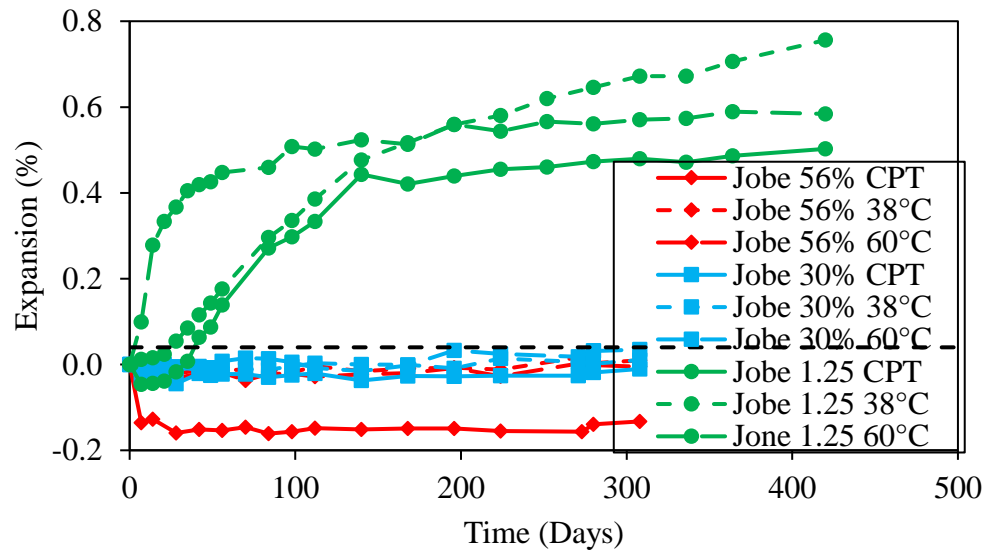
Figure 5.6: Expansion of UNBCCT Jobe 1.25% Na$_2$O$_e$ with and without fly ash

5.2. Comparison to CPT

5.2.1. Plain Portland cement Systems

The CPT method as denoted by ASTM C1293, is the preferred current standard for testing aggregates for susceptibility to ASR and evaluating the efficiency of preventative measures. When comparing the CPT to the UNBCCT after a year, the results between the two vary significantly. Figure 5.2 shows a comparison of samples cast and tested using ASTM C1293 and the UNBCCT at both 38°C and 60°C. It is evident that the UNBCCT shows damaging expansion in an accelerated fashion compared to the CPT for all cases except one (that being Spratt stored at 38°C).

104

Beside the ability to test samples with the same mix criteria as ASTM C1293, samples tested using the UNBCCT can be prepared at a range of alkali contents such that alkali thresholds can be observed. CPT and UNBCCT "job mixtures" can be seen in comparison in Figure 5.7, where the CPT was conducted only at 38°C and the UNBCCT at both 38°C and 60°C. Out of these 17 mixes at the one-year mark, 47.1% of the CPT samples, 64.7% of the UNBCCT-38°C samples, and 94.1% UNBCCT-60°C samples exceeded the 0.04% expansion mark. The samples that the CPT determined to be non-damaging were those with cement alkali contents in the range of 0.36 to 0.70%. Out of the 9 mixes that passed the CPT, 4 failed using both UNBCCT temperatures, 4 failed UNBCCT at 60°C, and only 1 passed all three tests (did not exceed 0.04%).
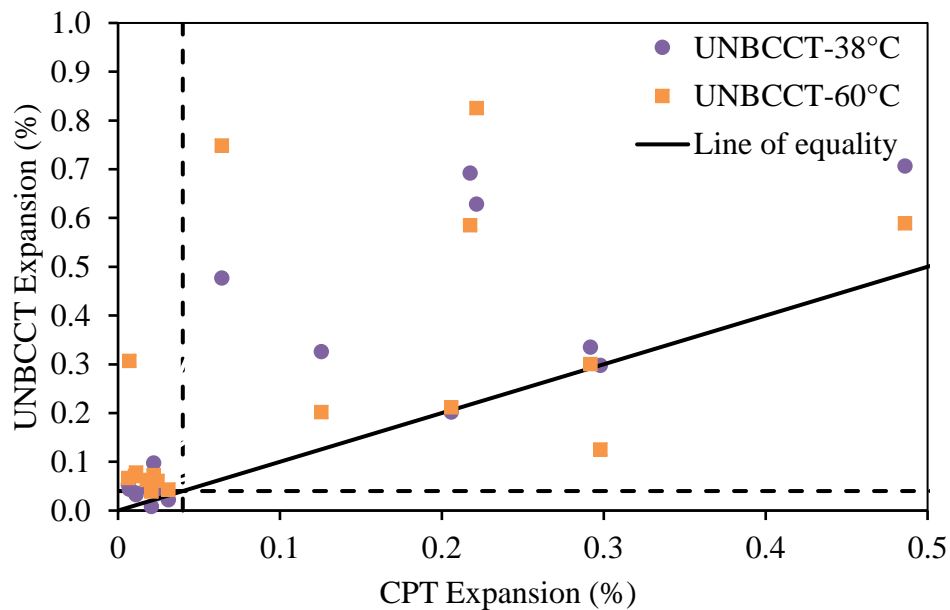
Figure 5.7: Pass Fail graph for CPT and UNBCCT portland cement systems

More expansion was observed in the UNBCCT and at a lower alkali content; in other words the alkali threshold required to initiate expansion was lower in the UNBCCT compared to the CPT. This was due to factors such as the size of the samples and the leaching of alkalis from the CPT. Larger samples tend to have more expansion due to their size (Zhang et al., 1999), the effects of size on leaching rates (Thomas et al. 2006), and the lack of leaching due to submersion in solution.

The time to initiate expansion varies between test methods as well. Figure 5.8, 5.9, and 5.10 demonstrate that as the alkali content decreases, the time to initiate damaging expansion (above 0.04%) increases. It can also be seen that a proportion of the CPT and UNBCCT at 38°C samples have yet to reach the 0.04% limit, where others of the same mixes have in samples of the UNBCCT at 60°C. This is noted by the CPT and UNBCCT at 38°C not having the same amount of data points as the UNBCCT at 60°C. All samples stored at 60°C had surpassed the 0.04% mark in a more rapid fashion than other test methods, leading yet again to the possibility of an accelerated test method.
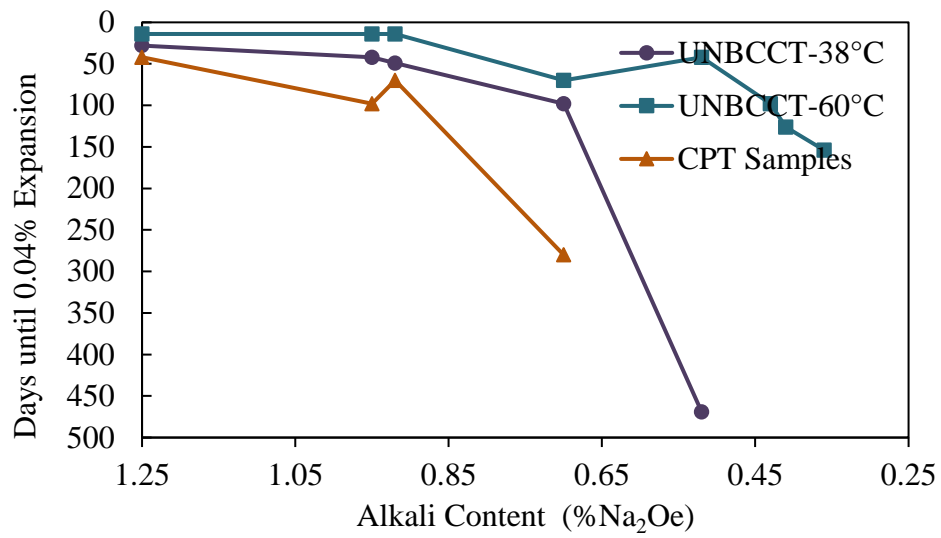
Figure 5.8: Time when expansion reaching 0.04% for Jobe Mixes
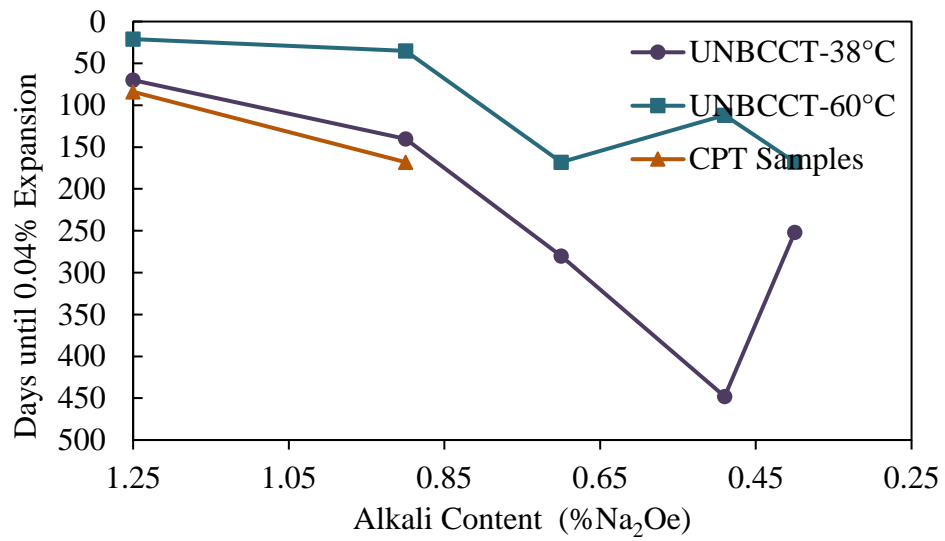
Figure 5.9: Time when expansion reaching 0.04 for Springhill Mixes
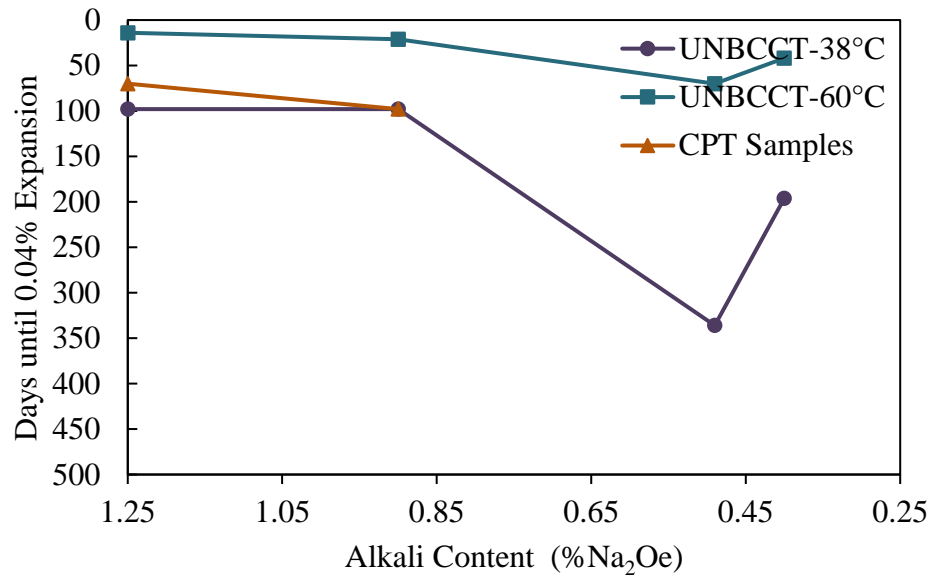
Figure 5.10: Time when expansion reaching 0.04 for Spratt Mixes

5.2.2. Binary and Ternary Systems

The data are not sufficiently advanced to evaluate the test methods with regards to SCMs at this time; neither test method has shown expansion at any temperature and longer term data are needed.

5.3. Comparison to Exposure Blocks

While ASR testing can be conducted in the controlled environment of a laboratory, the only way to view the long-term effects of the environment is to create and monitor exposure blocks. Exposure blocks are gaining popularity for their ability to act as a surrogate structure for the prediction of long-term potential and mitigation of ASR (Ideker et al.,

2012). The benefits of exposure blocks are their ability to test "job mixtures", but a disadvantage is the length of time required for testing.

5.3.1. Plain Portland Cement Systems

A comparison of exposure block data to that of the CPT and UNBCCT methods is presented in

Table 5.1 and Figure 5.3, 5.4, and 5.5. The data for these exposure blocks were retrieved from work done by Fournier et al. (2016) and Thomas et al (2013b) for Spratt and Springhill aggregates at the CANMET exposure site in Ottawa, and from work done by Stacey et al. (2016) at The University of Texas at Austin exposure site for Jobe sand. It is evident that exposure blocks see a greater level of expansion than the other test methods. This is due mainly to their size being much greater than that of the UNBCCT samples and their age. This is the same trend as noted for the comparison between the CPT and UNBCCT methods. However, the variance between that of the exposure block and the CPT is much greater than that seen between the UNBCCT and the exposure blocks due to the size effect, and leaching of alkalis in the CPT (Thomas et al., 2006). When comparing Figure 5.11 and Figure 5.7, it can be seen that the UNBCCT test shows a much greater agreement with the exposure block than that of the CPT. This leads to the observation that the UNBCCT resembles findings closer to field data than that of the CPT. This is supported by examining the coefficient of correlation of each method in comparison to exposure blocks. The test method with the lowest coefficient was that of the CTP at 0.5415. The UNBCCT at 38°C and 60°C have a coefficient of correlation of 0.6801 and 0.9457

respectively. These values show that there was a higher correlation between the UNBCT
and the exposure blocks than that of the CPT.

Table 5.1: Summary of expansion data for 100% Portland cement systems

Aggregate	PC Alkali (% Na$_2$O$_e$)	PC Alkali (kg/m³)	Expansion of lab Test (%)			Exposure Block Expansion (%)	Age of Blocks (years)
			CPT (38°C)	UNBCCT-38°C	UNBCCT-60°C		
Jobe	0.41	1.72	0.029	0.028	0.049	0.094	9.5
	0.52	2.18	0.011	0.041	0.413	1.108	10.4
	0.95	3.99	0.227	0.743	0.580	1.434	10.4
	1.25	5.25	0.503	0.756	0.584	1.751	9.56
Spratt	0.40	1.68	0.006	0.054	0.067	0.085	15.0
	0.90	3.78	0.298	0.298	0.125	0.206	15.0
	1.25	5.25	0.206	0.202	0.212	0.336	18.1
Springhill	0.40	1.68	0.016	0.046	0.085	0.029	15.0
	0.90	3.78	0.126	0.326	0.202	0.391	15.0
	1.25	5.25	0.292	0.335	0.300	0.495	18.1
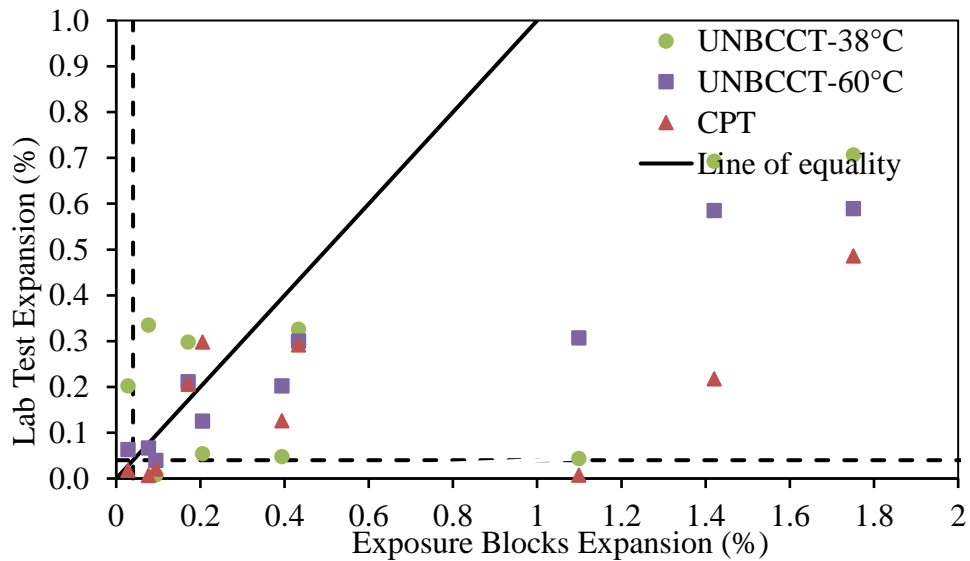
Figure 5.11: Pass/fail graph of 100% Portland cement UNBCCT and CPT vs exposure
blocks

As denoted above, the major flaw of the exposure block test is the time to reach the "damaging" expansion level of 0.04%. Some blocks as shown in Chapter 3 and by Fournier et al. (2009) take months, if not years to reach this level, where corresponding UNBCCT samples reach this level in a matter of weeks. This expansion in a fraction of the time allows for the UNBCCT to yield a verdict in a reasonable amount of time compared to the exposure blocks.

It should also be noted that exposure blocks see damaging expansion at lower alkali contents compared to laboratory tests such as CPT. The UNBCCT does expand at low alkali contents, but not all have reached the 0.04% expansion threshold. Examples of blocks that have caused damaging expansion, but have not had UNBCCT samples reach the threshold are Jobe 0.41% and 0.52% alkali at 38°C. It is likely that over time, these samples will reach and surpass 0.04% expansion at later ages.

5.3.2. Binary and Ternary Systems

The exposure block data for binary systems for Springhill and Spratt aggregates were retrieved from the work done by Fournier et al. (2016) at the CAMNET exposure site in Ottawa, Ontario. The exposure block data for the ternary system was retrieved from the work done by Hooton et al. (2013) at the Kingston, Ontario exposure site. Figure 5.12 shows the comparison of the exposure blocks and both the UNBCCT and CPT test methods. Most samples fall within the pass-pass zone, which is to be expected for samples comprised of SCMs, however, some outliers do exist. This may be due to the age of the UNBCCT samples being much younger than their counterpart blocks. The CPT samples

111

stray much farther from the line of equality that the UNBCCT counterparts. This yet again shows the shortcomings of CPT test through lack of likeness to exposure blocks. The coefficient of correlation for the CPT in comparison to the exposure blocks was 0.4384. The coefficient for the UNBCCT at both 38°C and 60°C was 0.4770 and 0.5967 respectively. These values once more the UNBCCT yields result more in line with exposure block than that of the CPT

Table 5.2: Summary of expansion data for binary and ternary systems

Aggregate	SCM and replacement level (%)	Expansion of lab Test (%)			Exposure Block Expansion (%)	Age of Blocks (years)
		CPT (38°C)	UNBCCT-38C	UNBCCT-60C		
Spratt	20% FA	0.002	0.004	0.018	0.062	15
	30% FA	-0.096	0.013	0.022	0.016	15
	50% SG	-0.033	0.010	0.014	0.022	15
	65% SG	0.026	-0.002	0.030	0.014	15
	25% SG 4% SF	-0.023	0.0031	0.034	0.030	20
Springhill	30% FA	-0.020	0.005	-0.002	0.067	15
	56% FA	-0.085	0.056	0.020	0.005	18.2
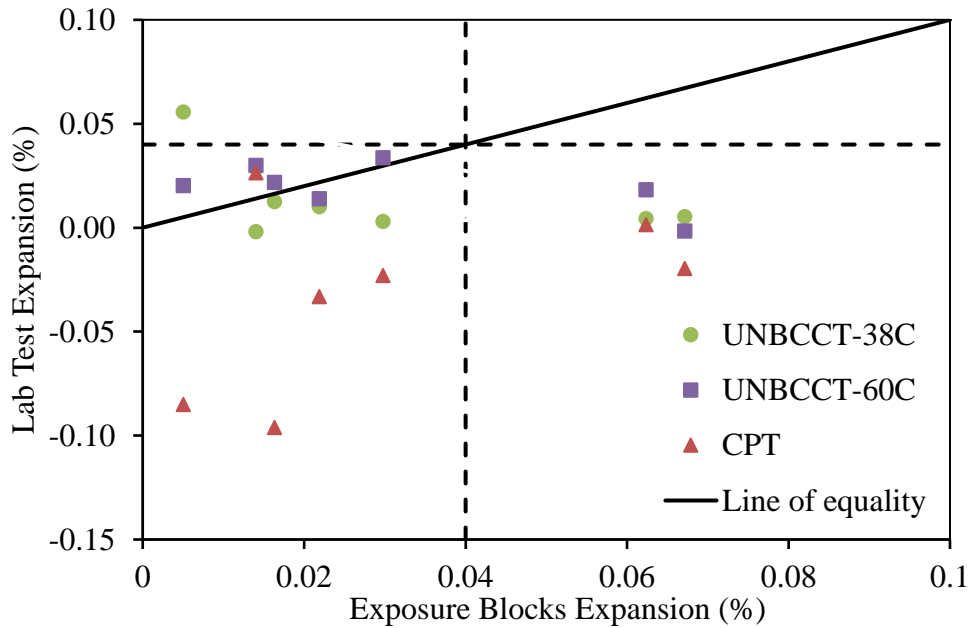
Figure 5.12: Pass/Fail graph of SCM Exposure Block vs CPT and UNBCCT

5.4. Comparison to the CCT

The CCT as reported by Stacey et al. (2016) uses cylinders cast in a mould with filter fabric placed around the interior circumference. The size of the mould recommended by Stacey et al. is 150mm x 300mm. The concrete is cast 6mm shorter than the mould to allow for ponding of water. The water with the help of the filter fabric was able to encompass the sample in a thin film, thus allowing the sample to stay at a 100% RH environment.

The CCT test method had flaws when dealing with low-alkali concrete mixtures. It was noted by Stacey et al. (2016) that the test lacked the ability to demonstrate that low-alkali concrete can cause damaging expansion as found in exposure blocks. Figure 4.1 to Figure 4.9 validates that the UNBCCT test can detect damage with an equivalent alkali content

as low as 0.41%, while the CCT was able to detect expansion with an alkali content of 0.52%. Figure 5.13 shows that expansion seen in the CCT at alkali contents of 0.52% and 0.78% at both 38°C and 60°C are dramatically lower than that found with the UNBCCT at a level of 0.52%. This difference shows that the CCT does not have as close resemblance to exposure blocks as the UNBCCT.
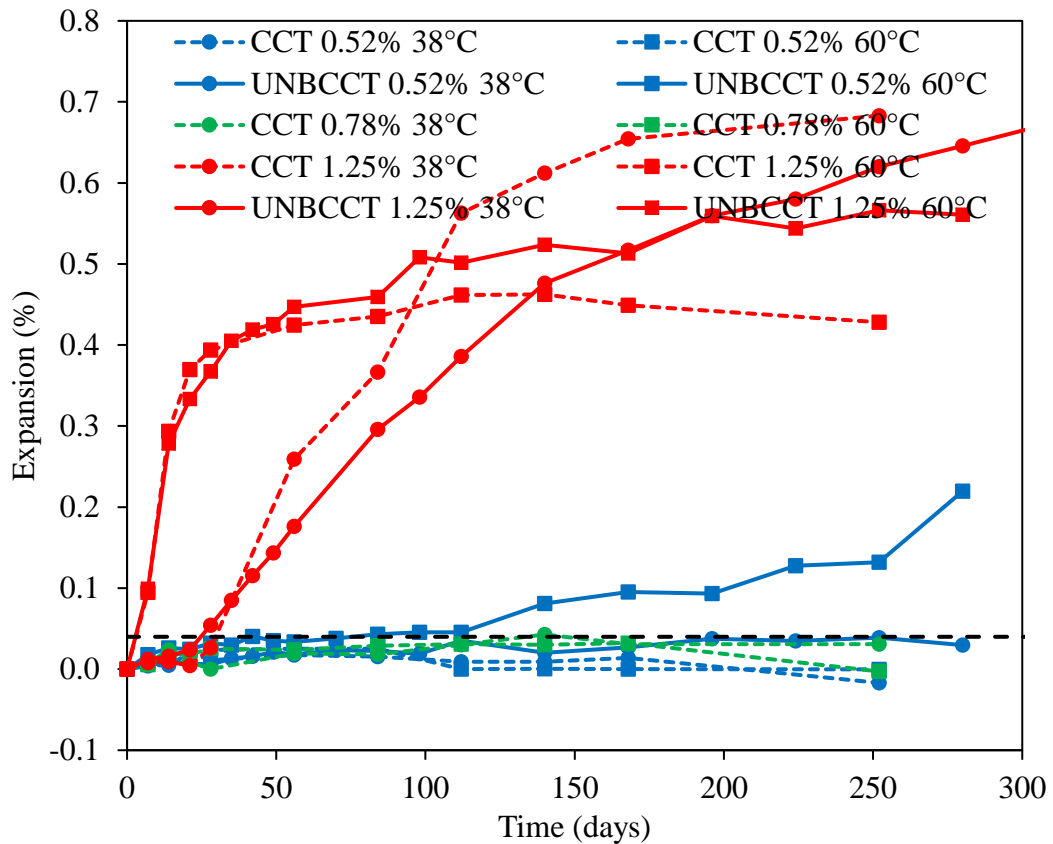
Figure 5.13: CCT expansion compared to UNBCCT

Time is another key factor when it comes to testing. The CCT has the potential to yield a pass/fail result in as little as 15 weeks. This short time frame bodes well if a highly reactive

aggregate were to be tested, but for slowly-reactive or moderately-reactive aggregates, more testing is still required to demonstrate the ability of the CCT as an accelerated test method. The UNBCCT likewise has only been tested with highly (Spratt) and extremely reactive (Springhill and Jobe) aggregates, therefore more testing is required to validate for less reactive aggregates.

The one benefit that the CCT has is that at a higher alkali contents the samples seem to have a more accelerated reaction at 38°C then those of the UNBCCT. Figure 5.13 demonstrates this by showing the CCT at 1.25% stored at 38°C expanding much more rapidly than the UNBCCT. However, the UNBCCT does produce a higher ultimate expansion.

5.5. Alkali Inventory

The alkali inventory work conducted shows an increase in both acid and water soluble alkalis over time as seen in Figure 4.14, 4.15, and 4.16. The acid soluble alkalis had much more variation than the water soluble. The data from the "bulk sample" generally agrees with that of the alkali profiles. The increase in alkalis is believed to come from a slight amount of migration from the pore solution to maintain equilibrium as alkalis were bound by CSH. It should be noted that the aggregate used was non-reactive, therefore the possibility of the alkalis being bound in a gel is not feasible. The decrease in equivalent alkalis observed by the host solution at both 38 and 60°C validates that as alkalis were being bound by the CSH, there was a small amount of migration happening in order to maintain equilibrium.

115

The profiles generated for the alkalis over time for both acid and water-soluble can be observed in Figure 4.14 and 4.15 respectively. It is evident from these figures that the alkali content is uniform across the interior of the sample, with a spike on the surface (where it was in contact with host solution) and in the center. The spike in the center is assumed to be noise in the data.

The pore solution data found in Figure 4.17 has a dramatic drop found between the 28 and 84 days. This drop was explained by Figures 4.18 and 4.19, where the equivalent alkali contents were broken down into sodium and potassium respectively. The drop was explained by the movement of potassium from the pore solution to the host solution in order to maintain equilibrium. However, the increase in potassium for the 38°C pore solution at 182 days was believed to be caused by an error, as no increase was seen by the 60°C pores solution sample.

The presence of leaching of alkalis was not fully observed in the non-reactive samples as the host solution did not see an increase in its sodium content, but only potassium. This observation can be applied to the reactive samples used for the other aspects of the testing program yielding the possibility of the movement of potassium from the pore to the host solution. However it is speculated that the movement of potassium would be less for the reactive samples, as some of the potassium would have reacted with the silica to form the gel.

6. Conclusions

The conclusions that can be drawn from these experiments presented in this dissertation revolve around the flaws found in current test methods (both standardized and experimental) and the similarity of the results to field data. The presence of leaching was also tested through an alkali inventory, as well as the feasibility of testing "job mixes". It was the hope of this work to improve on current tests such that a more reliable and accurate test could be developed. From the work conducted within this research, the following conclusions can be made:

- The UNBCCT was found to be more reliable than the CPT and other test methods for the determination of damaging expansion found in low-alkali cement concretes.
- The results generated for both 38°C and 60°C do not exactly mirror those found in exposure blocks, but do show a trend of rejecting the same damaging mixes.
- The use of a higher temperature can be used to accelerate the time of the test, however it will yield less expansion over time.
- The UNBCCT works well with both fine and coarse aggregates but sufficient data have yet to be generated to evaluate mixtures containing SCMs.

Leaching of alkalis was not fully prevented due to the movement of potassium from the pore solution the host solution. This could lead to a lower expansion level being seen than what would normally be generated.

7. Recommendations

In order to further develop the UNBCCT, the following modifications to the test method are recommended:

- The use of KOH in the host solution in addition to NaOH should be investigated in order to create a more realistic surrogate pore solution to mitigate the movement of potassium ions through the concrete.

- The production of specimens with a wide range of sizes and dimensions should be conducted in order to investigate the impacts on the reliability of the test when compared to exposure blocks.

- The use of more SCMs is required especially at various replacement levels to obtain a better grasp of their effects and the ability of this test method to determine their performance.

- The alkali profiling of reactive samples to further observed the movement of alkalis from the host solution into the pore solution.

References

ACI Committee 201. (1991). Guide to Durable Concrete Reported. *ACI Materials Journal*, *88*(5), 544–582.

ASTM International. (2008a). ASTM C1293: Standard Test Method for Determination of Length Change of Concrete Due to Alkali-silica reaction. In *Annual Book of ASTM Standards*. West Conshohocken,PA: ASTM International. https://doi.org/10.1520/C1293-08B.2

ASTM International. (2008b). ASTM C1567: Standard Test Method for Determining the Potential Alkali-Silica Reactivity of Combinations of Cementitious Materials and Aggregate (Accelerated Mortar - Bar Method). In *Annual Book of ASTM Standards*. West Conshohocken, PA: ASTM International. https://doi.org/10.1520/C1567-13.2

ASTM International. (2008c). ASTM C157: Standard Test Method for Length Change of Hardened Hydraulic-Cement Mortar and Concrete. In *Annual Book of ASTM Standards*. West Conshohocken, PA: ASTM International. https://doi.org/10.1520/C0157

ASTM International. (2010). ASTM C227: Standard Test Method for Potential Alkali Reactivity of Cement-Aggregate Combinations (Mortar-Bar Method). In *Annual Book of ASTM Standards*. West Conshohocken, PA: ASTM International. https://doi.org/10.1520/C0227-10.2

ASTM International. (2014). ASTM C1260: Standard Test Method for Potential Alkali Reactivity of Aggregates (Mortar-Bar Method). In *Annual Book of ASTM Standards*. West Conshohocken, PA: ASTM International. https://doi.org/10.1520/C1260-14.2

ASTM International. (2015a). ASTM C114: Standard Test Methods for Chemical Analysis of Hydraulic Cement. In *Annual Book of ASTM Standards*. West Conshohocken, PA: ASTM International. https://doi.org/10.1520/C0114-15.2

ASTM International. (2015b). ASTM C143: Standard Test Method for Slump of Hydraulic-Cement Concrete. In *Annual Book of ASTM Standards*. West Conshohocken, PA: ASTM International. https://doi.org/10.1520/C0143

ASTM International. (2016a). ASTM C1778: Standard Guide for Reducing the Risk of Deleterious Alkali-Aggregate Reaction. In *Annual Book of ASTM Standards*. West Conshohocken, PA: ASTM International. https://doi.org/10.1520/C1778-14.2

ASTM International. (2016b). ASTM C192: Standard Practice for Making and Curing Concrete Test Specimens in the Laboratory. In *Annual Book of ASTM Standards*. West Conshohocken, PA: ASTM International. https://doi.org/10.1520/C0192

ASTM International. (2016c). ASTM C33: Standard Specification for Concrete Aggregates. In *Annual Book of ASTM Standards*. West Conshohocken, PA: ASTM

International. https://doi.org/10.1520/C0033

ASTM International. (2017). ASTM C39: Standard Test Method for Compressive Strength of Cylindrical Concrete Specimens. In *Annual Book of ASTM Standards*. West Conshohocken, PA: ASTM International. https://doi.org/10.1520/C0039

Barneyback, R. S., Diamond, S., & Lafayette, W. (1981). Expression and Analysis of Pore Fluids from Hardened Cement Pastes and Mortars. *Cement and Concrete Research*, *11*, 279–285.

Beaman, N. (2005). *Prevention of Expansion due to Alkali Silica Reaction in Concrete Containing Reactive Aggregates from Mactaquac*. University of New Brunswick.

Blanks, R., & Meissner, H. (1946). The Expansion Test as a Measure of Alkali-Aggregate Reaction. *Journal of the American Concrete Institute*, *42*(4), 517–540.

Bleszynski, R. F., & Thomas, M. D. A. (1998). Microstructural Studies of Alkali-Silica Reaction in Fly Ash Concrete Immersed in Alkaline Solutions. *Advanced Cement Based Materials*, *7*(2), 66–78. https://doi.org/10.1016/S1065-7355(97)00030-8

Broekmans, M. A. T. M. (2004). Structural properties of quartz and their potential role for ASR. *Materials Characterization*, *53*, 129–140. https://doi.org/10.1016/j.matchar.2004.08.010

Brouwers, H. J. H., & van Eijk, R. J. (2003). Alkali concentrations of pore solution in hydrating OPC. *Cement and Concrete Research*, *33*, 191–196. https://doi.org/10.1016/S0008-8846(02)01022-0

Canadian Standards Association. (2014a). Potential expansivity of aggregates (procedure for length change due to alkali-aggregate reaction in concrete prisms at 38 °C) 1Scope. In *A23.1-14/A23.2-14 Concrete Materials and Methods of Concrete Construction / Test Methods and Standard Practices for Concrete* (pp. 350–362). Mississauga, Ontario: CSA Group.

Canadian Standards Association. (2014b). Standard practice to identify degree of alkali-reactivity of aggregates and to identify measures to avoid deleterious expansion in concrete. In *A23.1-14/A23.2-14 Concrete materials and methods of concrete construction/Test methods and standard practices for concrete* (pp. 439–451). Mississauga, Ontario: CSA Group.

Canadian Standards Association. (2014c). Test method for detection of alkali-silica reactive aggregate by accelerated expansion of mortar bars. In *A23.1-14/A23.2-14 Concrete Materials and Methods of Concrete Construction / Test Methods and Standard Practices for Concrete* (pp. 425–433). Mississauga, Ontario: CSA Group.

Diamond, S. (1996). Delayed ettringite formation - Processes and problems. *Cement and Concrete Composites*, *18*(3), 205–215. https://doi.org/10.1016/0958-9465(96)00017-

0

Diamond, S., & Penko, M. (1992). Alkali Silica Reaction Processes : The Conversion of Cement Alkalies to Alkali Hydroxide. *ACI Special Publication*, *131*, 153–168.

Feng, X., Thomas, M. D. A., Bremner, T. W., Balcom, B. J., & Folliard, K. J. (2005). Studies on lithium salts to mitigate ASR-induced expansion in new concrete: A critical review. *Cement and Concrete Research*, *35*(9), 1789–1796. https://doi.org/10.1016/j.cemconres.2004.10.013

Fletcher, J. (2016). Management of Alkali-Aggregate Reaction Affects at Mactaquac Generating Station. Fredericton, New Brunswick: NB Power.

Fournier, B., Chevrier, R., Bilodeau, A., Nkinamubanzi, P. C., & Nouziubaa, N. (2016). Comparative Field and Laboratory Investigations on the use of Supplementary Cementing Materuals (SCMs) to Control Alkali-Silica Reaction in Concrete. In *Proceedings of the 15th International Conference on Alkali-Aggregate Reaction (ICAAR)*. Sao Paulo, Brazil.

Fournier, B., Chevrier, R., de Grosbois, M., Lisella, R., Folliard, K. J., Ideker, J. H., … Baxter, S. (2004). The accelerated concrete prism test (60 °C): variability of the test method and proposed expansion limits. In *The 12th International Conference on Alkali–Aggregate Reaction in Concrete* (pp. 314–323). Beijing, China.

Fournier, B., Ideker, J. H., Folliard, K. J., Thomas, M. D. A., Nkinamubanzi, P. C., & Chevrier, R. (2009). Effect of environmental conditions on expansion in concrete due to alkali-silica reaction (ASR). *Materials Characterization*, *60*(7), 669–679. https://doi.org/10.1016/j.matchar.2008.12.018

Fournier, R. O., & Rowe, J. K. (1977). The solubility of amorphous silica in water at high temperatures and high pressures. *American Mineralogist*, *62*, 1052–1056.

Gautam, B. P., & Panesar, D. K. (2017). The effect of elevated conditioning temperature on the ASR expansion, cracking and properties of reactive Spratt aggregate concrete. *Construction and Building Materials*, *140*, 310–320. https://doi.org/10.1016/j.conbuildmat.2017.02.104

Giannini, E. R., & Folliard, K. J. (2013). *A Rapid Test to Determine Alkali-Silica Reactivity of Aggregates Using Autoclaved Concrete Prisms*. Skokie, Illinois, USA.

Hansen, W. C. (1944). Studies Relating to the Mechanism. *Journal of the American Concrete Institute*, *15*(3), 213–227.

Hooton, R. D., Rogers, C. A., MacDonald, C. A., & Ramlochan, T. (2013). Twenty-year field evaluation of alkali-silica reaction mitigation. *ACI Materials Journal*, *110*(5), 539–548.

Ideker, J. H., Bentivegna, A. F., Folliard, K. J., & Juenger, C. G. (2012). Do current

laboratory test methods accurately predict ASR. *ACI Materials Journal*, *109*(4), 395–402.

Ideker, J. H., Drimalas, T., Bentivegna, A. F., Folliard, K. J., Fournier, B., Thomas, M. D. A., … Rogers, C. A. (2012). Importance of Outdoor Exposure Site Testing. In T. Drimalas, J. H. Ideker, & B. Fournier (Eds.), *14th ICAAR* (p. 10). Austin, Texas.

Latifee, E. R., & Rangaraju, P. R. (2015). Miniature Concrete Prism Test : Rapid Test Method for Evaluating Alkali-Silica Reactivity of Aggregates. *Journal of Material in Civil Engineering*, *27*(7), 1–10. https://doi.org/10.1061/(ASCE)MT.1943-5533.0001183.

Lindgård, J., Andiç-Çakir, Ö., Fernandes, I., Rønning, T. F., & Thomas, M. D. A. (2012). Alkali-silica reactions (ASR): Literature review on parameters influencing laboratory performance testing. *Cement and Concrete Research*, *42*, 223–243. https://doi.org/10.1016/j.cemconres.2011.10.004

McGowan, J. K., & Vivian, H. E. (1952). Studies in cement-aggregate reaction: correlation between crack development and expansion of mortars. *Australian Journal of Applied Science*, *3*, 228–232.

Oberholster, R. E., & Davies, G. (1986). An accelerated method for testing the potential alkali reactivity of siliceous aggregates. *Cement and Concrete Research*, *16*(2), 181–189. https://doi.org/10.1016/0008-8846(86)90134-1

Pedneault, A. (1996). *No Development of testing and analytical procedures for the evaluation of the residual potential of reaction, expansion, and deterioration of concrete affected by ASR*. Laval University, Quebec City, Canada.

Powers, T. C., & Steinour, H. H. (1955). An Interpretation of Some Published Researches on the Alkali-Aggregate Reaction: Part 1-The Chemical Reaction and Mechanism of Expansion. *Journal of the American Concrete Institute*, *26*(6), 497–516.

Ramyar, K., Topal, A., & Andiç, Ö. (2005). Effects of aggregate size and angularity on alkali-silica reaction. *Cement and Concrete Research*, *35*, 2165–2169. https://doi.org/10.1016/j.cemconres.2005.03.010

Sibbick, R. G., & Page, C. L. (1992). Threshold alkali contents for expansion of concretes containing British aggregates. *Cement and Concrete Research*, *22*, 990–994. https://doi.org/10.1016/0008-8846(92)90123-D

Stacey, S., Folliard, K. J., Drimalas, T., & Thomas, M. D. A. (2016). An Accelerated and more Accurate Test Method to ASTM C1293: The Concrete Cylinder Test. In *The 15th International Conference on Alkali–Aggregate Reaction in Concrete*. Sao Paulo, Brazil.

Stanton, T. E. (1940). Expansion of Concrete through Reaction between Cement and

Aggregate. In *Proceedings of American Society of Civil Engineers 66* (pp. 1781–1811).

Stanton, T. E., Porter, O. J., & Nicil, A. M. L. C. (1942). California Experience with the Expansion of Concrete Through Reaction Between Cement and Aggregate. *Journal of the American Concrete Institute*, *38*(3), 210–236.

Stark, D. (1991). The Moisture Condition of Field Concrete Exhibiting Alkali-Silica Reactivity. *ACI Special Publication*, *126*, 973–988. https://doi.org/10.14359/2467

Tang, M.-S., & Su-fen, H. (1980). Effect of Ca (OH)2 on alkali-silica reaction. In *8th International Congress on the Chemistry of Cement. Vol. 2*.

Thomas, M. D. A. (2001). The role of Calcium Hydroxide in Alkali Recycling in Concrete. (J. Skalny, J. Gebauer, & I. Odler, Eds.), *Materials Science of Concrete Special Volume on Calcium Hydroxide in Concrete*. Westerville, OH: American Ceramic Society.

Thomas, M. D. A. (2016a). Alkali-Silica Reactions: CIV 1299 Chemistry of Cements and Concrete. Toronto, Ontario: University of Toronto.

Thomas, M. D. A. (2016b). Delayed ettringite formation: CIV 1299 Chemistry of Cements and Concrete. Toronto, Ontario: University of Toronto.

Thomas, M. D. A., Fournier, B., & Folliard, K. J. (2013a). *Alkali-Aggregate Reactivity (AAR) Facts Book*. Washington DC: Federal Highway Administration.

Thomas, M. D. A., Fournier, B., Folliard, K. J., & Drimalas, T. (2013b). *A Review of ASR Expansion Data from Field-Exposure Sites in Ottawa and Texas*. Fredericton, New Brunswick.

Thomas, M. D. A., Fournier, B., Folliard, K. J., Ideker, J. H., & Shehata, M. (2006). Test methods for evaluating preventive measures for controlling expansion due to alkali-silica reaction in concrete. *Cement and Concrete Research*, *36*(10), 1842–1856. https://doi.org/10.1016/j.cemconres.2006.01.014

Thomas, M. D. A., Hooton, R. D., & Folliard, K. J. (2017). Prevention of Alkali-Silica Reaction. In I. Smith & A. Poole (Eds.), *Alkali-Aggregate Reaction in Concrete: A World Review* (pp. 89–118). Boca Raton, Florida: CRC Press.

Thomas, M. D. A., & Innis, F. (1999). Use of the Accelerated Mortar Bar Test for Evaluating the Efficacy of Mineral Admixtures for Controlling Expansion due to Alkali-Silica Reaction. *Cement, Concrete and Aggregates*, *21*(2), 157–164. https://doi.org/10.1520/CCA10429J

Urhan, S. (1987). Alkali silica and pozzolanic reactions in concrete. Part 1: Interpretation of published results and an hypothesis concerning the mechanism. *Concrete and Concrete Research*, *17*, 141–152.

Wood, S. G., Kimble, M. L., Klenke, N. D., Fiore, B., Tanner, J. E., & Giannini, E. R. (2016). Inter-Laboratory Comparison of Expansions From the Autoclaved Concrete Prism Test. In *Proceedings of the 15th International Conference on Alkali-Aggregate Reaction (ICAAR)*. Sao Paulo, Brazil.

Xu, Z., Lan, X., Deng, M., & Tang, M.-S. (2002). A new accelerated method for determining the potential alkali-carbonate reactivity. *Cement and Concrete Research*, *32*(6), 851–857. https://doi.org/10.1016/S0008-8846(01)00758-X

Zhang, C., Wang, A., Tang, M., & Zhang, N. (1999). Influence of dimension of test specimen on alkali-aggregate reactive expansion. *ACI Materials Journal*, *96*(2), 204–207.

Appendix A: Mix Design

Mix Name: Jobe 0.36

W/CM=	0.42		**Date Cast:**	2016-02-19		**Batch Size:**	50 **L**
Total Cem. =	420		**Slump:**	203.20	**mm**		
Water Cont. =	176.4		**28 Day Strength:**	53.5	**MPa**		
Alkali Content	0.36						

Material	ABS	Proportions	Density	Volume	M/C	Correction	Batch
		kg/m³	**kg/m³**	**m³**	**%**	**kg**	**kg**
Paulding Cement		0	3140	0.00			0.00
Brooksville Cement		420	3140	0.13			21.00
NaOH		0	2130	0.00			0.00
Water		176	1000	0.18		184.69	9.23
Coarse Agg.	0.44	1045	2691	0.39	0.00%	1040.42	52.02
Fine Agg.	0.54	729	2589	0.28	2.74%	725.11	36.26
Air Content				0.02			
		SUM:		1.000		**Total Wt. :**	118.51 **kg**
		Sand/Agg:		42%		**Theoretical Density:**	2370.23 **kg/m3**

Mix Name: Jobe 0.41

					Date Cast:	2016-02-18		Batch Size:	50 L
W/CM=	0.42				**Slump:**	203.20	**mm**		
Total Cem. =	420				**28 Day Strength:**	50	**MPa**		
Water Cont. =	176.4								
Alkali Content	0.41								

Material	ABS	Proportions	Density	Volume	M/C	Correction	Batch
		kg/m³	kg/m³	m³	%	kg	kg
Paulding Cement		300	3140	0.10			15.00
Brooksville Cement		120	3140	0.04			6.00
NaOH		0	2130	0.00			0.00
Water		176	1000	0.18		184.69	9.23
Coarse Agg.	0.44	1045	2691	0.39	0.00%	1040.42	52.02
Fine Agg.	0.54	729	2589	0.28	2.74%	725.11	36.26
Air Content				0.02			
			SUM:	1.000		**Total Wt. :**	118.51 **kg**
			Sand/Agg:	42%		**Theoretical**	
						Density:	2370.23 **kg/m3**

Mix Name: Jobe 0.43

W/CM=	0.42	Date Cast:	2016-02-10		Batch Size:	50	L
Total Cem. =	420	Slump:	76.20	mm			
Water Cont. =	176.4	28 Day Strength:	41	MPa			
Alkali Content	0.43						

Material	ABS	Proportions kg/m³	Density kg/m³	Volume m³	M/C %	Correction kg	Batch kg
Paulding Cement		420	3140	0.13			21.00
Brooksville Cement		0.00	3140	0.00			0.00
NaOH		0.00	2130	0.00			0.00
Water		176	1000	0.18		184.69	9.23
Coarse Agg.	0.44	1045	2691	0.39	0.00%	1040.42	52.02
Fine Agg.	0.54	729	2589	0.28	2.74%	725.11	36.26
Air Content				0.02			
		SUM:		1.000		Total Wt. :	118.51 kg
		Sand/Agg:		42%		Theoretical Density:	2370.23 kg/m3

Mix Name: Jobe 0.52

			Date Cast:	2016-02-09		Batch Size:	50 L
W/CM=	0.42		**Slump:**	228.60	**mm**		
Total Cem. =	420		**28 Day Strength:**	32.5	**MPa**		
Water Cont. =	176.4						
Alkali Content	0.52						

Material	ABS	Proportions kg/m³	Density kg/m³	Volume m³	M/C %	Correction kg	Batch kg
Whitehall Cement		77	3140	0.02			3.86
Paulding Cement		343	3140	0.11			17.14
NaOH		0.00	2130	0.00			0.00
Water		176	1000	0.18	0.00%	184.69	9.23
Coarse Agg.	0.44	1045	2691	0.39	0.00%	1040.42	52.02
Fine Agg.	0.54	729	2589	0.28	2.74%	725.11	36.26
Air Content				0.02			
		SUM:		1.000		**Total Wt. :**	118.51 **kg**
		Sand/Agg:	42%			**Theoretical Density:**	2370.23 **kg/m3**

Mix Name: Jobe 0.70							
Date Cast: 2016-03-16					**Batch Size:**	50	**L**
W/CM= 0.42							
Total Cem. = 420							
Water Cont. = 176.4							
Slump: 292.10 **mm**							
28 Day Strength: 41.5 **MPa**							
Alkali Content 0.7							
Material	**ABS**	**Proportions**	**Density**	**Volume**	**M/C**	**Correction**	**Batch**
		kg/m³	**kg/m³**	**m³**	**%**	**kg**	**kg**
Whitehall Cement		231	3140	0.07			11.57
Paulding Cement		189	3140	0.06			9.43
NaOH		0.0	2130	0.00			0.00
Water		176	1000	0.18	0.00%	184.69	9.23
Coarse Agg.	0.44	1045	2691	0.39	0.00%	1040.42	52.02
Fine Agg.	0.54	729	2589	0.28	2.74%	725.11	36.26
Air Content				0.02			
		SUM:		1.000		**Total Wt. :**	118.51 **kg**
		Sand/Agg:	42%			**Theoretical**	
						Density:	2370.23 **kg/m3**

130

Mix Name: Jobe 0.92

			Date Cast:	2016-03-17		Batch Size:	50 L
W/CM=	0.42		Slump:	203.20 mm			
Total Cem. =	420		28 Day Strength:	39.5 MPa			
Water Cont. =	176.4						
Alkali Content	0.92						

Material	ABS	Proportions kg/m³	Density kg/m³	Volume m³	M/C %	Correction kg	Batch kg
Whitehall Cement		420	3140	0.13			21.00
Paulding Cement		0.00	3140	0.00			0.00
NaOH		0.00	2130	0.00			0.00
Water		176	1000	0.18		184.69	9.23
Coarse Agg.	0.44	1045	2691	0.39	0.00%	1040.42	52.02
Fine Agg.	0.54	729	2589	0.28	2.74%	725.11	36.26
Air Content				0.02			
			SUM:	1.000		Total Wt. :	118.51 kg
			Sand/Agg:	42%		Theoretical Density:	2370.23 kg/m3

131

Mix Name: Jobe 0.95

				Date Cast:	2016-03-22		Batch Size:	50 L
W/CM=	0.42							
Total Cem. =	420			**Slump:**	209.55	**mm**		
Water Cont. =	176.4			**28 Day Strength:**	39	**MPa**		
Alkali Content	0.95							

Material	**ABS**	**Proportions**	**Density**	**Volume**	**M/C**	**Correction**	**Batch**
		kg/m3	**kg/m3**	**m3**	**%**	**kg**	**kg**
Whitehall Cement		420	3140	0.13			21.00
Paulding Cement		0.00	3140	0.00			0.00
NaOH		0.16	2130	0.00			0.01
Water		176	1000	0.18		184.69	9.23
Coarse Agg.	0.44	1045	2691	0.39	0.00%	1040.42	52.02
Fine Agg.	0.54	729	2589	0.28	2.74%	725.11	36.26
Air Content				0.02			
			SUM:	1.000		**Total Wt. :**	118.52 **kg**
			Sand/Agg:	42%		**Theoretical Density:**	2370.39 **kg/m3**

132

Mix Name: Jobe 1.25

		Date Cast:	2016-03-29			Batch Size:	50 L
W/CM=	0.42						
Total Cem. =	420	**Slump:**	215.90	**mm**			
Water Cont. =	176.4	**28 Day Strength:**	38.5	**MPa**			
Alkali Content	1.25						

Material	**ABS**	**Proportions**	**Density**	**Volume**	**M/C**	**Correction**	**Batch**
		kg/m³	**kg/m³**	**m³**	**%**	**kg**	**kg**
Whitehall Cement		420	3140	0.13			21.00
Paulding Cement		0.00	3140	0.000			0.00
NaOH		1.79	2130	0.00			0.09
Water		176	1000	0.18		184.69	9.23
Coarse Agg.	0.44	1045	2691	0.39	0.00%	1040.42	52.02
Fine Agg.	0.54	729	2589	0.28	2.74%	725.11	36.26
Air Content				0.02			
		SUM:		1.000		**Total Wt. :**	118.60 **kg**
		Sand/Agg:	42%			**Theoretical**	
						Density:	2372.02 **kg/m3**

Mix Name: Jobe 30% FA

		Date	2016-08-25				
W/CM=	0.42	Cast:				Batch Size	50 L
Total Cem. =	420	Slump:	101.60 mm				
Portland Cement=	294	28 Day Strength:	29.5 MPa				
Water Cont. =	176.4						
Fly Ash	30%						
Alkali Content	1.25						
Material	ABS	Proportions	Density	Volume	M/C	Correction	Batch
		kg/m³	kg/m³	m³	%	kg	kg
Whitehall Cement		294	3140	0.09			14.70
Fly Ash		126	2400	0.05			6.30
NaOH		1.25	2130	0.00			0.06
Water		176	1000	0.18		174.32	8.72
Coarse Agg.	0.44	1045	2691	0.39	100.00%	1050.83	52.54
Fine Agg.	0.54	697	2589	0.27	0.00%	693.06	34.65
Air Content				0.02			
		SUM:	1.000			Total Wt. :	116.97 kg
		Sand/Agg:	41%			Theoretical Density:	2339.45 kg/m3

Mix Name: Jobe 56% FA

			Date Cast:	2016-08-23		Batch Size	50	L
W/CM=	0.42		Slump:	203.20	mm			
Total Cem. =	420		28 Day Strength:	25	MPa			
Portland Cement=	184.8							
Water Cont. =	176.4							
Fly Ash	56%							
Alkali Content	1.25							

Material	ABS	Proportions	Density	Volume	M/C	Correction	Batch
		kg/m3	kg/m3	m3	%	kg	kg
Whitehall Cement		185	3140	0.06			9.24
Fly Ash		235.2	2400	0.10			11.76
NaOH		0.79	2130	0.00			0.04
Water		176	1000	0.18		184.40	9.22
Coarse Agg.	0.44	1020	2691	0.38	0.00%	1015.53	50.78
Fine Agg.	0.54	693	2589	0.27	2.74%	689.56	34.48
Air Content				0.02			
				SUM:	1.000	Total Wt. :	115.51	kg
				Sand/Agg:	41%	Theoretical Density:	2310.28	kg/m3

Mix Name: Springhill 0.40

			Date	2016-03-			
W/CM=	0.42		Cast:	02		Batch Size:	50 L
Total Cem. =	420		Slump:	146.05	mm		
Water Cont. =	176.4		28 Day Strength:	49	MPa		
Alkali Content	0.40						

Material	ABS	Proportions	Density	Volume	M/C	Correction	Batch
		kg/m³	**kg/m³**	**m³**	**%**	**kg**	**kg**
Paulding Cement		240.00	3140	0.08			12.00
Brooksville Cement		180.00	3140	0.06			9.00
NaOH		0	2130	0.00			0.00
Water		176	1000	0.18		183.93	9.20
Coarse Agg.	0.40	1020	2535	0.40	0.00%	1015.94	50.80
Fine Agg.	0.53	694	2594	0.27	2.74%	690.36	34.52
Air Content				0.02			
			SUM:	1.000		**Total Wt. :**	115.51 **kg**
						Theoretical	
			Sand/Agg:	40%		**Density:**	2310.23 **kg/m3**

Mix Name: Springhill 0.49

W/CM=	0.42
Total Cem. =	420
Water Cont. =	176.4
Alkali Content	0.49

Date Cast: 2016-03-03 **Batch Size:** 50 L

Slump: 190.50 mm

28 Day Strength: 37 MPa

Material	ABS	Proportions kg/m³	Density kg/m³	Volume m³	M/C %	Correction kg	Batch kg
Whitehall Cement		51.43	3140	0.02			2.57
Paulding Cement		368.57	3140	0.12			18.43
NaOH		0.00	2130	0.00			0.00
Water		176	1000	0.18		183.93	9.20
Coarse Agg.	0.40	1020	2535	0.40	0.00%	1015.94	50.80
Fine Agg.	0.53	694	2594	0.27	2.74%	690.36	34.52
Air Content				0.02			
			SUM:	1.000		Total Wt. :	115.51 kg

Sand/Agg: 40%

Theoretical Density: 2310.23 kg/m3

Mix Name: Springhill 0.70

W/CM=	0.42	Date Cast:	2016-05-25		Batch Size:	50	L
Total Cem. =	420	Slump:	63.50	mm			
Water Cont. =	176.4	28 Day Strength:	48.5	MPa			
Alkali Content	0.70						

Material	ABS	Proportions	Density	Volume	M/C	Correction	Batch
		kg/m³	kg/m³	m³	%	kg	kg
Whitehall Cement		231.43	3140	0.07			11.57
Paulding Cement		188.57	3140	0.06			9.43
NaOH		0.00	2130	0.00			0.00
Water		176	1000	0.18		183.93	9.20
Coarse Agg.	0.40	1020	2535	0.40	0.00%	1015.94	50.80
Fine Agg.	0.53	694	2594	0.27	2.74%	690.36	34.52
Air Content				0.02			
			SUM:	1.000		Total Wt. :	115.51 kg
			Sand/Agg:	40%		Theoretical Density:	2310.23 kg/m3

Mix Name: Springhill 0.90

		Date Cast:	2016-05-31		Batch Size:	50	L
W/CM=	0.42						
Total Cem. =	420	**Slump:**	50.80	**mm**			
Water Cont. =	176.4	**28 Day Strength:**	43.5	**MPa**			
Alkali Content	0.90						

Material	ABS	Proportions	Density	Volume	M/C	Correction	Batch
		kg/m³	kg/m³	m³	%	kg	kg
Whitehall Cement		402.86	3140	0.13			20.14
Paulding Cement		17.14	3140	0.01			0.86
NaOH		0.00	2130	0.00			0.00
Water		176	1000	0.18		183.93	9.20
Coarse Agg.	0.40	1020	2535	0.40	0.00%	1015.94	50.80
Fine Agg.	0.53	694	2594	0.27	2.74%	690.36	34.52
Air Content				0.02			
			SUM:	1.000		**Total Wt. :**	115.51 **kg**
			Sand/Agg:	40%		**Theoretical** **Density:**	2310.23 **kg/m3**

Mix Name: Springhill 1.25

W/CM=	0.42
Total Cem. =	420
Water Cont. =	176.4
Alkali Content	1.25

Date Cast:	2016-06-01
Slump:	63.50 mm
28 Day Strength:	45 MPa

Batch Size: 50 L

Material	ABS	Proportions kg/m³	Density kg/m³	Volume m³	M/C %	Correction kg	Batch kg
Whitehall Cement		420	3140	0.13			21.00
Paulding Cement		0.00	3140	0.00			0.00
NaOH		1.79	2130	0.00			0.09
Water		176	1000	0.18		183.93	9.20
Coarse Agg.	0.40	1020	2535	0.40	0.00%	1015.94	50.80
Fine Agg.	0.53	694	2594	0.27	2.74%	690.36	34.52
Air Content				0.02			
			SUM:	1.000			
			Sand/Agg:	40%			

Total Wt. : 115.60 kg
Theoretical Density: 2312.02 kg/m3

Mix Name: Springhill 30% FA

		Date Cast:	2016-08-23			Batch Size	50	L
		Slump:	203.20 mm					
		28 Day Strength:	44 MPa					

		W/CM=	0.42
		Total Cem. =	420
		Portland Cement=	294.0
		Water Cont. =	176.4
		Fly Ash	30%
		Alkali Content	0.90

Material	ABS	Proportions kg/m³	Density kg/m³	Volume m³	M/C %	Correction kg	Batch kg
Whitehall Cement		282.82	3140	0.09			14.14
Paulding Cement		11.18	3140	0.00			0.56
Fly Ash		126	2400	0.05			6.30
NaOH		0.00	2130	0.00			0.00
Water		176	1000	0.18		181.98	9.10
Coarse Agg.	0.40	1020	2535	0.40	17.64%	1017.73	50.89
Fine Agg.	0.53	662	2594	0.26	2.74%	658.43	32.92
Air Content				0.02			
			SUM:	1.000		Total Wt. :	113.91 kg
			Sand/Agg:	39%		Theoretical Density:	2278.14 kg/m3

Mix Name: Springhill 56% FA

		Date Cast:	2016-10-13	
W/CM=	0.42	Slump:	203.20 mm	Batch Size 50 L
Total Cem. =	420	28 Day Strength:	39.5 MPa	
Portland Cement=	184.8			
Water Cont. =	176.4			
Fly Ash	56%			
Alkali Content	1.25			

Material	ABS	Proportions kg/m³	Density kg/m³	Volume m³	M/C %	Correction kg	Batch kg
Whitehall Cement		185	3140	0.06			9.24
Fly Ash		235.2	2400	0.10			11.76
NaOH		0.79	2130	0.00			0.04
Water		176	1000	0.18		181.84	9.09
Coarse Agg.	0.40	1020	2535	0.40	17.64%	1017.73	50.89
Fine Agg.	0.53	634	2594	0.24	2.74%	630.75	31.54
Air Content				0.02			
			SUM:	1.000		Total Wt. :	112.56 kg
			Sand/Agg:	38%		Theoretical Density:	2251.11 kg/m3

Mix Name: Spratt 0.40

		Date Cast:	2016-05-09		Batch Size:	50	L
W/CM=	0.42	Slump:	76.20	mm			
Total Cem. =	420	28 Day Strength:	52.5	MPa			
Water Cont. =	176.4						
Alkali Content	0.40						

Material	ABS	Proportions kg/m³	Density kg/m³	Volume m³	M/C %	Correction kg	Batch kg
Paulding Cement		240.00	3140	0.08			12.00
Brooksville Cement		180.00	3140	0.06			9.00
NaOH		0	2130	0.00			0.00
Water		176	1000	0.18		186.38	9.32
Coarse Agg.	0.61	1070	2670	0.40	0.00%	1063.51	53.18
Fine Agg.	0.53	698	2594	0.27	2.74%	694.54	34.73
Air Content				0.02			
			SUM:	1.000		Total Wt. :	118.22 kg
			Sand/Agg:	40%		Theoretical Density:	2364.43 kg/m3

Mix Name: Spratt 0.49

			Date				
W/CM=	0.42		**Cast:**	2016-05-16		**Batch Size:**	50 **L**
Total Cem. =	420		**Slump:**	38.10	**mm**		
Water Cont. =	176.4		**28 Day Strength:**	47.5	**MPa**		
Alkali Content	0.49						

Material	ABS	Proportions kg/m³	Density kg/m³	Volume m³	M/C %	Correction kg	Batch kg
Whitehall Cement		51.43	3140	0.02			2.57
Paulding Cement		368.57	3140	0.12			18.43
NaOH		0.00	2130	0.00			0.00
Water		176	1000	0.18		186.38	9.32
Coarse Agg.	0.61	1070	2670	0.40	0.00%	1063.51	53.18
Fine Agg.	0.53	698	2594	0.27	2.74%	694.54	34.73
Air Content				0.02			
				SUM: 1.000		**Total Wt. :**	118.22 **kg**
						Theoretical	
				Sand/Agg: 40%		**Density:**	2364.43 **kg/m3**

144

Mix Name: Spratt 0.90

			Date	2016-05-			
W/CM=	0.42		**Cast:**	17		**Batch Size:**	50 **L**
Total Cem. =	420		**Slump:**	177.80	**mm**		
Water Cont. =	176.4		**28 Day Strength:**	49	**MPa**		
Alkali Content	0.90						

Material	ABS	Proportions kg/m³	Density kg/m³	Volume m³	M/C %	Correction kg	Batch kg
Whitehall Cement		402.86	3140	0.13			20.14
Paulding Cement		17.14	3140	0.01			0.86
NaOH		0.00	2130	0.00			0.00
Water		176	1000	0.18		186.38	9.32
Coarse Agg.	0.61	1070	2670	0.40	0.00%	1063.51	53.18
Fine Agg.	0.53	698	2594	0.27	2.74%	694.54	34.73
Air Content				0.02			
				SUM: 1.000		**Total Wt. :**	118.22 **kg**
						Theoretical	
			Sand/Agg: 40%			**Density:**	2364.43 **kg/m3**

Mix Name: Spratt 1.25

W/CM=	0.42	Date	2016-05-24
Total Cem. =	420	Cast:	
Water Cont. =	176.4	Slump:	63.50 mm
Alkali Content	1.25	28 Day Strength:	28.5 MPa
		Batch Size:	50 L

Material	ABS	Proportions kg/m³	Density kg/m³	Volume m³	M/C %	Correction kg	Batch kg
Whitehall Cement		420	3140	0.13			21.00
Paulding Cement		0.00	3140	0.00			0.00
NaOH		1.79	2130	0.00			0.09
Water		176	1000	0.18		186.38	9.32
Coarse Agg.	0.61	1070	2670	0.40	0.00%	1063.51	53.18
Fine Agg.	0.53	698	2594	0.27	2.74%	694.54	34.73
Air Content				0.02			
		SUM:		1.000		Total Wt. :	118.31 kg
		Sand/Agg:		40%		Theoretical Density:	2366.22 kg/m3

146

Mix Name: Spratt 20% FA

			Date	2016-08-		Batch Size	50	L
W/CM=	0.42		Cast:	10				
Total Cem. =	420		Slump:	177.80	mm			
Portland Cement=	336		28 Day Strength:	53	MPa			
Water Cont. =	176.4							
Fly Ash	20%							
Alkali Content	0.90							

Material	ABS	Proportions kg/m³	Density kg/m³	Volume m³	M/C %	Correction kg	Batch kg
Whitehall Cement		321.47	3140	0.10			16.07
Paulding Cement		14.53	3140	0.00			0.73
Fly Ash		84	2400	0.04			4.20
NaOH		0.00	2130	0.00			0.00
Water		176	1000	0.18		186.27	9.31
Coarse Agg.	0.61	1070	2670	0.40	0.00%	1063.51	53.18
Fine Agg.	0.53	677	2594	0.26	2.74%	673.25	33.66
Air Content				0.02			
			SUM:	1.000		Total Wt. :	117.15 kg
			Sand/Agg:	39%		Theoretical Density:	2343.03 kg/m3

Mix Name: Spratt 30% FA

		Date	2016-08-				
W/CM=	0.42	Cast:	11		Batch Size	50	L
Total Cem. =	420	Slump:	139.70	mm			
Portland Cement=	294	28 Day Strength:	38.5	MPa			
Water Cont. =	176.4						
Fly Ash	30%						
Alkali Content	0.90						

Material	ABS	Proportions	Density	Volume	M/C	Correction	Batch
		kg/m³	kg/m³	m³	%	kg	kg
Whitehall Cement		282.82	3140	0.09			14.14
Paulding Cement		11.18	3140	0.00			0.56
Fly Ash		126	2400	0.05			6.30
NaOH		0.00	2130	0.00			0.00
Water		176	1000	0.18		186.22	9.31
Coarse Agg.	0.61	1070	2670	0.40	0.00%	1063.51	53.18
Fine Agg.	0.53	666	2594	0.26	2.74%	662.60	33.13
Air Content				0.02			
		SUM:		1.000		Total Wt. :	116.62 kg
						Theoretical	
		Sand/Agg:	39%			Density:	2332.33 kg/m3

148

Mix Name: Spratt 50% SG

		Date Cast:	2016-08-18			Batch Size	50 L
		Slump:	63.50 mm				
		28 Day Strength:	48.5 MPa				

		W/CM=	0.42
		Total Cem. =	420
		Portland Cement=	210
		Water Cont. =	176.4
		Slag	50%
		Alkali Content	0.90

Material	ABS	Proportions kg/m³	Density kg/m³	Volume m³	M/C %	Correction kg	Batch kg
Whitehall Cement		201.43	3140	0.06			10.07
Paulding Cement		8.57	3140	0.00			0.43
Slag		210	1375	0.15			10.50
NaOH		0.00	2130	0.00			0.00
Water		176	1000	0.18		185.26	9.26
Coarse Agg.	0.61	1070	2670	0.40	0.00%	1063.51	53.18
Fine Agg.	0.53	475	2594	0.18	2.74%	472.96	23.65
Air Content				0.02			
		SUM:		1.000		Total Wt. :	107.09 kg
		Sand/Agg:	31%			Theoretical Density:	2141.74 kg/m3

Mix Name: Spratt 65% SG

		Date	2016-11-28		Batch Size	50	L
W/CM=	0.42	Cast:					
Total Cem. =	420	Slump:	63.50	mm			
Portland Cement=	147	28 Day Strength:	55.5	MPa			
Water Cont. =	176.4						
Slag	65%						
Alkali Content	0.90						

Material	ABS	Proportions kg/m³	Density kg/m³	Volume m³	M/C %	Correction kg	Batch kg
Whitehall Cement		140.39	3140	0.04			7.02
Paulding Cement		6.61	3140	0.00			0.33
Slag		273	1375	0.20			13.65
NaOH		0.00	2130	0.00			0.00
Water		176	1000	0.18		184.93	9.25
Coarse Agg.	0.61	1070	2670	0.40	0.00%	1063.51	53.18
Fine Agg.	0.53	409	2594	0.16	2.74%	406.49	20.32
Air Content				0.02			
			SUM:	1.000		Total Wt. :	103.75 kg
			Sand/Agg:	28%		Theoretical Density:	2074.93 kg/m3

Mix Name: Spratt 25% SG 4% SF							
W/CM=	0.42		**Date**	2016-08-22			
Total Cem. =	420		**Cast:**			**Batch Size**	50 **L**
Portland Cement=	298.2		**Slump:**	38.10 **mm**			
Water Cont. =	176.4		**28 Day Strength:**	49 **MPa**			
Slag	25%						
Silica Fume	4%						
Alkali Content	1.25						
Material	**ABS**	**Proportions**	**Density**	**Volume**	**M/C**	**Correction**	**Batch**
		kg/m³	**kg/m³**	**m³**	**%**	**kg**	**kg**
Whitehall Cement		298.20	3140	0.09			14.91
Paulding Cement		0.00	3140	0.00			0.00
Slag		105	1375	0.08			5.25
Silica Fume		16.8	2200	0.01			0.84
NaOH		1.27	2130	0.00			0.06
Water		176	1000	0.18		185.71	9.29
Coarse Agg.	0.61	1000	2670	0.37	0.00%	993.94	49.70
Fine Agg.	0.53	649	2594	0.25	2.74%	645.52	32.28
Air Content				0.02			
				SUM: 1.000		**Total Wt. :**	112.32 **kg**
				Sand/Agg: 40%		**Theoretical Density:**	2246.43 **kg/m3**

151

Mix Name: Alkali Inventory

		Date Cast 38C:	2017-01-11.		Batch Size:	40	L
		Date Cast 60C:	2017-01-12.				
		Slump:	165.10	**mm**			
		28 Day Strength:	45.3	**MPa**			

W/CM=	0.42
Total Cem. =	420
Water Cont. =	176.4
Alkali Content	0.70

Material	ABS	Proportions	Density	Volume	M/C	Correction	Batch
		kg/m³	**kg/m³**	**m³**	**%**	**kg**	**kg**
Whitehall Cement		231.43	3140	0.07			9.26
Paulding Cement		188.57	3140	0.06			7.54
NaOH		0.00	2130	0.00			0.00
Water		176	1000	0.18		224.04	8.96
Coarse Agg.	3.12	1000	2470	0.40	0.00%	969.74	38.79
Fine Agg.	2.68	673	2540	0.26	2.74%	655.67	26.23
Air Content				0.02			
			SUM:	1.000		**Total Wt. :**	90.78 kg
						Theoretical	
			Sand/Agg:	40%		**Density:**	2269.46 kg/m3

Appendix B: Graphs of Expansion with all data shown

Jobe 0.70% Alkali

154
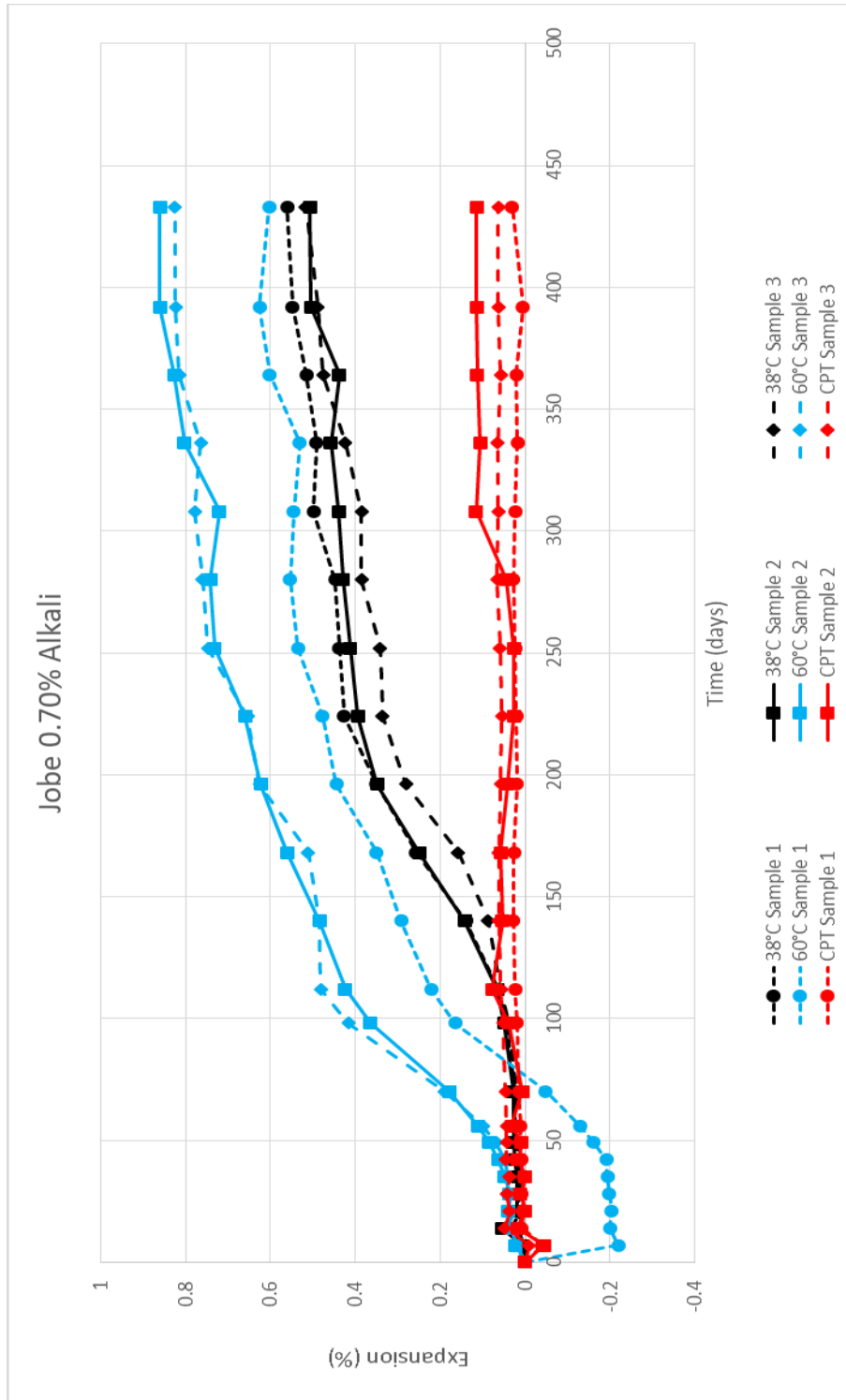
Appendix C: Graphs of Expansion with Error Bars
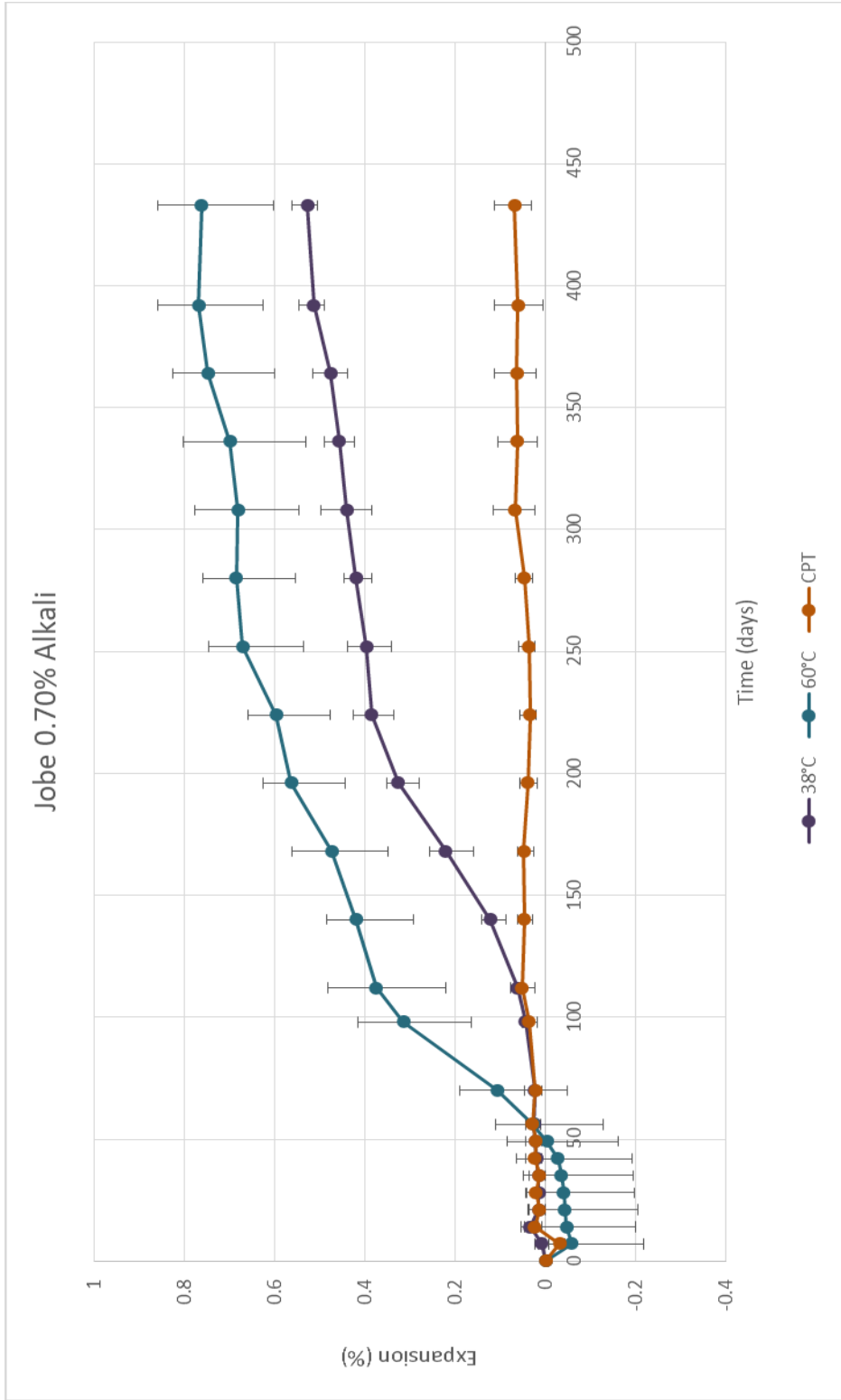
Jobe 0.70% Alkali

Appendix D: Graphs of Expansion for Individual Mix Designs

Jobe 0.36% Alkali
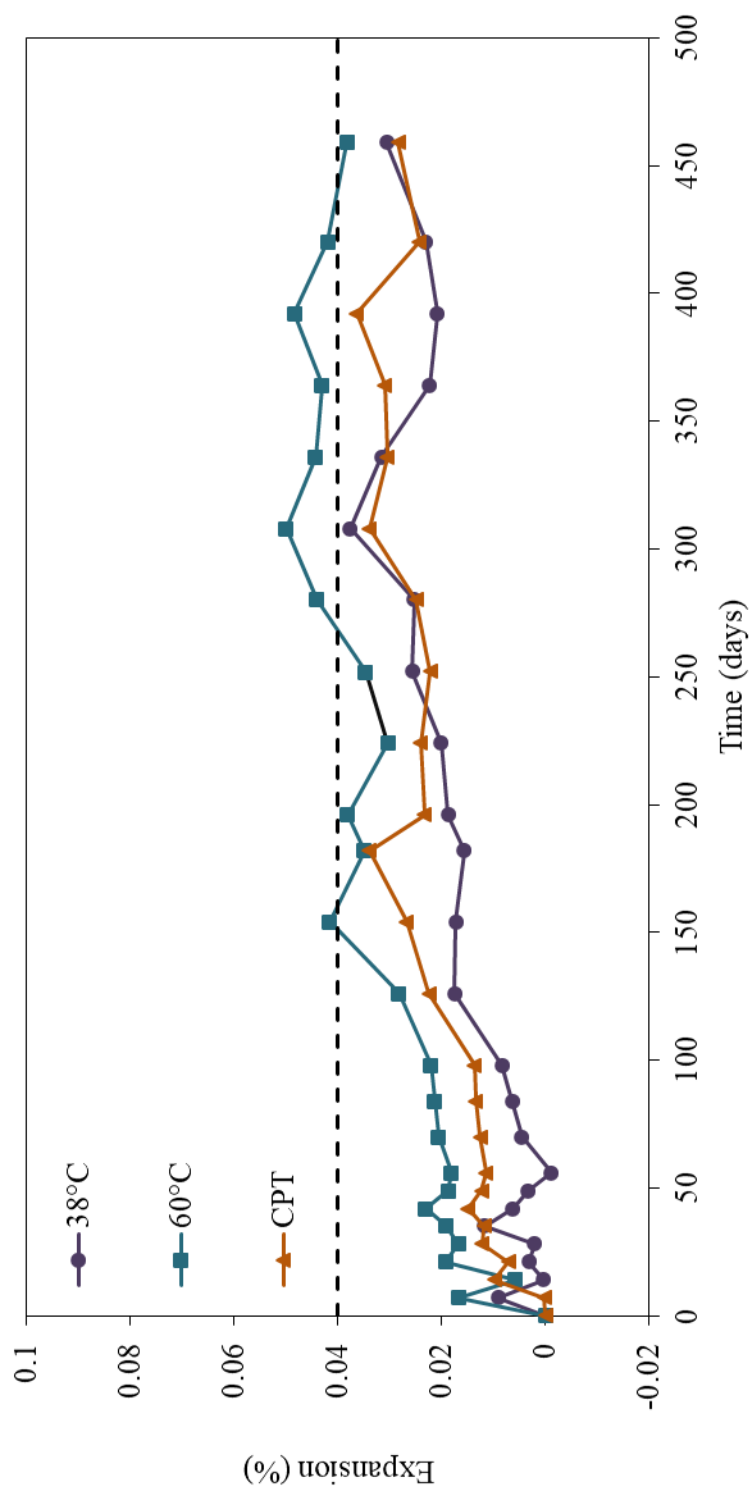
Jobe 0.41% Alkali

Jobe 0.43% Alkali

160

Jobe 0.52% Alkali

38°C
60°C
CPT

Jobe 0.70% Alkali

162
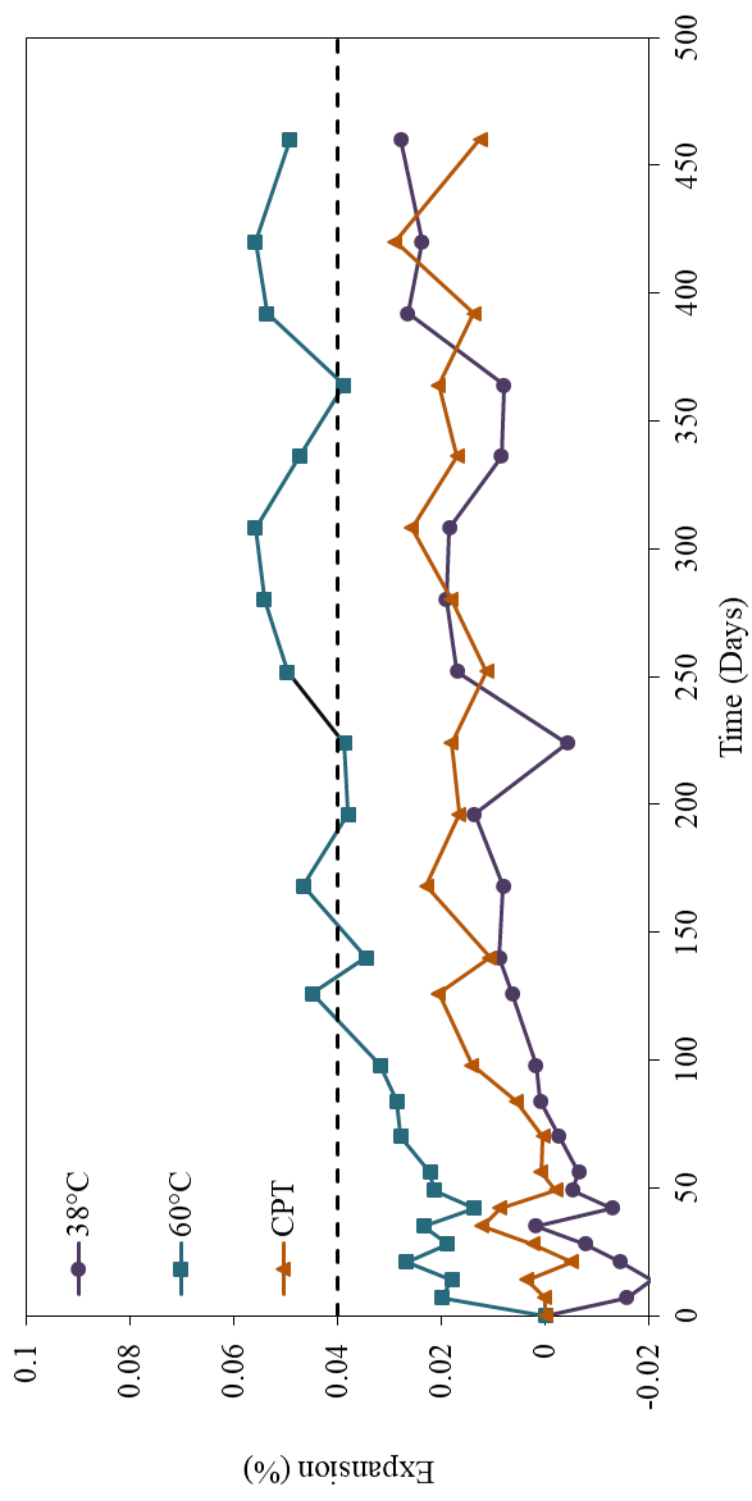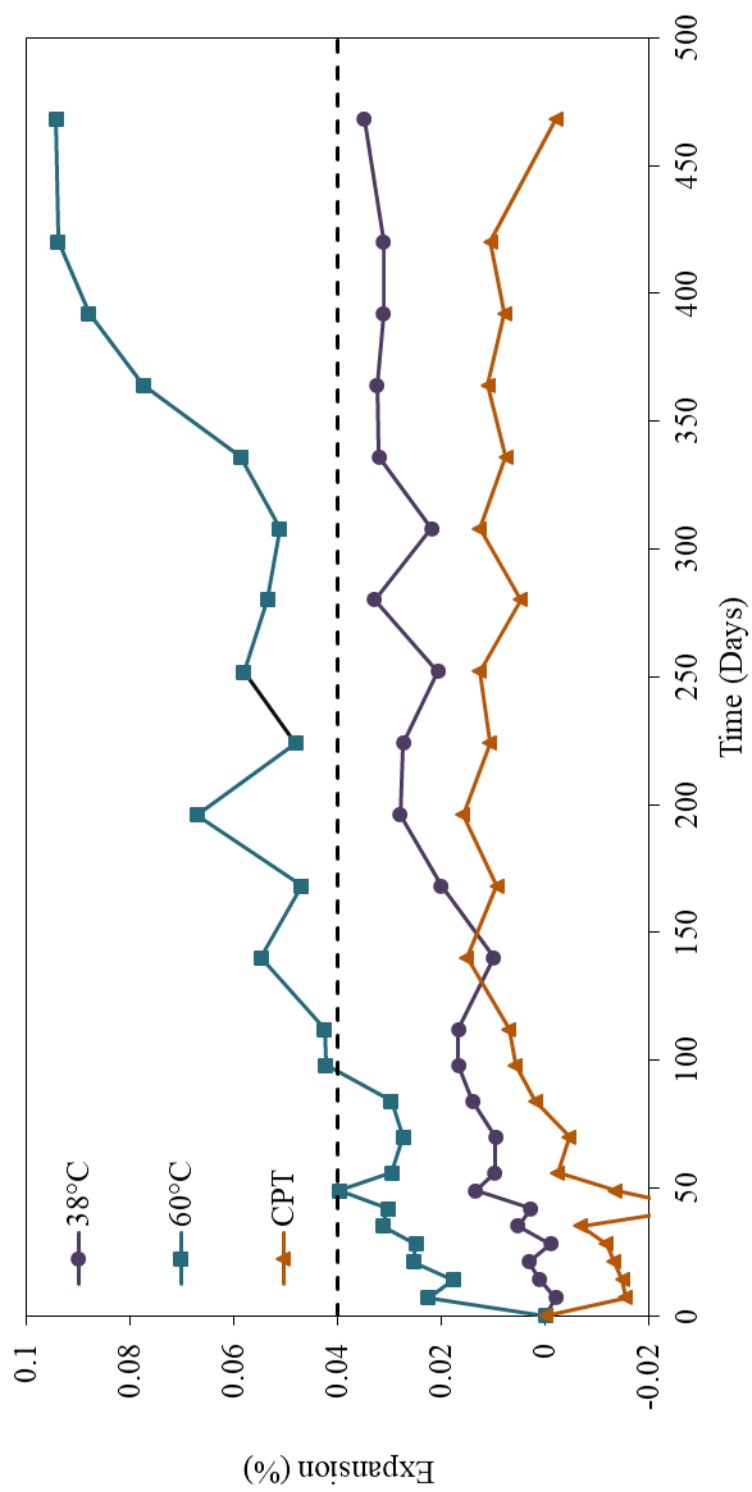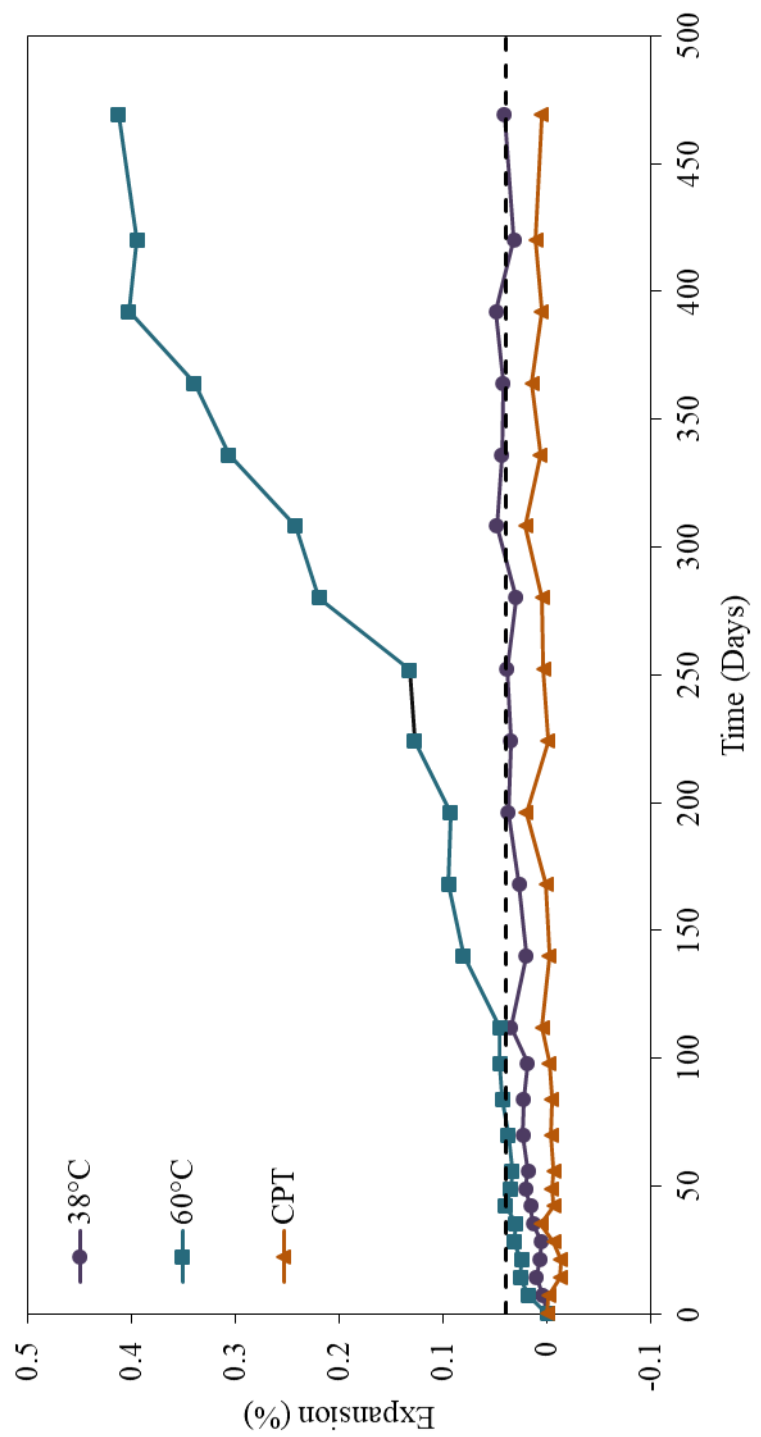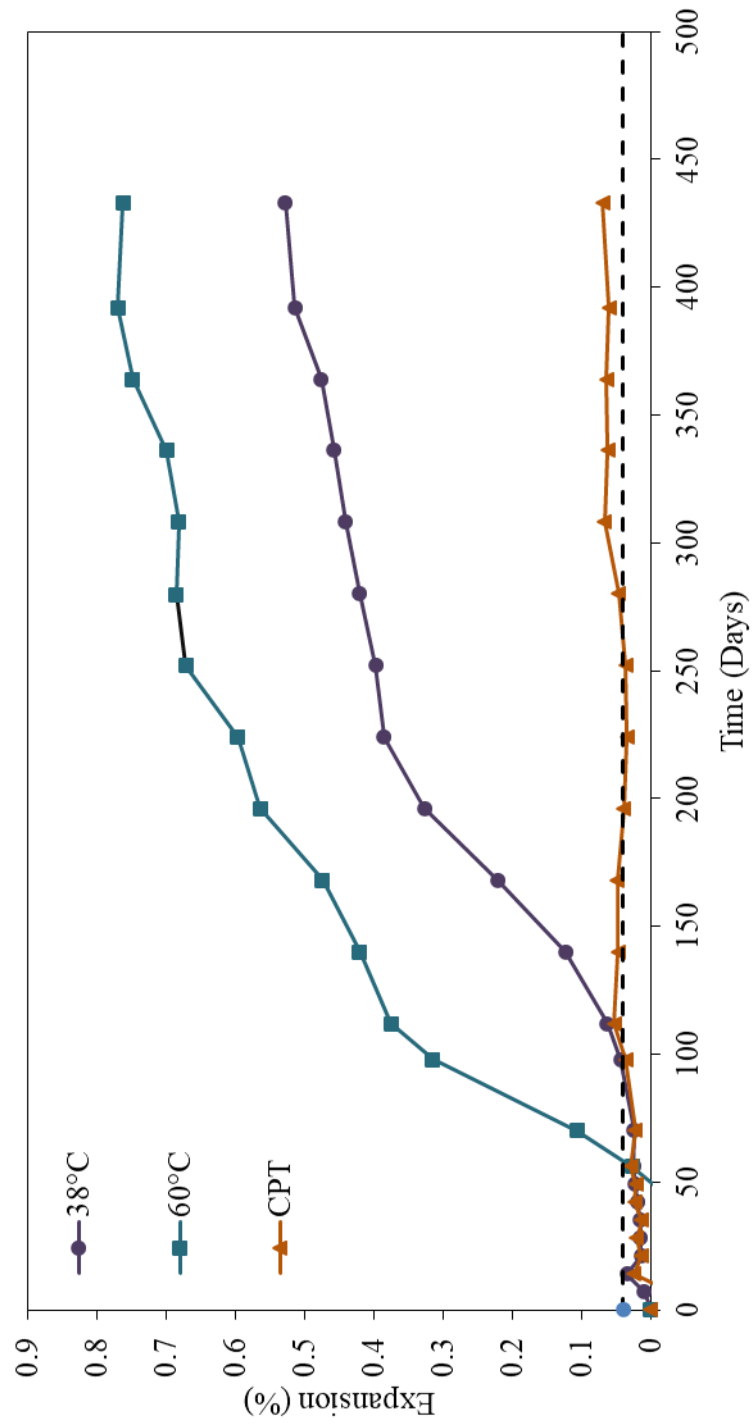
Jobe 0.92% Alkali

Jobe 0.95% Alkali

164

Jobe 1.25% Alkali

165
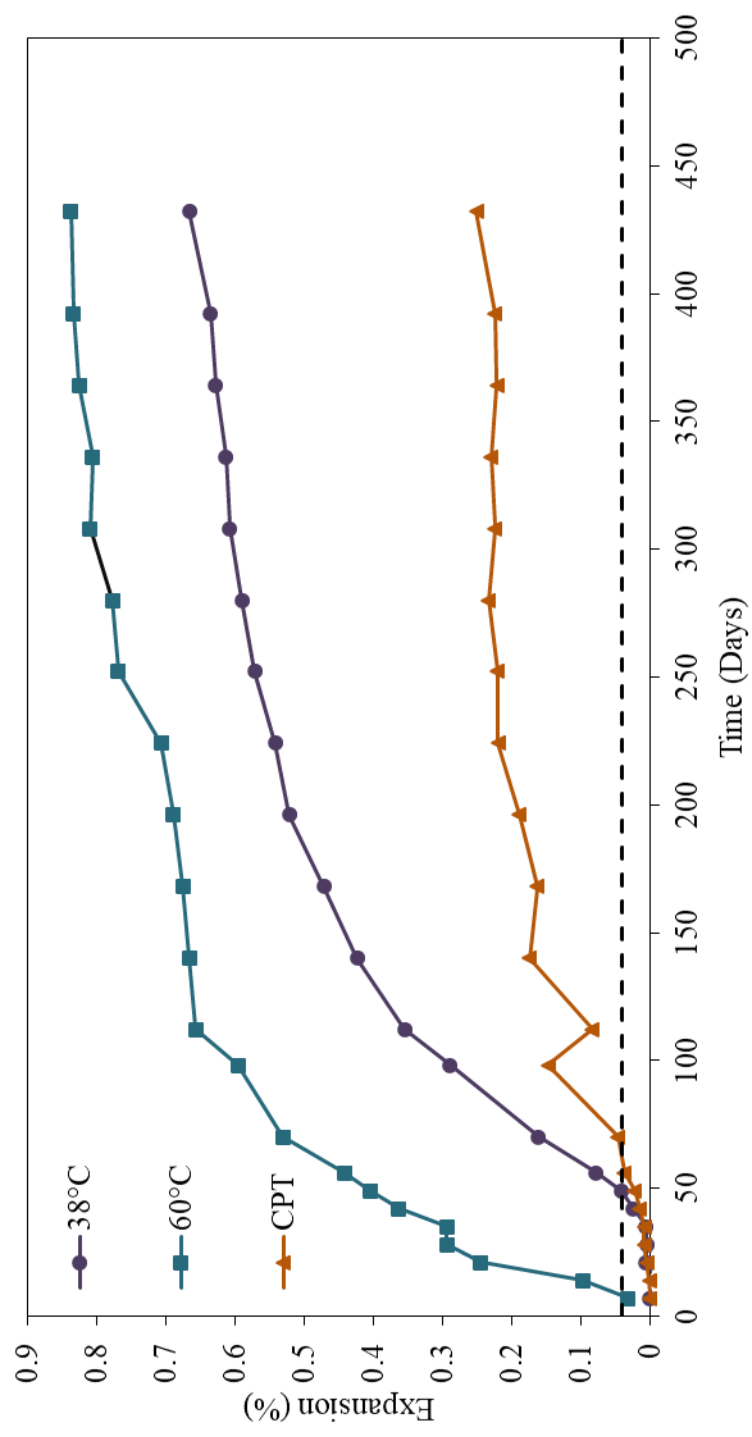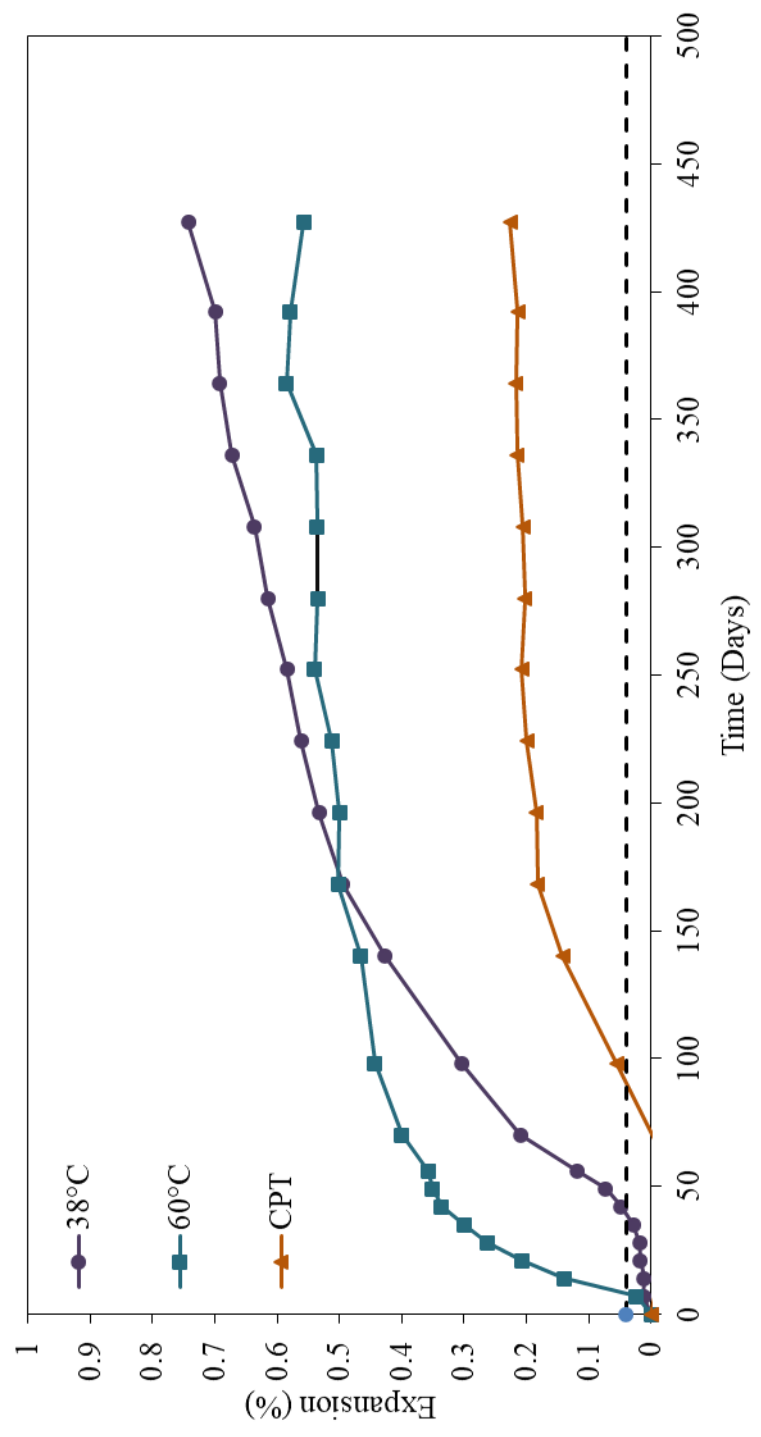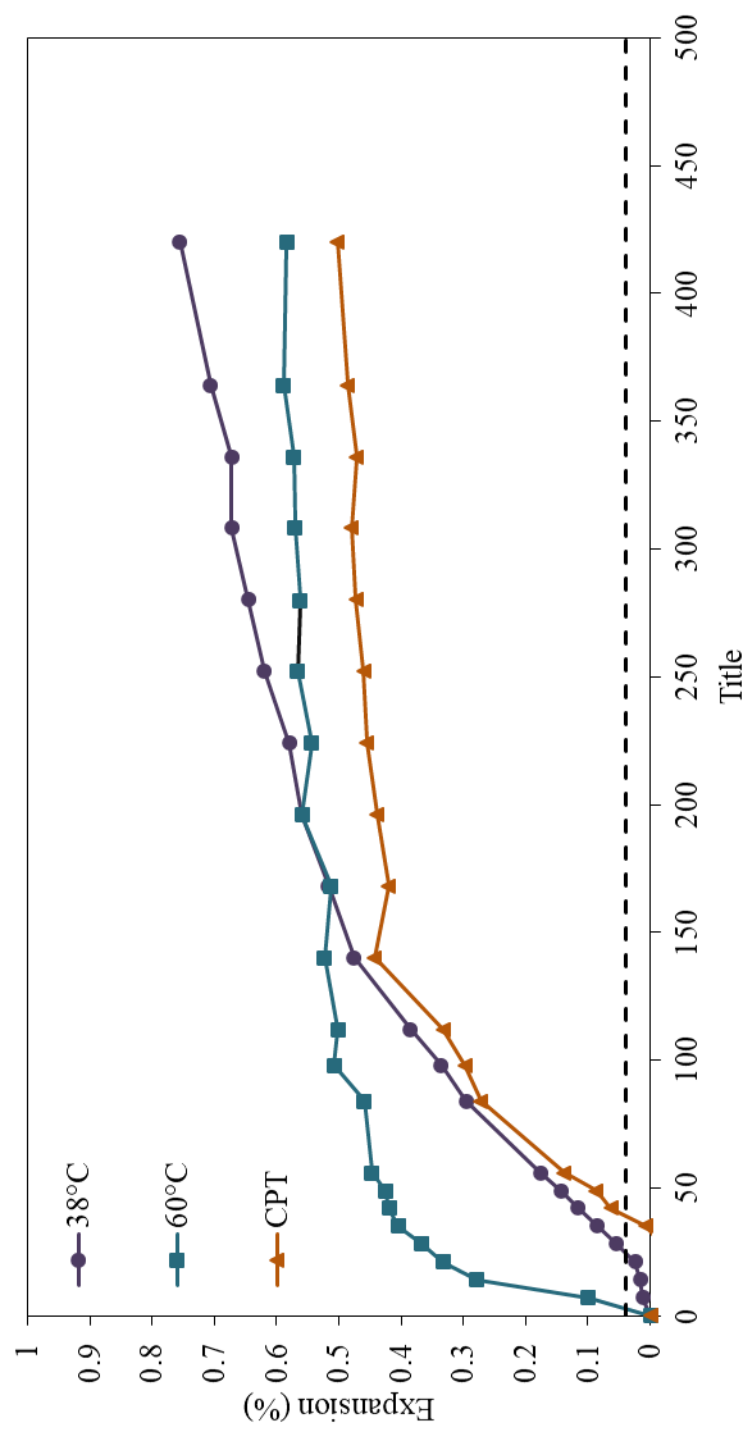
Jobe 30% Fly Ash

Jobe 56%Fly Ash

167
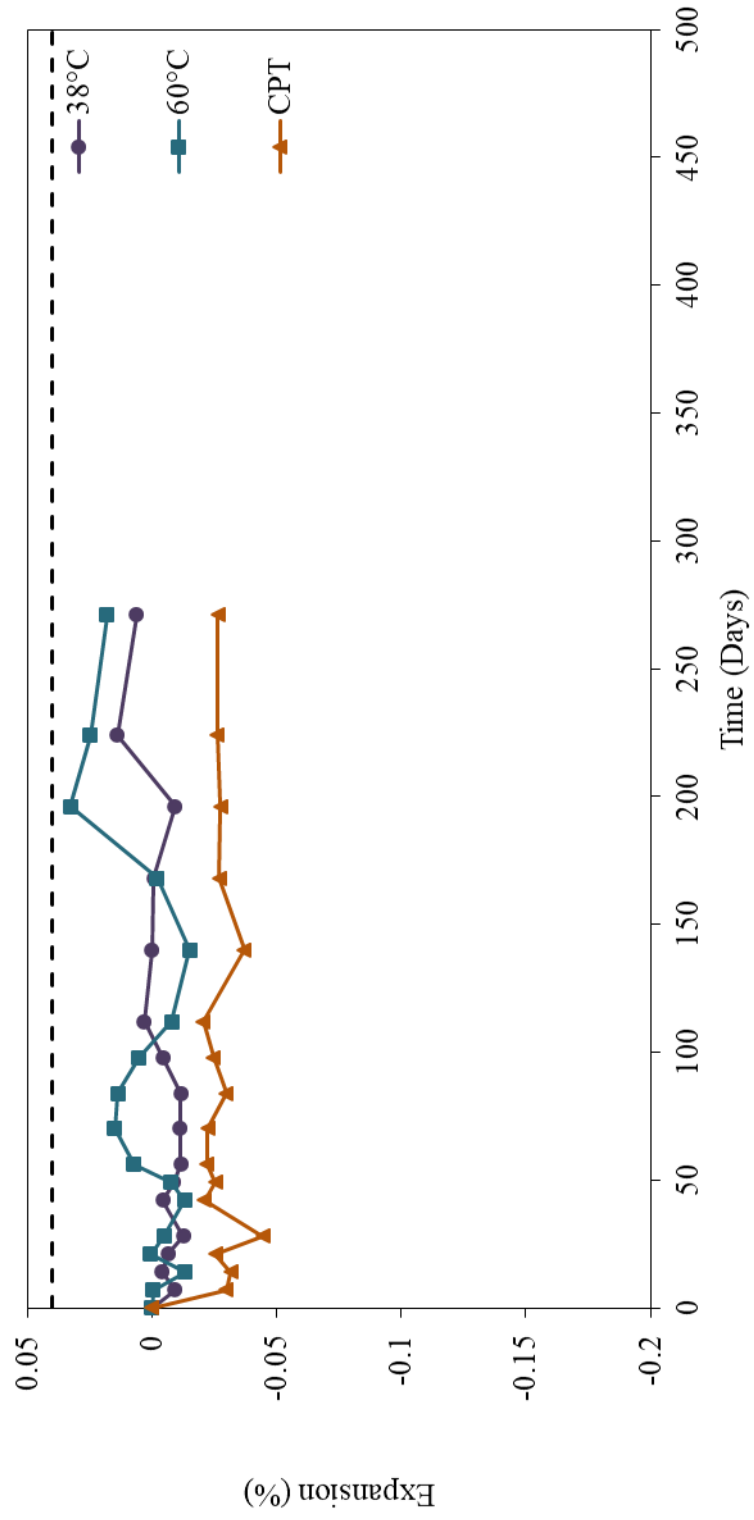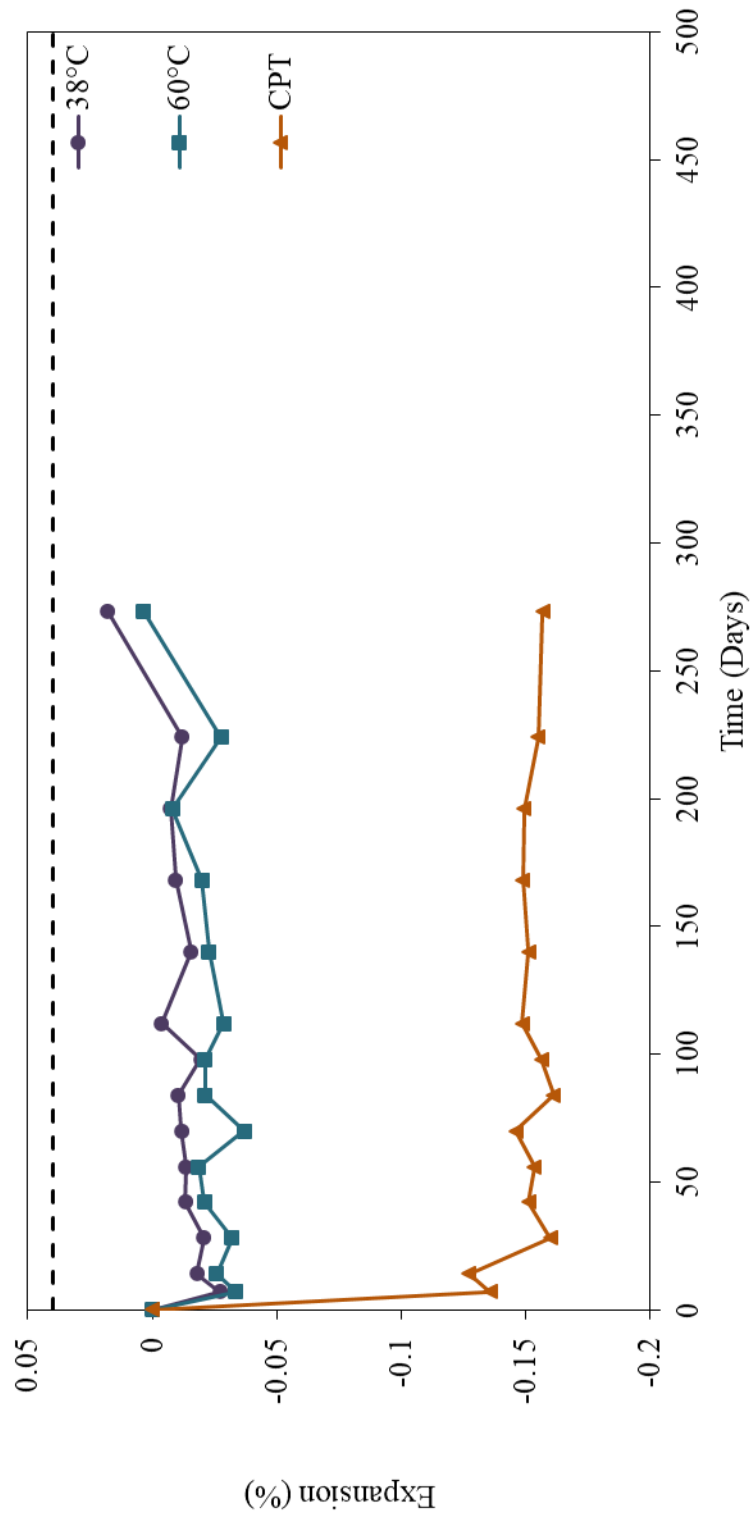
Springhill 0.4% Alkali
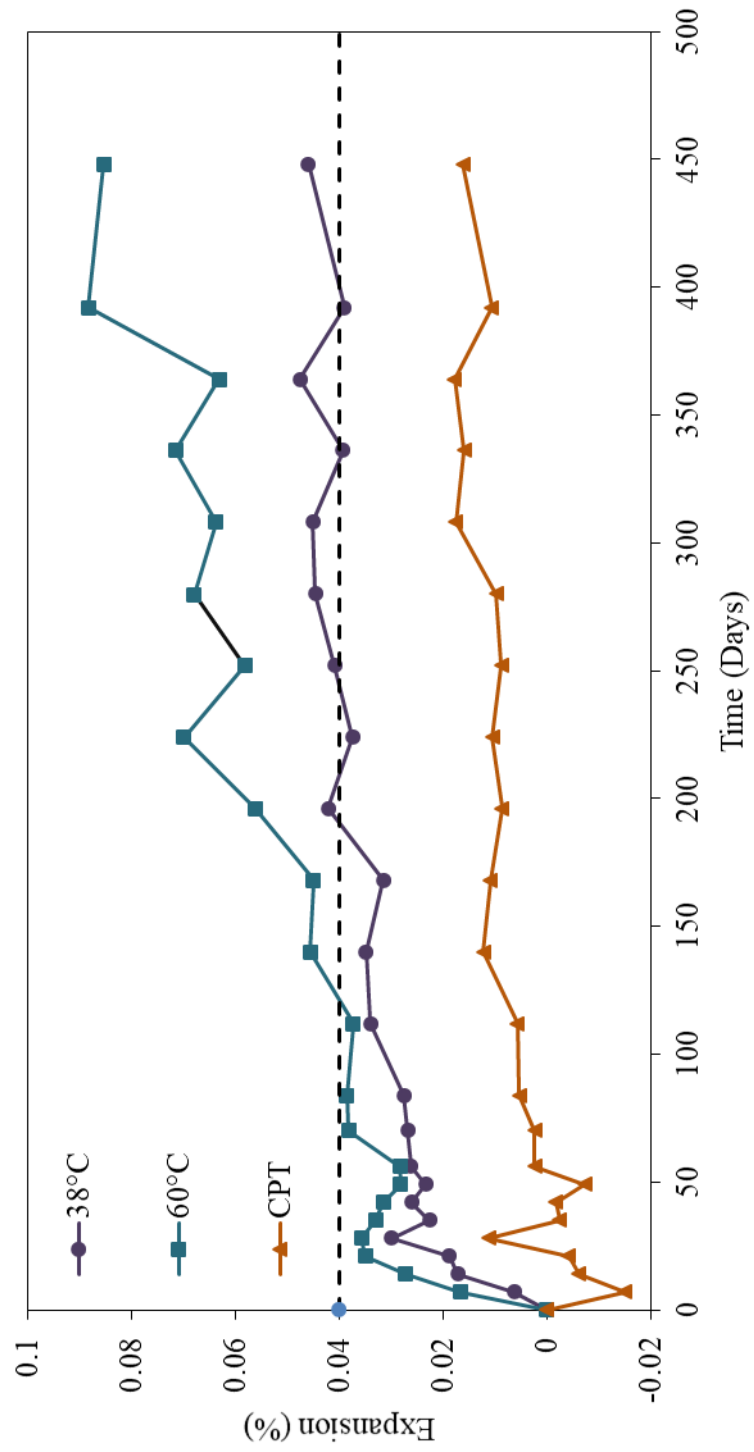
Springhill 0.49% Alkali

169
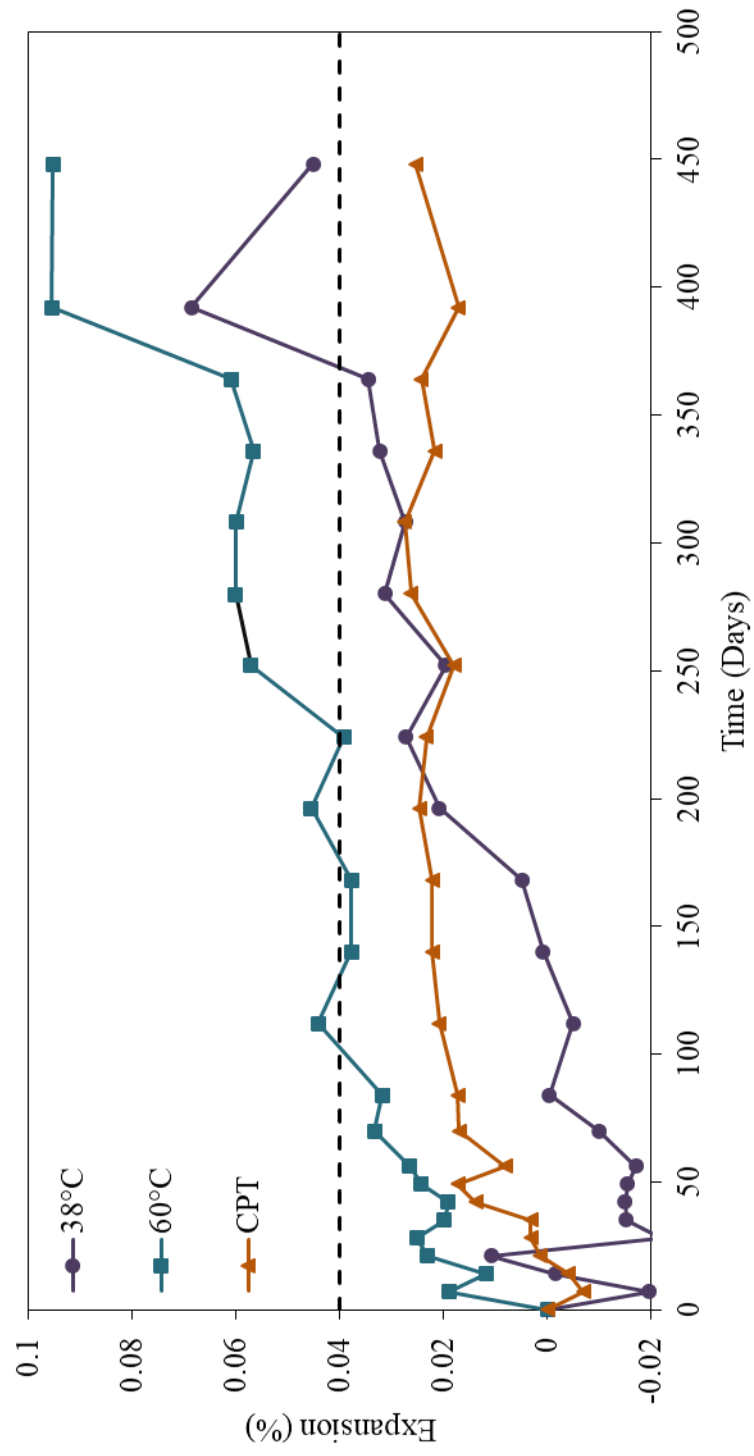
Springhill 0.7% Alkali
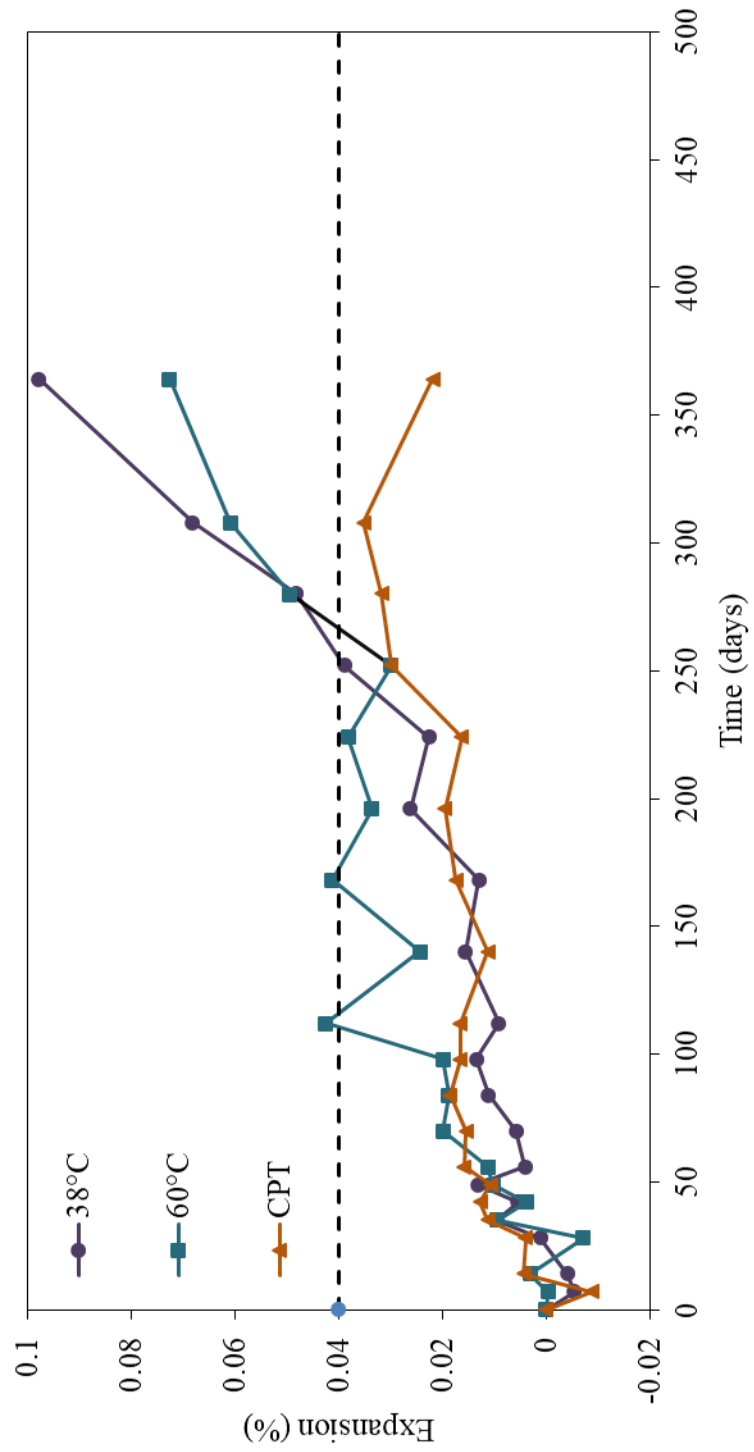
Springhill 0.9% Alkali
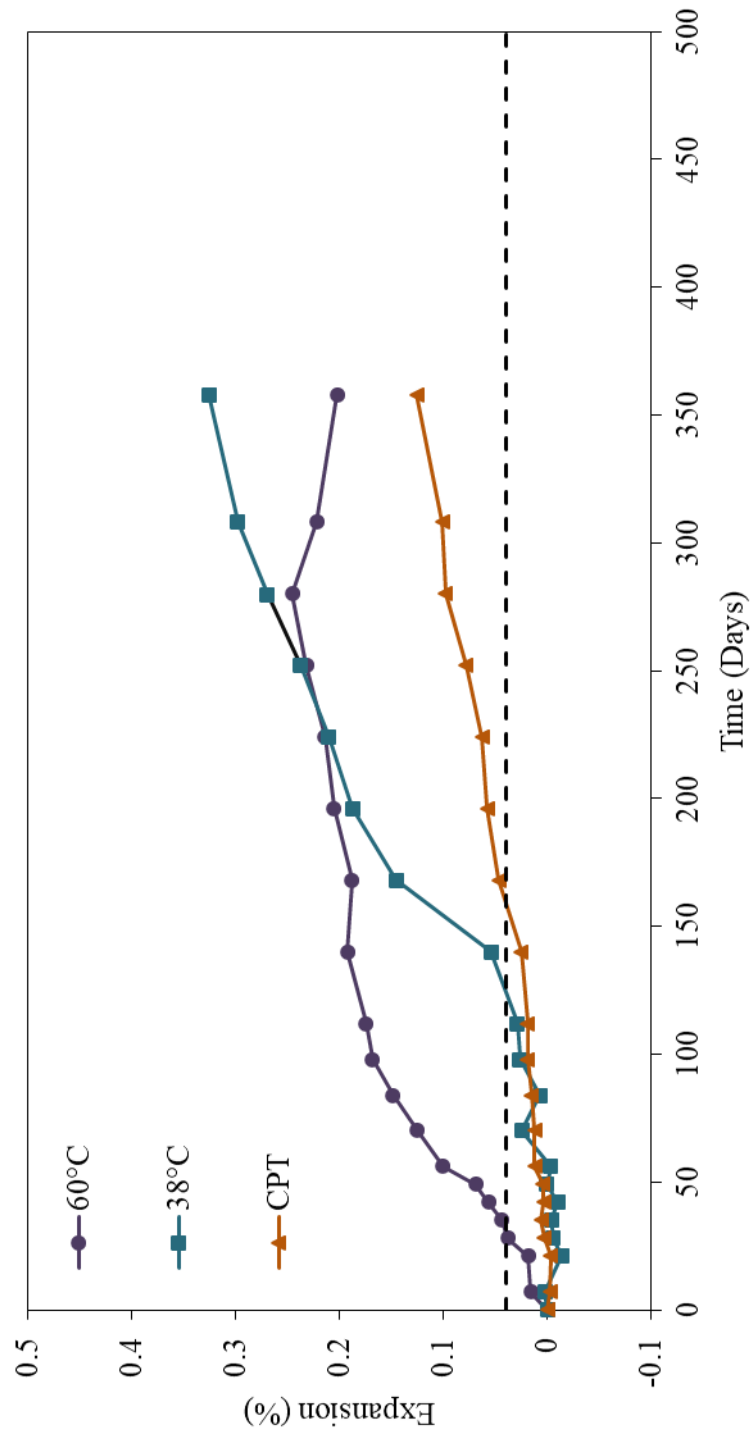
Springhill 1.25% Alkali
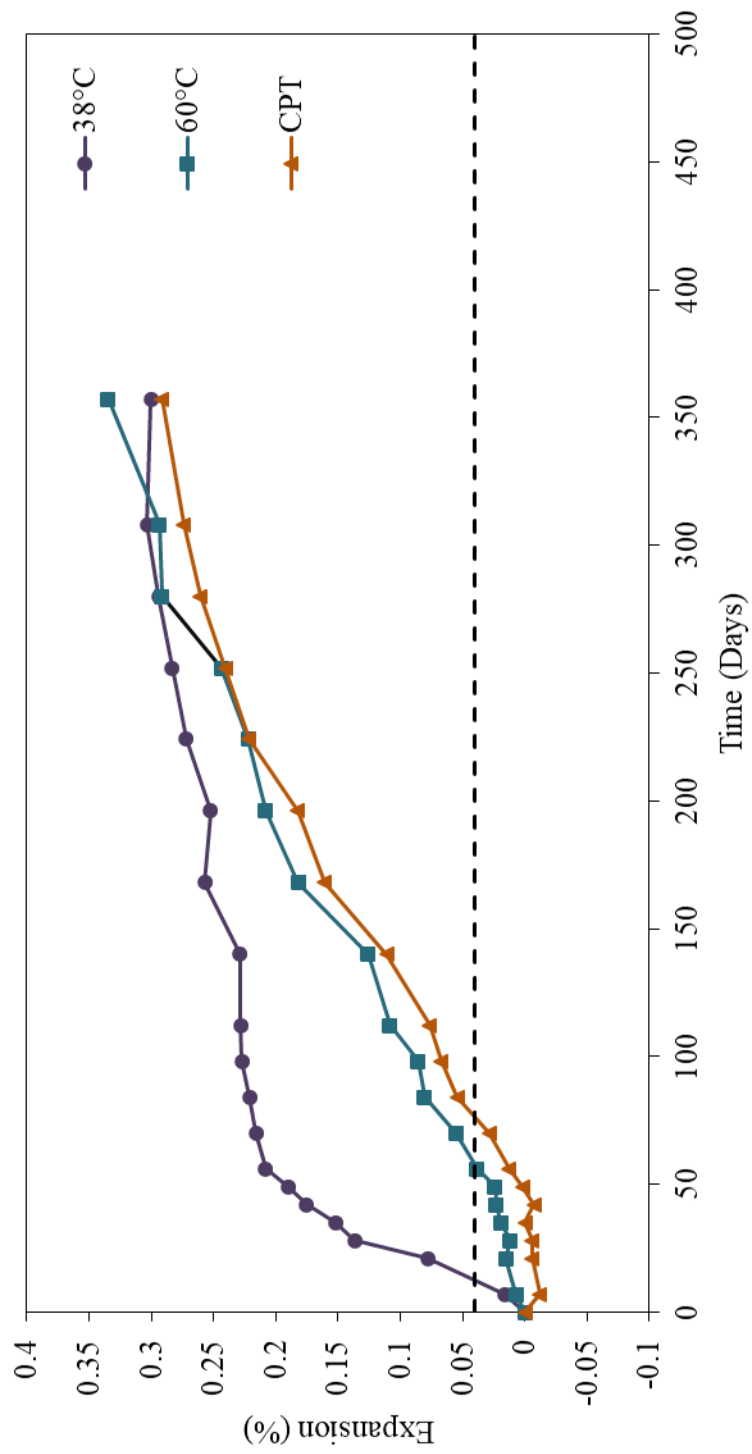
Springhill 30% Fly Ash
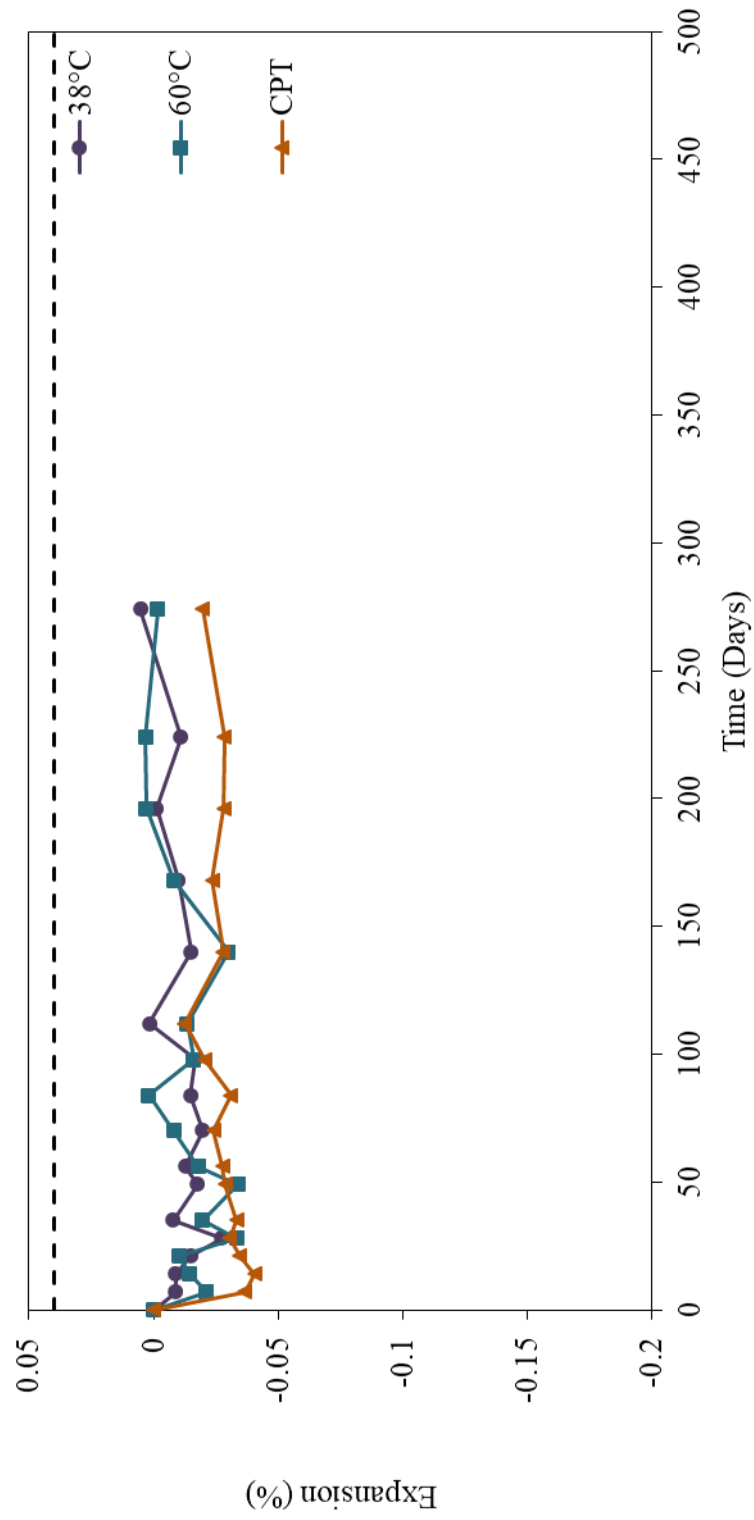
Springhill 56% Fly Ash
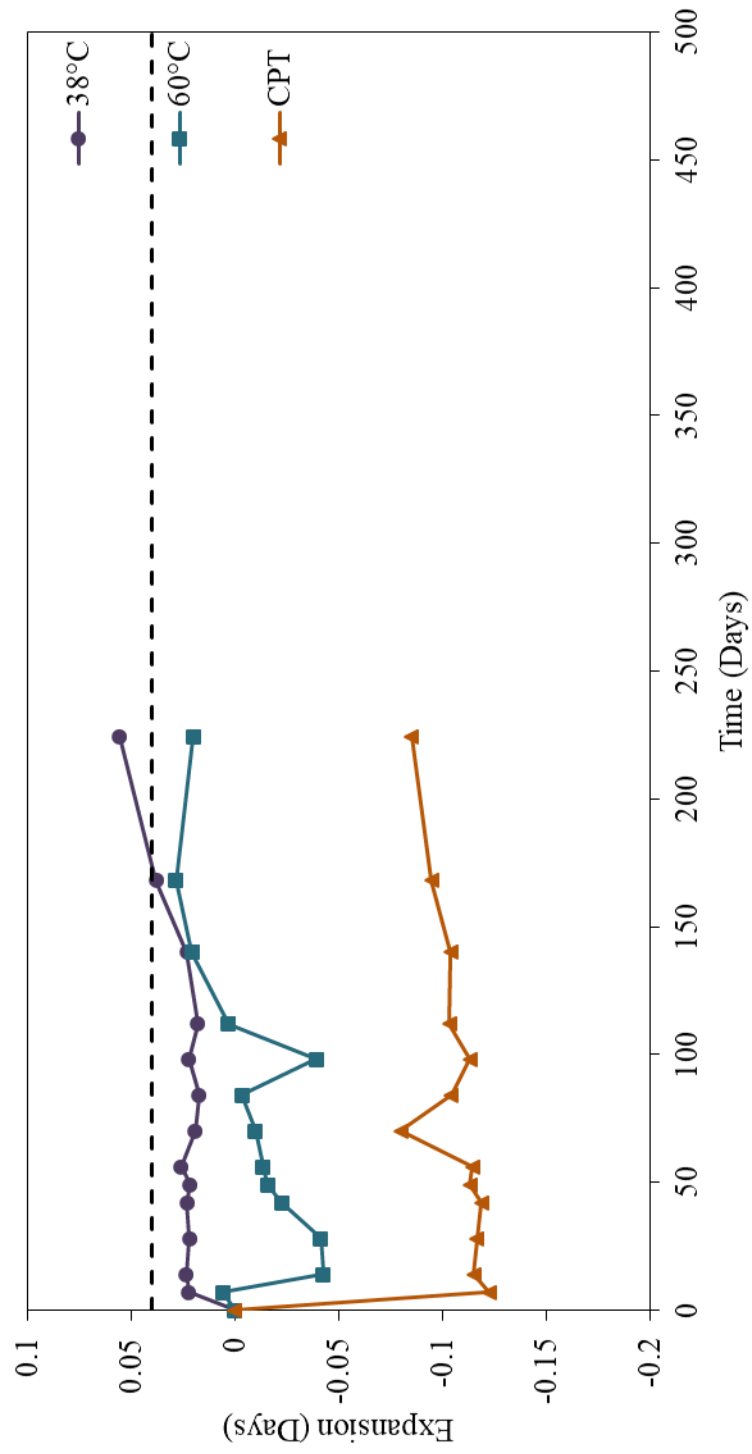
Spratt 0.40% Alkali
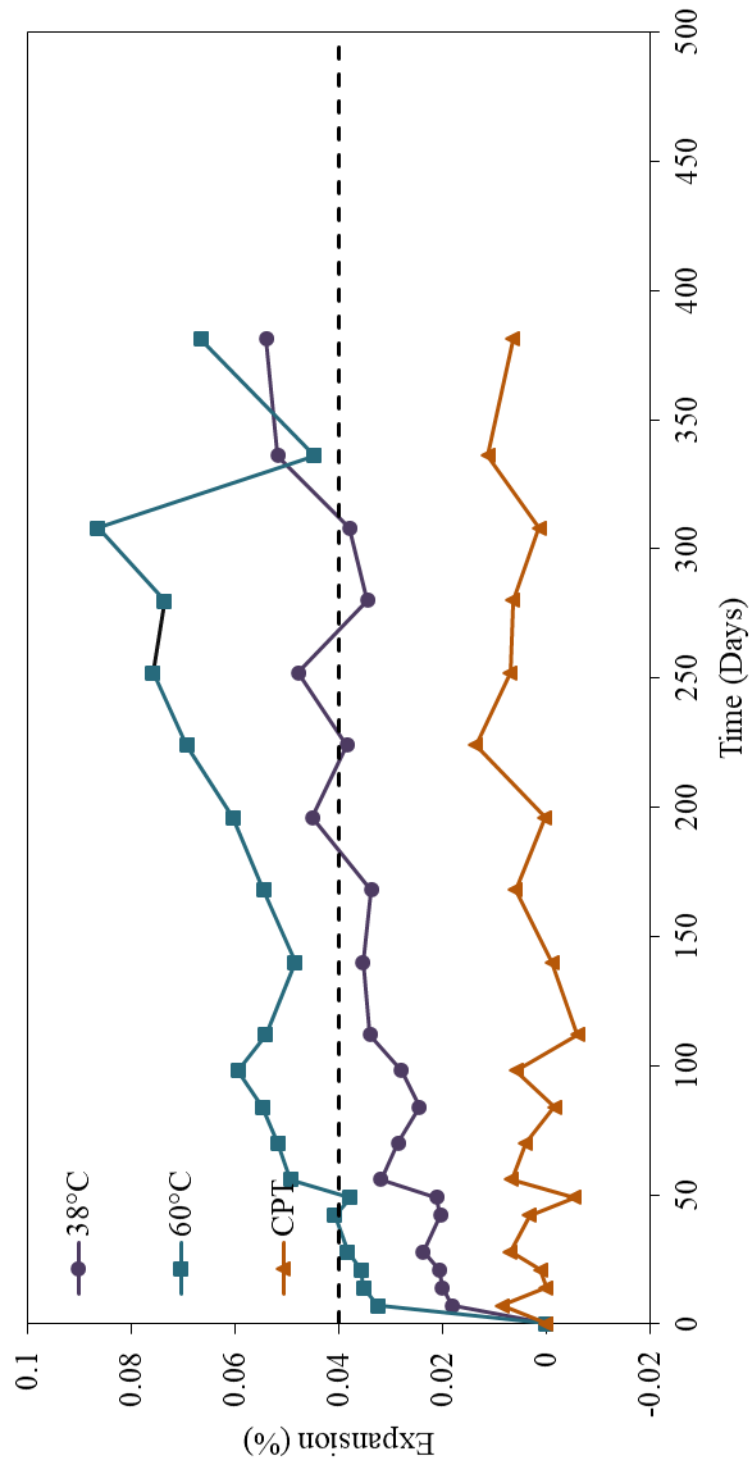
Spratt 0.49% Alkali
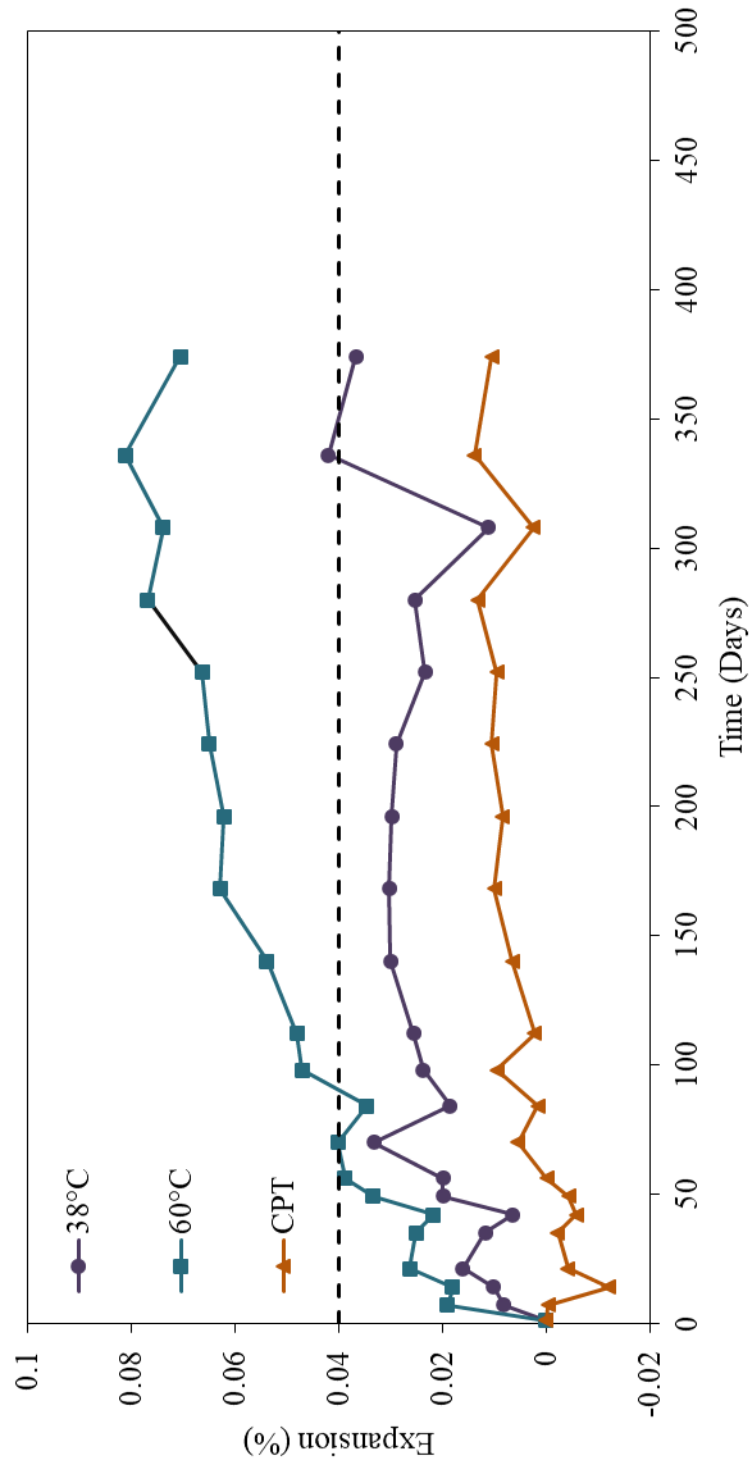
Spratt 0.90% Alkali
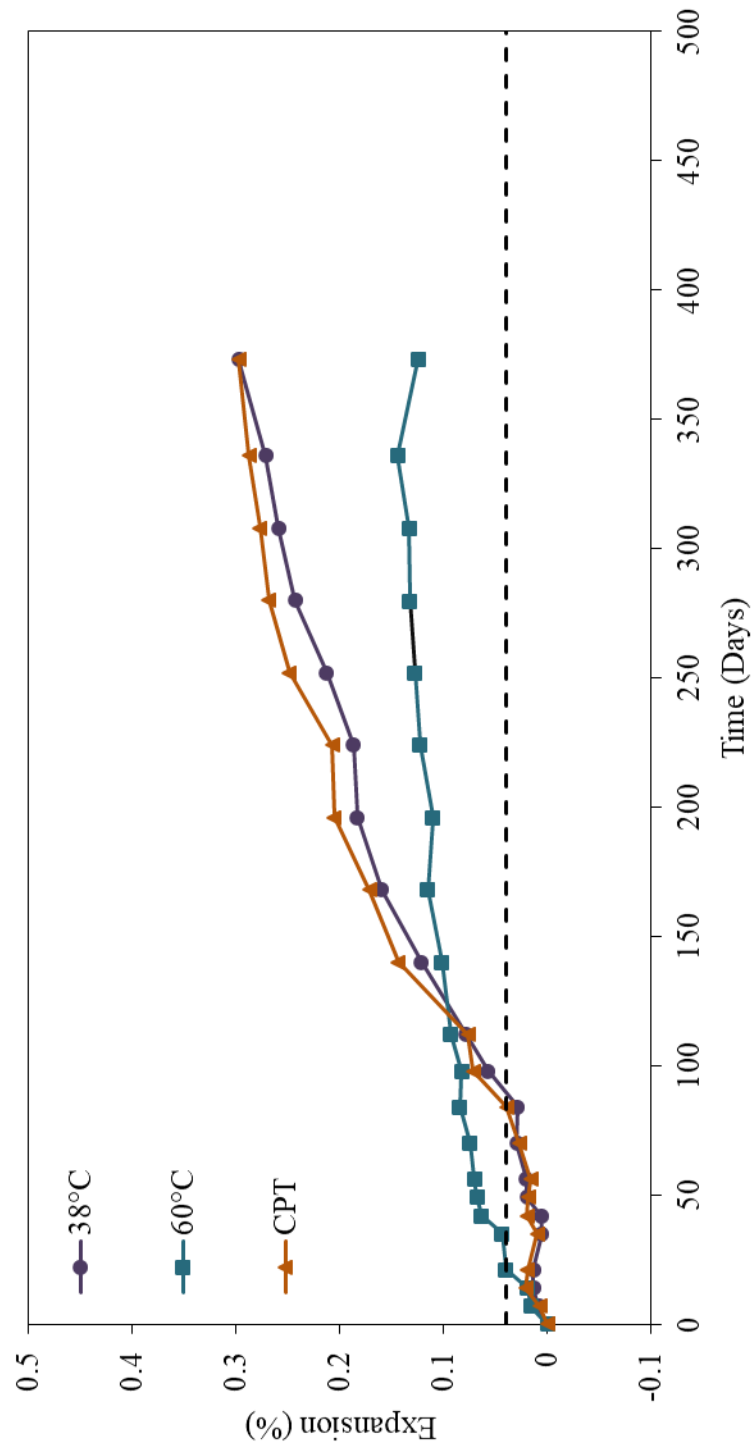
Spratt 1.25% Alkali
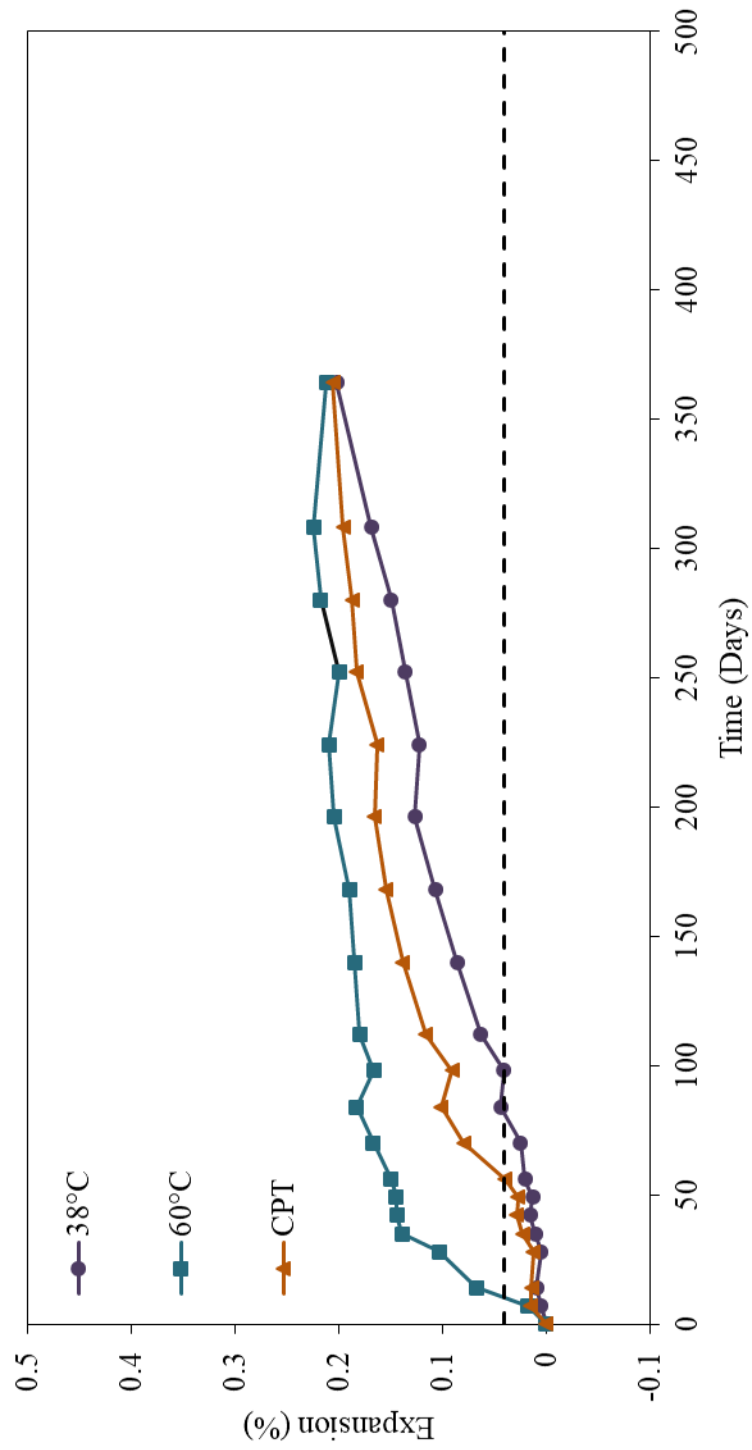
Spratt 20% Fly Ash
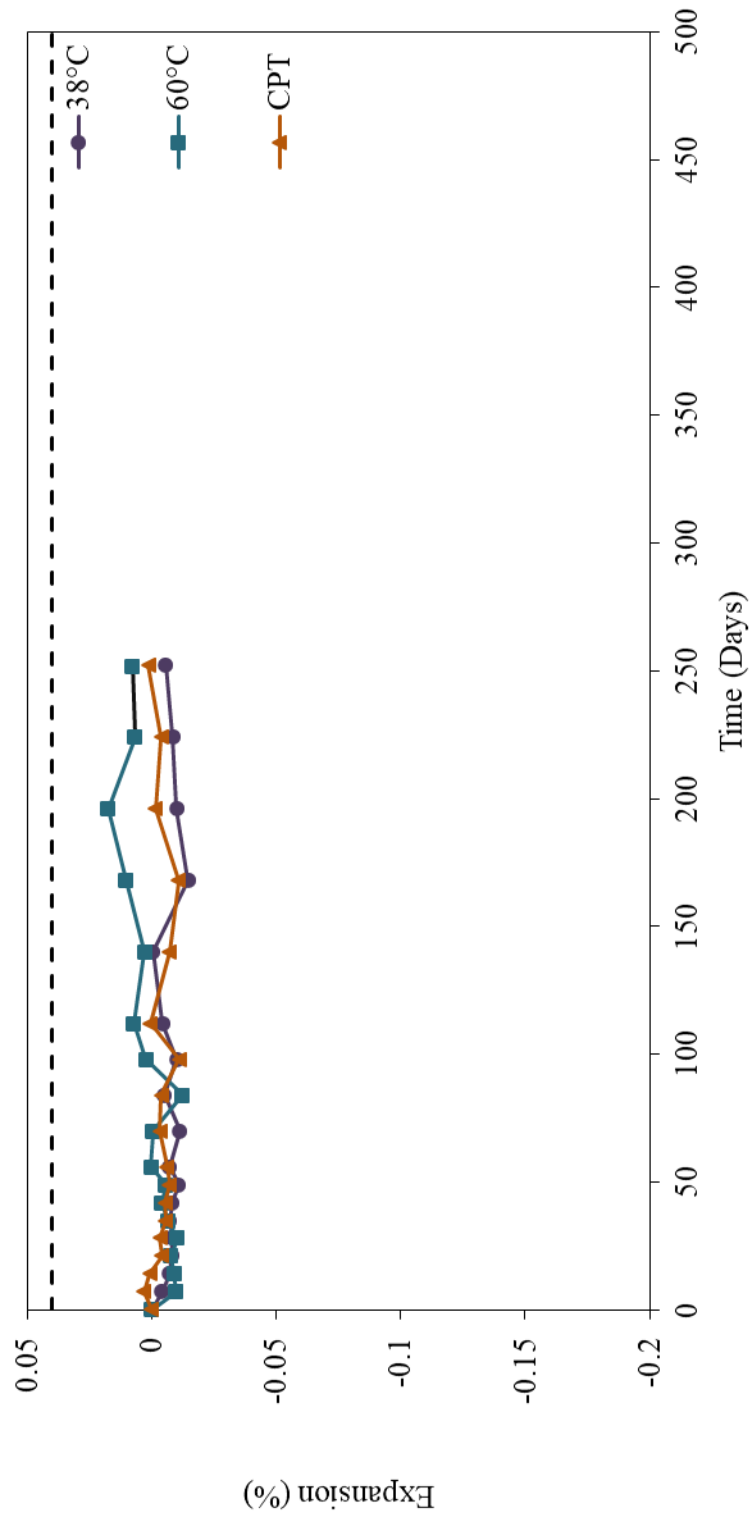
Spratt 30% Fly Ash
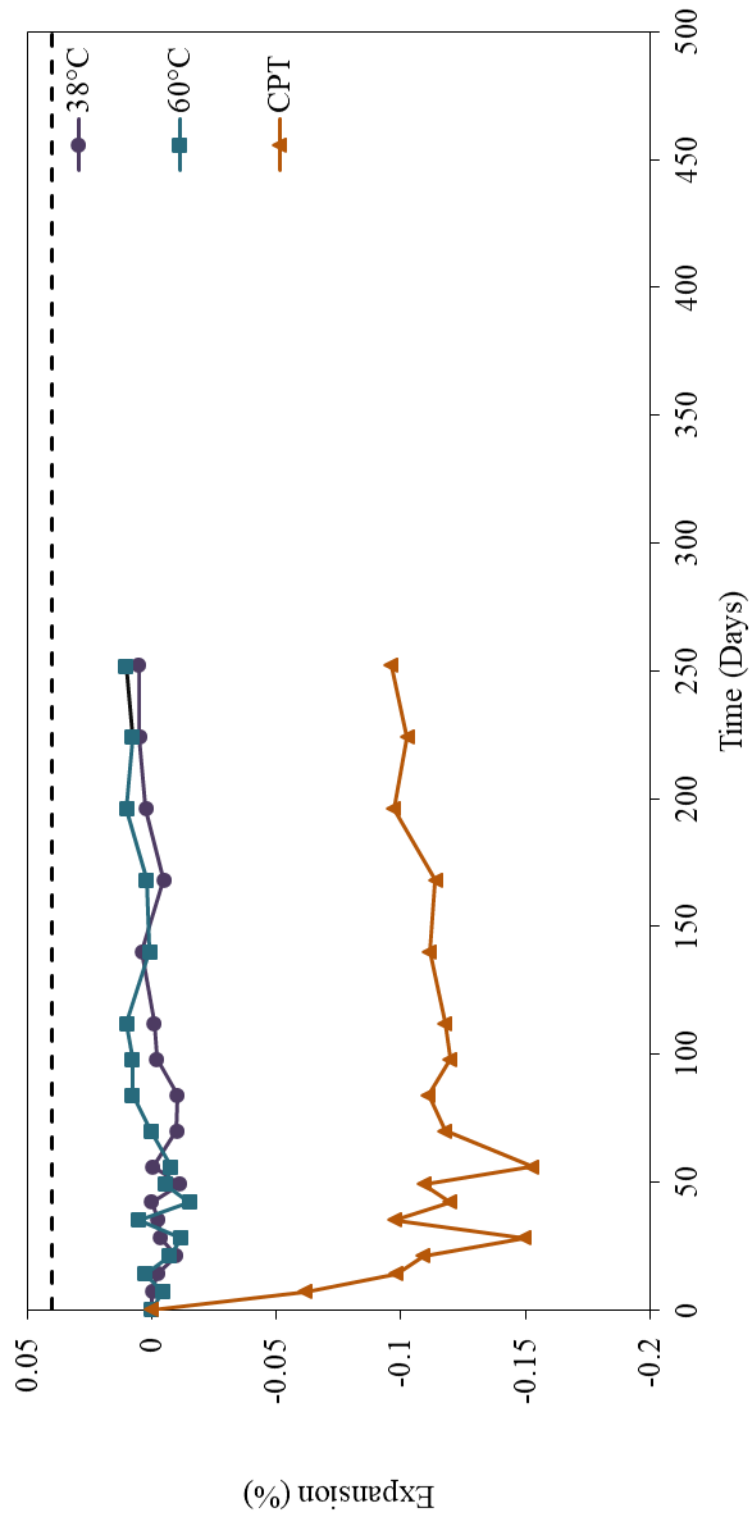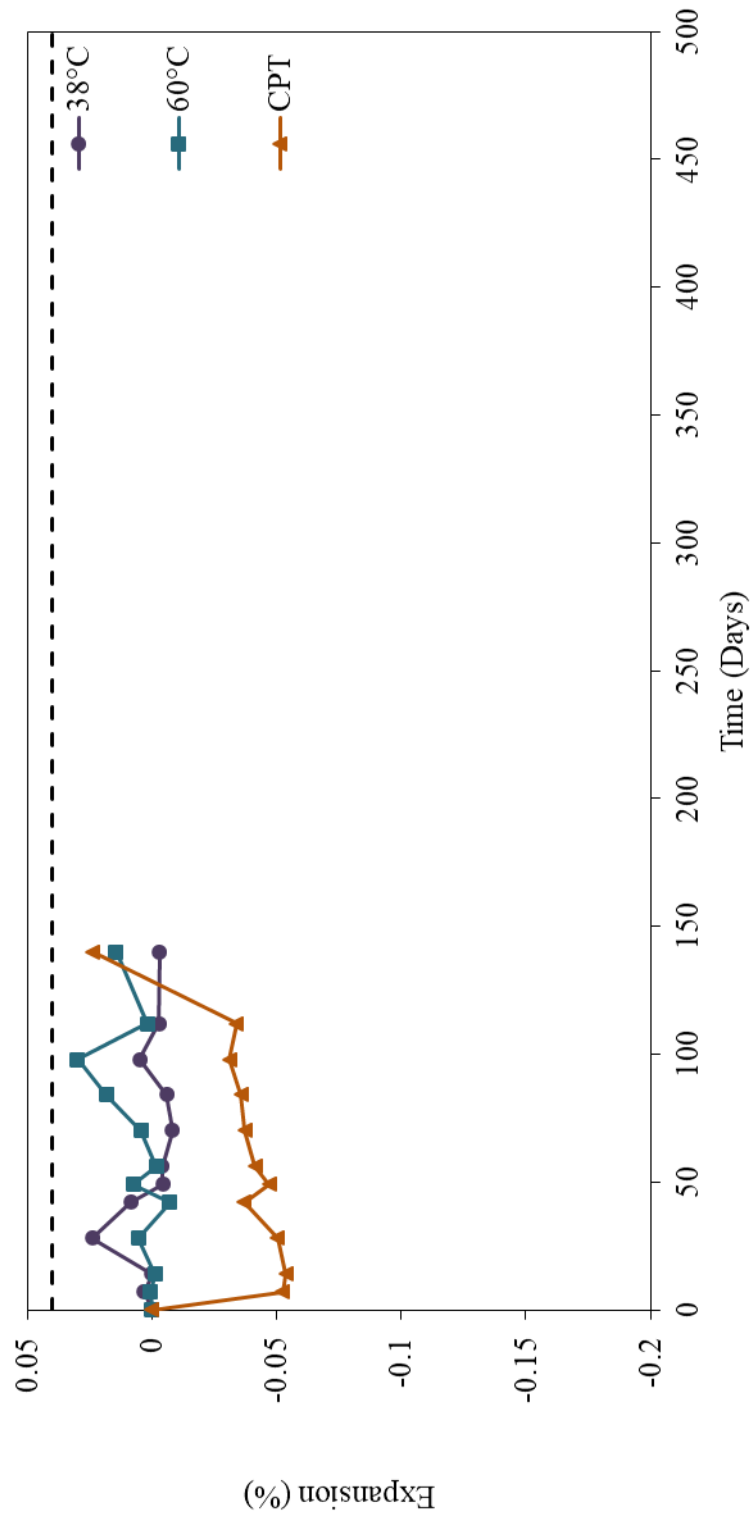
Spratt 50% Slag
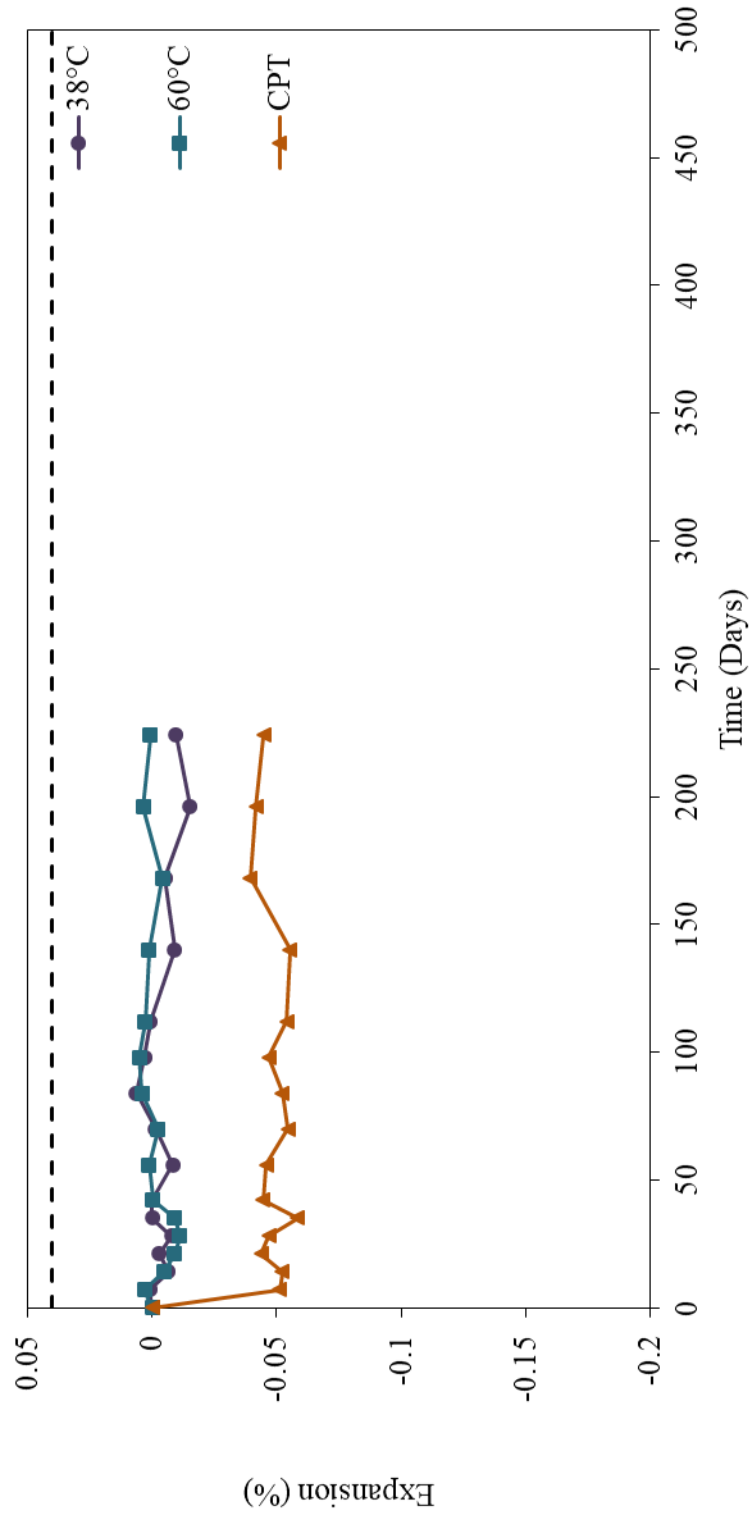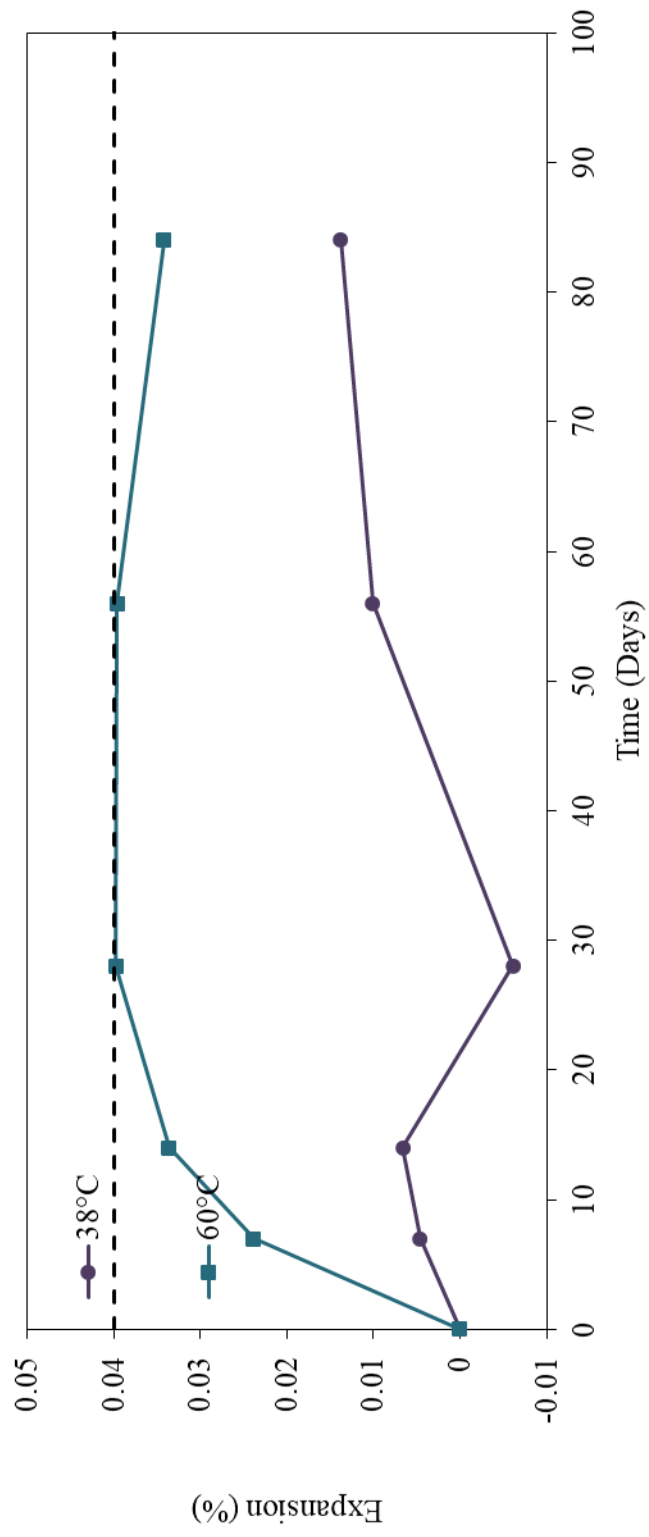
Spratt 25% Slag 4% Silica Fume
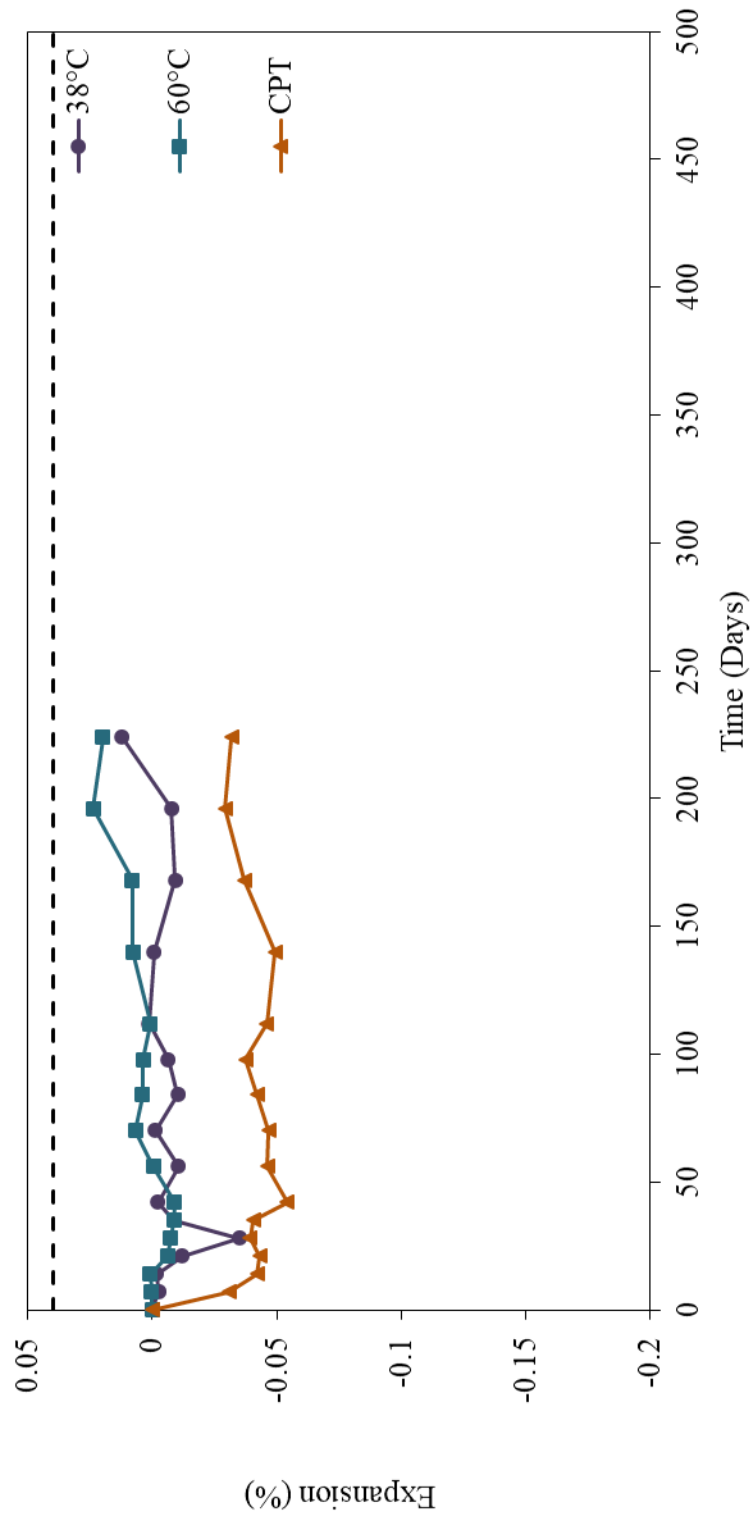
Spratt 65% Slag

San Antonino & Austin (Non-Reactive) 0.70% Alkali

Curriculum Vitae

Candidate's full name:

Michael Joseph Laskey

Universities attended:

University of New Brunswick (2011-2015); B.Sc.E.

Publications: None

Conference Presentations:

A New Test Method for the Determination of Susceptibility of Aggregates to ASR: The UNB Concrete Cylinder Test. American Concrete Institute, Philadelphia, Pennsylvania, November 2016

ASR: The UNB Concrete Cylinder Test and Other Current Test Methods. Atlantic Concrete Association, Saint John, New Brunswick, February 2017

The UNB Concrete Cylinder Test: An Update. American Concrete Institute, Detroit, Michigan, March 2017